
Opportunities and limitations of the cosmic-ray neutron soil moisture sensor under humid conditions

PhD-thesis

By

JOOST IWEMA



Department of Civil Engineering
UNIVERSITY OF BRISTOL

A dissertation submitted to the University of Bristol in accordance with the requirements of the degree of DOCTOR OF PHILOSOPHY in the Faculty of Engineering.

DECEMBER 2017

ABSTRACT

A scale gap in soil moisture measurement techniques, at scales of metres to hundreds of metres in horizontal space and minutes to a day in time, has been existing for decades. These are the typical scales of relevant hydrometeorological and biogeochemical processes, and of modern hydrological models. A new soil moisture measurement technique that can help fill this scale gap was developed a decade ago. This technique, the Cosmic-Ray Neutron Sensor (CRNS), estimates root zone soil moisture in the surrounding tens of metres by measuring natural neutron radiation above the ground. The objective of this thesis was to investigate the opportunities and limitations of the CRNS to help fill the scale gap in soil moisture measurement techniques by improving the knowledge of the CRNS, especially at humid sites. This objective was achieved through three separate studies. The first, a land surface model calibration study, showed that compared to point-scale soil moisture data, CRNS soil moisture data did not lead to overall better latent heat flux estimation across sites, based on two-objective calibrations (soil moisture and latent heat flux). This result was attributed mainly to the limited effect of calibrating model parameters on soil moisture dynamics. The second study showed that the traditional assumption that only one soil sampling day would be sufficient to calibrate the CRNS, was insufficient to obtain accurate soil moisture estimates. Multiple, but no more than six calibration days are advised for humid sites instead. The novelty of the third study was the separate analysis of the accuracy and precision of both the CRNS neutron count and the derived soil moisture estimate, which are affected differently by natural conditions and can be improved in different ways. One outcome was that, at the three humid sites investigated, the soil moisture precision was largely a function of the soil moisture content itself. Temporal integration times below fifteen hours were sufficient to achieve precision similar to traditional point-scale techniques at these sites, at any time. Overall, this thesis shows the CRNS is an accurate and precise soil moisture measurement technique for humid sites if multiple calibrations are done and if all relevant hydrogen pools are quantified. To use CRNS data to its full potential for land surface modelling, using soil moisture dynamics as calibration objective rather than the absolute soil moisture, could be investigated.

COSMIC-RAY NEUTRON SENSOR LITERATURE REVIEW

A technique that may help to fill the intermediate scale gap in soil moisture measurements (Chapter 1) is the Cosmic-Ray Neutron Sensor (CRNS; Fig. 1.2; Zreda et al., 2008). This above ground sensor has a footprint radius of 130-240 m at sea level and a measurement depth of ~12-76 cm depending on soil wetness (Desilets et al., 2010; Köhli et al., 2015). Therefore this sensor can provide soil moisture information at scales within the intermediate scale gap as shown in Figure 1.7. The CRNS-technique makes use of the slowing down and thermalisation of high-energy cosmic-ray neutrons by hydrogen atoms in the soil (Zreda et al., 2008). An extensive literature review on the CRNS functioning and the relevant processes affecting its measurements is given in this chapter. First, in Section 2.1, the nuclear physics of cosmic-ray neutrons is explained. Next, older technologies that also employed neutron radiation to measure soil moisture content are briefly discussed in Section 2.2. Then, in Section 2.3, it is explained how the novel above ground Cosmic-Ray Neutron Sensor technically works. In Section 2.4 three methods to obtain soil moisture estimates from measured neutron counts are presented. In the following Section 2.5 the procedure to calibrate these three models using soil samples is elaborated on. Not only soil moisture affects the CRNS measured signal. Naturally changing conditions, for instance atmospheric pressure and the presence of other water containing landscape elements affect the neutron radiation. All relevant natural factors are therefore addressed in Section 2.6. The size of the soil volume represented by the CRNS measurements also depends on natural conditions and can change in time and varies from location to location. The CRNS footprint size has been subject to debate over the past decade and the knowledge on this issue has improved, as explained in Section 2.7. Like with any measurement technique, the CRNS observations are subject to uncertainties. This uncertainty stems from both accuracy and precision issues and is affected by a range of natural and human influenced factors. The measurement uncertainty

is discussed in Section 2.8, which is especially relevant with respect to Chapter 5 of this thesis. Since the development of the first CRNS, sensor networks have been established in different parts of the world. These networks are introduced in Section 2.9. A mobile version of the CRNS, the CRNS ‘Rover’ is discussed in Section 2.10. In the for-last Section 2.11, linking specifically to the main purpose of the CRNS, the use of CRNS measurements in hydrological and land surface process studies till date is discussed. This chapter finishes with an outlook on expected developments in the CRNS research community, in Section 2.12.

2.1 Origin and nuclear physics of cosmic-ray neutrons

The neutrons detected by the Cosmic-Ray Neutron Sensor ultimately originate from extraterrestrial radiation, so-called *primary cosmic-rays* (Hess et al., 1959). Most primary cosmic-rays originate from beyond our solar system but within our galaxy and are created after supernovas (Blasi, 2014). These primary cosmic-rays are mostly protons, but also include other charged particles. If a primary cosmic-ray has sufficient energy, it may pass the magnetic fields of the Sun and of the Earth. The number of cosmic-rays reaching the Earth’s magnetosphere reduces during periods of higher solar activity. Cosmic-rays that do reach the Earth’s magnetosphere can still be prevented from reaching the Earth’s atmosphere by the planet’s magnetic field. The possible fate of a cosmic-ray that does reach the top of the atmosphere is depicted in Fig. 2.1, where a cosmic-ray (proton) is shown as a black arrow.

2.1.1 High-energy, fast, epithermal, and thermalised neutrons

Secondary cosmic-ray particles, including high-energy neutrons (red lines in Fig. 2.1), can be created by reactions between cosmic-rays and nitrogen and oxygen in the Earth’s atmosphere (Letaw and Normand, 1991; Desilets and Zreda, 2001a; Köhli et al., 2015). These secondary cosmic-rays have an energy level of between about 11 MeV¹ and 10 GeV, and with its peak around 100 MeV (Simpson, 1951; Gudima et al., 1983; Desilets and Zreda, 2001a; Köhli et al., 2015). These so-called high energy neutrons can subsequently travel downward through the atmosphere and create cascades of neutrons, which can ultimately reach the Earth’s surface (upper panel of Fig. 2.1). In Figure 2.2, the energy spectrum of high-energy neutrons at the Earth’s surface is indicated in pink/red (Köhli et al., 2015; Goldhagen et al., 2002). Near the surface, high-energy neutrons can collide with other nuclei. During such collisions, fast neutrons, with lower energy levels (~1 MeV, green in Figure 2.2, blue lines in Fig. 2.1) are released (Simpson, 2000; Desilets and Zreda, 2001a). Due to further collisions, these fast neutrons continue to lose energy. The blue domain in Figure 2.2 shows the energy levels (0.2 eV–100 keV) at which so-called elastic collisions dominate (represented with blue lines in Fig. 2.1, Hess et al. (1959); Desilets and Zreda

¹An electronvolt eV is a measure of a particle’s energy. It is defined as the change in amount of energy of an electron moving over one volt of electric potential difference.

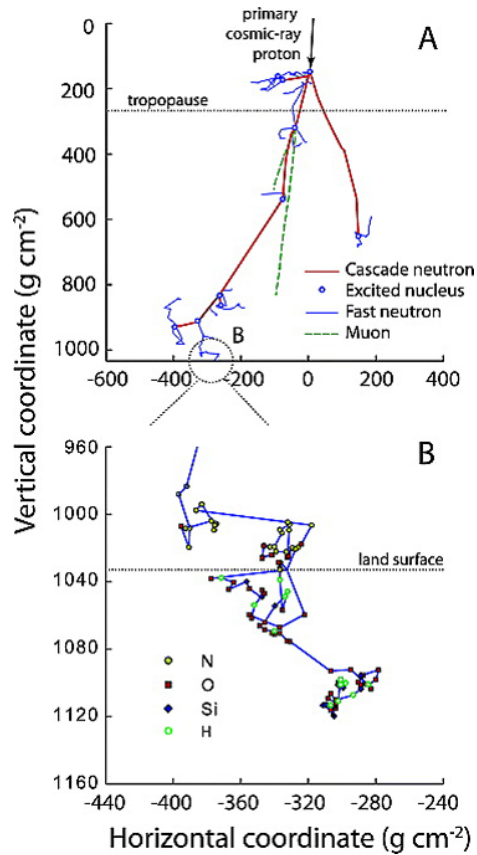


FIGURE 2.1. Simulated particle track from primary cosmic-ray proton reaching the top of the atmosphere to fast neutrons interacting in the soil. High-energy neutrons are shown in red (cascade neutrons). In the upper panel the particle paths from the top of the atmosphere to the land surface are shown. In the lower panel the paths just above and just below the land surface are shown. The units on both axes are in shielding mass, which is the actual distance multiplied with the mass of material above. Due to the higher density of soil than of air, the distances below the surface appear much greater compared to the distances above the land surface. The actual distances in metres are in the order of less than 1 m. The simulations were done with radiation transport model Monte Carlo N-Particle Extended (MCNPX, Pelowitz, 2005) and the figure was copied with permission from Desilets et al. (2010).

(2001a) and Köhli et al., 2015). The neutrons within this sub-range of the fast neutron spectrum are called epithermal neutrons. In an ideal elastic collision kinetic energy is equally transferred between the moving neutron and the target nucleus. Due to the relatively low kinetic energy of the target nucleus, the travelling neutron either keeps most of its kinetic energy in case the target nucleus has a much higher mass, or, if the target nucleus has a mass similar to that of the neutron, most kinetic energy is transferred to the target nucleus. In the latter case the neutron is effectively stopped, because it retains a small bit of its kinetic energy only. After losing most of

its energy, a neutron can become thermalised, i.e. it reaches an energy level below ~ 0.2 eV (gray area in Figure 2.2, Hess et al. (1959); Desilets and Zreda (2001a) Köhli et al., 2015). At those energy levels the neutrons are in thermal equilibrium, also called vibrational equilibrium, with the molecules in their surroundings (Desilets and Zreda, 2001a). The average energy level of the thermal neutrons therefore depends on the temperature and corresponds with the equilibrium energy level ('equilibrium' peak in Fig. 2.2). Nuclei can absorb thermal neutrons more easily than they can absorb epithermal–fast neutrons. Due to their neutral charge (i.e. they are insensitive to electrical potential differences) neutrons cannot regain energy by taking energy from charged nuclei. Thermal neutrons can therefore not accelerate back to the fast energy spectrum and cannot affect fast neutron energy radiation intensities.

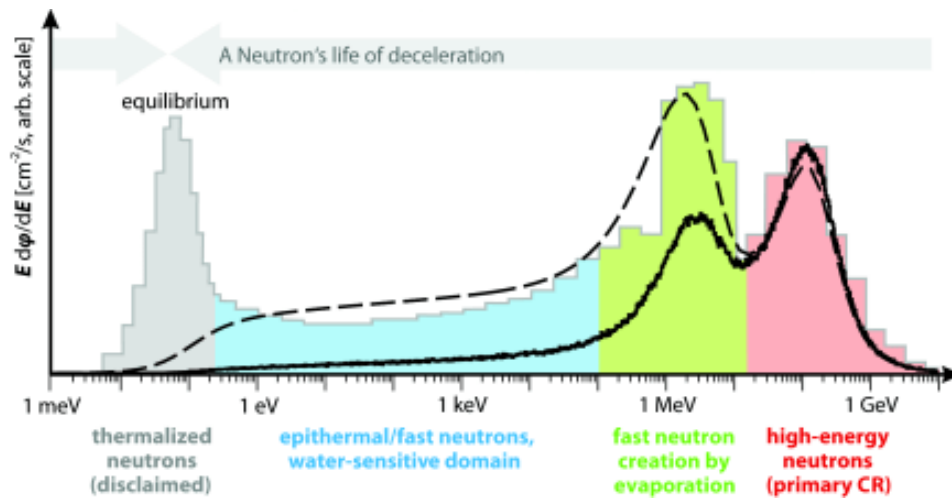


FIGURE 2.2. Neutron energy spectra at the Earth's surface. Measured spectra by Goldhagen et al. (2002) are shown in grey and colors. The red/pink colour shows high-energy neutrons. Interaction of these neutrons with heavy atoms yields fast/evaporation neutrons (green). Elastic collisions with light atoms, dominated by hydrogen, yield epithermal/fast neutrons to which the CRNS is especially sensitive. Finally, neutrons can reach thermal equilibrium energy levels (grey). Neutron spectrum simulations by Sato and Niita (2006) are shown shown with the dashed line. The observations and simulations at the thermal spectrum do not match due to model choices. Köhli et al. (2015) added the continuous line showing the net incoming spectrum after subtracting the radiation reflected by a pure water surface. They used this spectrum as input for their simulations. Copied with permissions from Köhli et al. (2015) and Goldhagen et al. (2002).

2.1.2 The effect of soil moisture on epithermal–fast neutrons

Because of their small size and mass, hydrogen atoms have a high slow down power for epithermal–fast neutrons through elastic collisions, implying hydrogen can stop these neutrons effectively (Bethe et al., 1940). Therefore, and because of the high abundance of water in

the subsurface, hydrogen dominates the moderation of fast neutrons in soils (Bethe et al., 1940; Hendrick and Edge, 1966; Desilets and Zreda, 2001a; Köhli et al., 2015). The moderation and hence intensity of thermal neutrons is not only affected by hydrogen, but is also substantially affected by other elements present near the land surface, like Boron. Moreover, thermal neutron intensity has a different dependency on hydrogen prevalence than fast neutrons (Desilets and Zreda, 2001a; Zreda et al., 2008). Therefore, if the goal is to measure soil moisture, a detector is needed that is sensitive to epithermal–fast neutron radiation, but insensitive to thermal neutron radiation. Due to the described moderating power of hydrogen, epithermal–fast neutron intensity is inversely correlated with soil moisture content (Hendrick and Edge, 1966; Kodama et al., 1985; Zreda et al., 2008). This relationship is the basis for soil moisture measurement with the Cosmic-Ray Neutron Sensor, which is mostly sensitive to epithermal neutrons.

2.2 Below ground neutron sensors

The technique of using epithermal neutron radiation to measure soil moisture is not a novelty of the above ground Cosmic-Ray Neutron Sensor as such. The effects of hydrogen and soil moisture on epithermal–fast neutron radiation was known in the fifties of the twentieth century already (Gardner and Kirkham, 1952). The effects of, more specifically, hydrogen in (lunar) soil (Lingenfelter et al., 1961) and of soil moisture on Earth (Hendrick and Edge, 1966) on natural fast–epithermal neutron radiation were known from the sixties of the twentieth century. These researchers were however more interested in natural neutron radiation near the land surface for different purposes, for instance the effects of nuclear weapons (Hendrick and Edge, 1966). During the second half of the twentieth century below ground neutron sensors were used to measure local ($< 1 \text{ m}^3$) soil moisture content. Two types of below ground sensors have been used. The first type, ‘active’ (e.g. Gardner and Kirkham, 1952) below ground neutron sensors, used an artificial neutron radiation source. The neutron radiation moderated by the soil and water surrounding the buried sensor was measured with a separate neutron detector. The artificial radiation sources however posed a serious health hazard to humans taking the measurements (Kodama et al., 1985). Kodama et al. (1985) therefore developed a passive below ground neutron sensor taking example in passive neutron radiation based snow water content sensors (Kodama, 1980). This passive sensor employed cosmic-ray neutron background radiation (Section 2.1). The background epithermal neutron radiation was detected by a tube filled with 10-boron trifluoride ($^{10}\text{BF}_3$; includes non-radioactive boron-10 isotope). Kodama et al. (1985) found good correlations between soil moisture contents and neutron measurements between 20 and 40 cm depth.

2.3 Above ground Cosmic-Ray Neutron Sensor (CRNS)

The modern above ground Cosmic-Ray Neutron Sensor was developed after epithermal neutron measurements above a field in Arizona, USA, showed a correlation with point-scale soil moisture

measurements made in the surrounding field (Figure 2.3, Zreda et al., 2008). The innovation of the Cosmic-Ray Neutron Sensor was therefore, compared to the more traditional below ground neutron based soil moisture sensors, that it provides a soil moisture measurement representing a larger area in horizontal space; in the order of hectometres (Zreda et al., 2008). Moreover, it provides a measurement integrated over the entire surface soil moisture volume measured, instead of a measurement at one or a few spots only.

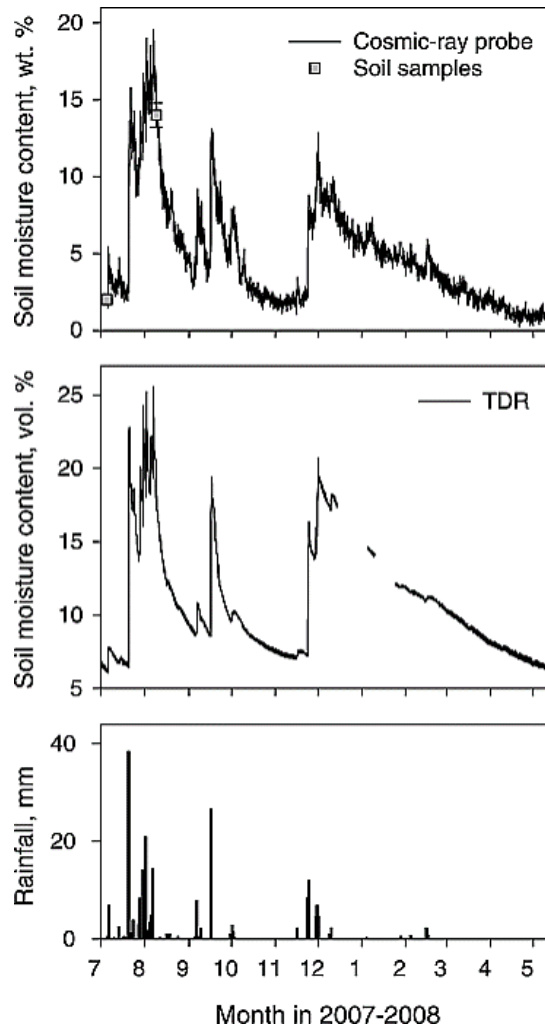


FIGURE 2.3. This figure from Zreda et al. (2008) shows Cosmic-Ray Neutron Sensor measurements (upper panel) at a site in Arizona correlated well independent soil moisture measurements made with co-located Time Domain Transmissivity sensors (middle panel). Copied with permission.

2.3.1 How does the CRNS measure epithermal neutron radiation?

To measure epithermal neutron radiation, the above ground Cosmic-Ray Neutron Sensor counts each neutron that collides with the sensor element (Knoll, 2000; Zreda et al., 2008, 2012). The sensor element is a metal tube filled with Helium-3 gas (^3He ; a non-radioactive Helium isotope) or boron-10 trifluoride gas (number 3 in Figure 2.4, number 4 is a bare counter, explained in the next section). The metal does not stop neutrons from reaching the gas inside because neutrons are not charged and hence do not interact with the charged metal lattice. To measure epithermal-fast neutron radiation only, a shield of high-density polyethylene, which can stop thermal neutrons is placed around the sensor element (number 3 in Figure 2.4). This shielded sensor is alternatively called a moderated Cosmic-Ray Neutron Sensor. Despite the polyethylene shield, estimations based on neutron modelling and field data indicated that 30% of the neutrons detected is thermal (McJannet et al., 2014). Their findings did however not provide conclusive proof and they recommended further research.

Andreasen et al. (2016) added a layer of cadmium (cadmium difference method; Lingenfelter et al. (1961) and Knoll, 2010) on top of the polyethylene shield to prevent thermal neutrons from affecting the soil moisture measurement. They derived site-specific correction functions to isolate the epithermal-fast neutron component from the total neutron count measured with a moderated neutron sensor. Besides a moderated neutron sensor and a cadmium shielded moderated neutron sensor, a so-called 'bare counter' (number 4 in Figure 2.4) is needed to measure the thermal neutron radiation intensity. This allowed to directly compare measured epithermal neutrons (0.2 eV–100 keV; the blue region in Figure 2.2) and neutrons modelled with neutron simulation models, which are typically in the range of 10 eV–1 keV (within the blue region in Figure 2.2). Another finding from this study (Andreasen et al., 2016) was that a moderated Cosmic-Ray Neutron Sensor measures about 45 % of thermal neutrons a bare detector measures. The bare detector was however found to be quite insensitive to epithermal neutrons, measuring about 5 % of epithermal neutrons the moderated detector measures. At the ground surface the thermal contribution to the moderated counter signal was with ~30% similar to the value reported by McJannet et al. (2014). The ratio between epithermal and thermal neutron intensity however differed with height above the land surface and was different between sites, due to different chemical compositions of the surroundings. To apply this cadmium difference method at a new field site a moderated counter, a cadmium shielded moderated counter, and a bare counter are needed to find site-specific thermal neutron radiation correction models. This is currently not the case at most Cosmic-ray Neutron Sensor sites. Most sites have a moderated and bare sensor only (Zreda et al., 2012; Evans et al., 2016; Baatz et al., 2015) and some have just a moderated sensor (e.g. CosmOz; Hawdon et al. (2014) and the AMUSED project sites at Sheepdrove Organic Farm, Berkshire, UK, see Chapter 5). All Cosmic-Ray Neutron Sensor data used in this thesis are from *non-cadmium shielded moderated counters*.

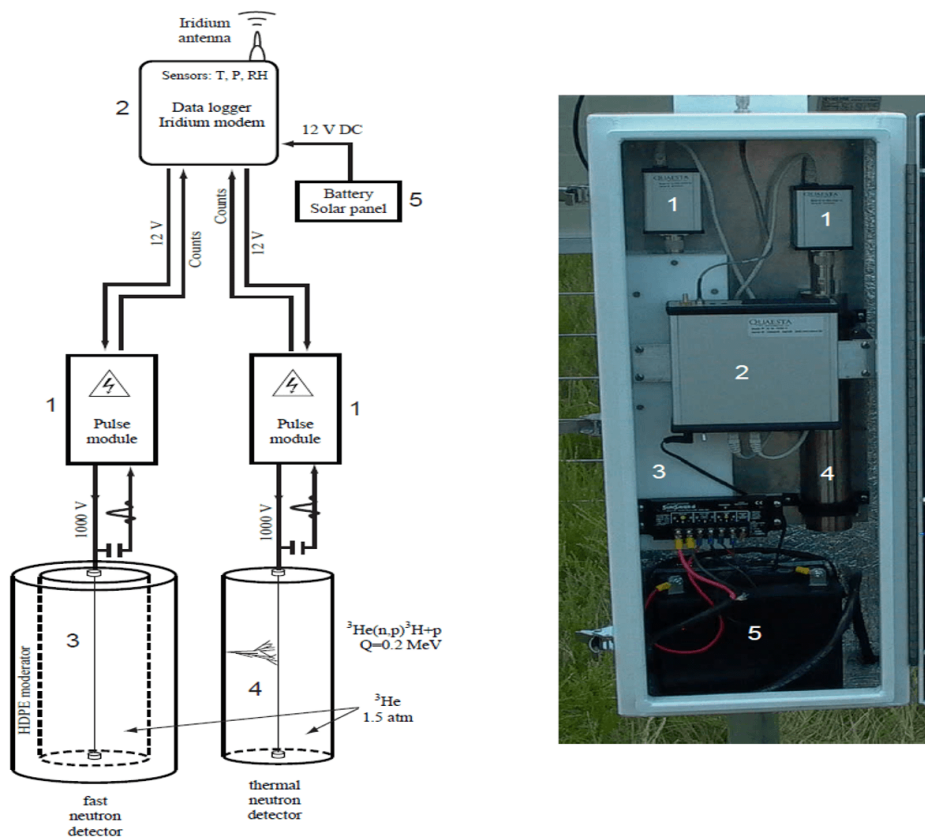


FIGURE 2.4. Schematic and photo of the box interior of a CRS1000 Cosmic-Ray Neutron Sensor (HydroInnova Inc., ^3He -filled). The ‘bare’ counter is indicated with number 4 and the moderated counter is indicated with number 3. The other elements shown include units for electrical signal and data storage and transmission (number 1 and 2), and number 5, the power supply (solar panel) and storage (battery). Figure copied from Zreda et al. (2012) with permission.

2.3.2 How are the neutron counts recorded?

As mentioned before, the epithermal–fast neutron intensity is measured by ‘counting’ each neutron that enters the helium-3 gas or boron-10 trifluoride gas filled in the sensor tube (Knoll, 2000). When an epithermal–fast neutron collides with a helium-3 or boron-10 nucleus, it is absorbed within this target nucleus. Due to the change in ratio of number of protons and neutrons in the core of the target nucleus, the electrical charge changes (becomes relatively less positive and hence more negative). To compensate for this increased negative charge, an electron is released. This electron is then a free electron; it is not part of an atom. A free electron can have a high kinetic energy and can be easily accelerated by the electrical potential difference applied within the sensor tube. This electrical potential difference is $\sim 1\text{ kV}$ (Zreda et al., 2012) and is applied between the wall of the sensor tube (negatively charged; *cathode*) and a wire

in the core of the tube (positively charged; *anode*, shown as a vertical line in number 3 and 4 in Figure 2.4). The free electron can collide with neutral particles in the gas inside the tube, freeing additional electrons, creating a cascade of free electrons, called a *Townsend avalanche* (Knoll, 2000). This process creates an electrical potential difference within the gas chamber, with all electrons travelling to the anode. The electrical current generated by this process is further amplified and passed through an electrical filter mechanism (Zreda et al., 2012). From the resulting electrical signal the neutron count is derived. This neutron count is communicated to a data logger (number 2 in Figure 2.4) via an electrical signal (number 1 in Figure 2.4). The user can collect the data by directly downloading it from the data logger using for instance a cable to a laptop or by copying the data from an SD-card connected to the data logger. Depending on the sensor installation, the data can also be send over an Iridium satellite connection (antenna shown in Figure 2.4). The neutron counts can be recorded at different temporal resolutions but the default for the Cosmic-ray Soil Moisture Observation System (COSMOS network, Sec. 2.9) is one hour (Zreda et al., 2012). However, the measured neutron count rate is usually expressed in counts per hour (cph).

2.3.3 Differences between individual CRNS

Differences in CRNS sensor type (e.g. CRS1000 versus CRS1000B), size, shielding, and gas type (^3He versus $^{10}\text{BF}_3$) will yield different neutron counts under the same conditions (Zreda et al., 2012). Even sensors of the same type can differ due to variations during the manufacturing process. In case neutron count values of CRNSs located at different sites need to be compared, these sensor-to-sensor differences should be corrected for. A common way to apply this correction is to install the tubes close to each other for a certain time, obtain a sensor-to-sensor scaling factor, and then move them to their intended field locations. The counting rate efficiency correction factor obtained this way is referred to as fe (-) and the efficiency corrected neutron count is called Ne (cph). (Zreda et al., 2012)

2.4 Translating neutrons to soil moisture

As described in Section 2.3, the Cosmic-Ray Neutron Sensor measures epithermal-fast neutron radiation by counting neutrons colliding with the sensor element. To obtain soil moisture values, the variable of interest, multiple methods have been developed over the past seven years. The first method was a mathematically simple empirical formula (the N_0 method; Desilets et al. (2010); Section 2.4.1) presenting a relationship between soil moisture content and neutron count only. Another method (the Hydrogen Molar Fraction (HMF) method; Franz et al. (2013a); Section 2.4.2) was designed to take into consideration the effects of hydrogen pools other than soil moisture (e.g. vegetation), especially needed when taking measurements with mobile Cosmic-Ray Neutron Sensors. A third method (the COsmic-ray Soil Moisture Interaction Code (COSMIC);

Shuttleworth et al. (2013); Section 2.4.3), which took into consideration vertical heterogeneity in soil moisture contents, was developed to be used in the context of hydrological and land surface models especially.

2.4.1 N_0 method

To obtain soil moisture values, the variable of interest, Desilets et al. (2010) established a non-linear relationship between neutron count and soil moisture (Figure 2.5). They used a neutron interaction model called Monte Carlo N-Particle eXtended (MCNPX; Pelowitz, 2005), which simulates the paths of individual particles (e.g. neutrons) and their interactions with other particles. It does this by simulating the release of many (e.g. millions of) high-energy neutrons at the top of the atmosphere and the neutron cascades through the atmosphere that follow. The interactions of high-energy neutrons and subsequent epithermal–fast neutrons with the land surface environment are simulated. The user needs to define the material (e.g. soil) properties and can execute these simulations for different soil moisture contents. Doing so, Desilets et al. (2010) derived a relationship between observed neutron count and soil moisture content (SM), called the N_0 -formula (Eq. 2.1):

$$(2.1) \quad SM = \frac{a_0}{N/N_0 - a_1} - a_2,$$

where the parameter values $a_0 = 0.0808(\text{cm}^3 \text{g}^{-1})$, $a_1 = 0.372(-)$, and $a_2 = 0.115(\text{cm}^3 \text{g}^{-1})$ are assumed site-independent constants. N is the measured neutron count in counts per hour (cph), and corrected for certain, but not necessarily all, effects from other factors than soil moisture (Section 2.6). The soil moisture content (SM) represents an average over the footprint of the Cosmic-Ray Neutron Sensor (see also Section 2.7.1).

N_0 (cph) is a time-constant normalisation parameter whose site dependent value can be derived by taking multiple soil samples spatially distributed within the CRNS footprint on at least one day (the calibration procedure is explained in detail in Section 2.7.1 and in Section A.1). One calibration day provides one calibration point and this was originally assumed sufficient (Desilets et al., 2010) because the shape of the N_0 -curve was assumed fixed by the three a -coefficients.

The N_0 method is theoretically only valid for gravimetric soil moisture content values above 0.02g g^{-1} , but due to the presence of other hydrogen containing elements in the soil, this threshold is usually exceeded in most soils (Zreda et al., 2012). The value of N_0 represents dry conditions; when the neutron count is equal to the value of the N_0 parameter, the soil moisture content is approximately zero. McJannet et al. (2014) argued that the limited physical definition of parameter N_0 is a drawback of the N_0 method, which they said, requires numerous calibration points to obtain sufficiently low uncertainty. The N_0 formula was derived for silica rich soils (Desilets et al., 2010) but has been used for different, silica poor soils like clay soils (Zreda et al., 2012).

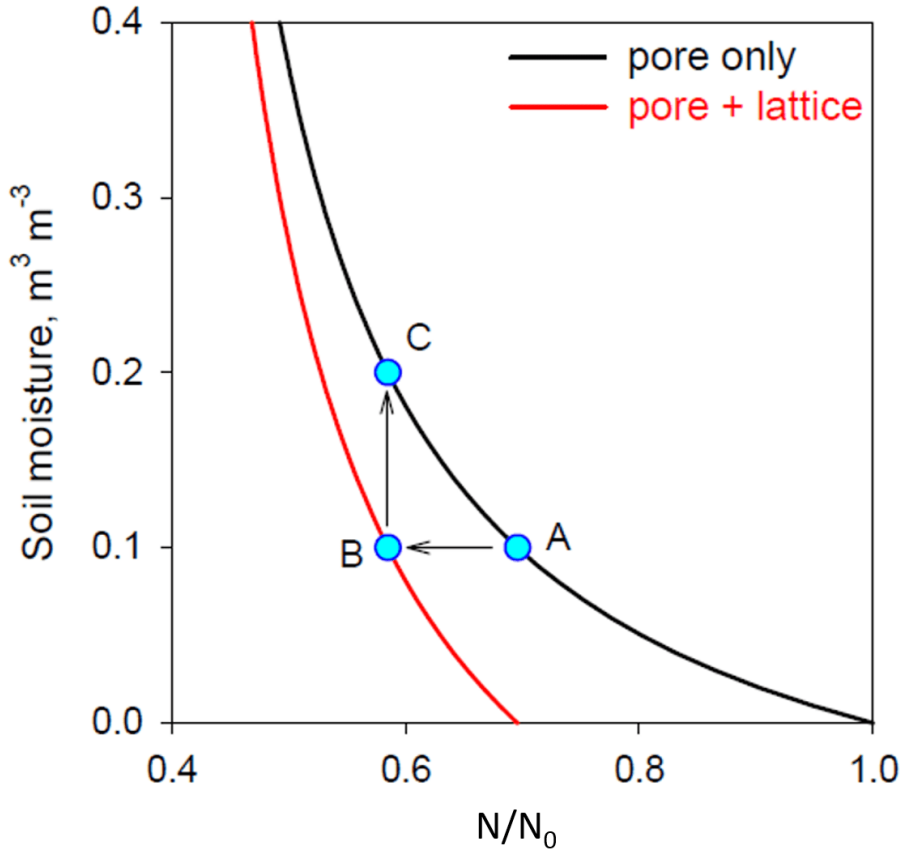


FIGURE 2.5. Examples of the N_0 -curve. The black line shows the curve when interstitial/lattice water is not taken into account and the red line shows the curve when this variable is taken into account. On the horizontal axis the neutron count normalised with respect to parameter N_0 is shown. On the vertical axis is the volumetric soil moisture content. Adding this time invariant variable shifts the position of the curve to the left. Copied with permission from Zreda et al. (2012).

The formula was initially assumed to be valid for both gravimetric (u ; g water g^{-1} dry soil) and volumetric (θ ; m^3 water m^{-3} dry soil) soil moisture content. Bogena et al. (2013) introduced some changes to the N_0 method to explicitly represent volumetric soil moisture content (θ) by incorporating the dry soil bulk density. It is necessary to compute volumetric soil water content if the data are used in hydrological models, because these typically calculate with soil volumes. They also added lattice water and soil organic matter water equivalent² (Eq. 2.2):

$$(2.2) \quad \theta = \frac{a_0 \cdot \rho_s}{N/N_0 - a_1} - a_2 \cdot \rho_s - lw - w_{SOM},$$

²Organic matter contains hydrogen (H). The equivalent amount of water (H_2O) is computed using the molar ratio of hydrogen to cellulose (10:1), the molar ratio of hydrogen to water (2:1) and the molar masses of hydrogen, water, and cellulose.

Parameters lw and w_{SOM} are the CRNS-footprint average volumetric lattice water content and soil organic matter equivalent water content ($\text{cm}^3 \text{cm}^{-3}$) respectively, and ρ_s (g cm^{-3}) is the dry soil bulk density, usually determined from soil samples.

Baatz et al. (2015) extended the formula of Bogena et al. (2013) to include above ground biomass (see also Section 2.6). In case of high biomass (e.g. forest) or changes in biomass (e.g. cropped fields) a biomass correction is needed to obtain soil moisture estimates from neutron count measurements. In this formula, the $N_{0,AGB=0}$ parameter represents conditions without biomass ($AGB = 0$; Eq. 2.3):

$$(2.3) \quad \theta = \frac{\alpha_0 \cdot \rho_s}{N_{AGB-corr.}/N_{0,AGB=0} - \alpha_1} - \alpha_2 \cdot \rho_s - lw - w_{SOM},$$

where $N_{AGB-corr.}$ is the measured neutron count corrected for biomass (see Section 2.6 for correction function).

2.4.2 HMF method

The HMF method was first developed to avoid site-specific calibration of the CRNS where soil sampling is difficult and also to facilitate the application of the mobile cosmic-ray soil moisture sensors (i.e. rover applications, Section 2.10, Franz et al., 2013b). In such cases soil moisture could be calculated provided neutron intensity and other hydrogen sources are known. However, for sites for which reliable soil moisture samples can be obtained, the HMF method can also be used for site-specific calibration of the CRNS. In the HMF method, the epithermal-fast neutron intensity is calculated with Eq. (2.4):

$$(2.4) \quad N = N_s \cdot \{4.486e^{(-48.1 \cdot \text{hmf})} + 4.195e^{(-6.181 \cdot \text{hmf})}\},$$

hmf is $\Sigma(H)/\Sigma(E_{\text{all}})$; the total hydrogen molar fraction (mol H/total mol). $\Sigma(H)$ is the sum of all hydrogen (mol), including hydrogen in above ground biomass, lattice water hydrogen, hydrogen in and bound to soil organic matter, and soil water hydrogen. $\Sigma(E_{\text{all}})$ (mol) is the sum of all elements: atmospheric nitrogen and oxygen, soil solids (quartz), lattice water, soil organic matter water equivalent, soil water, above ground biomass (usually assumed to be cellulose, see Section 2.6) and water inside above ground biomass. N_s (cph) is a normalisation parameter which needs to be site-calibrated and is defined as the neutron count over a deep ($> 1 \text{ m}$) and wide ($\sim 500 \text{ m}$) water body. When the neutron count (N) is equal to N_s , the hydrogen molar fraction is $0.23 \text{ mol mol}^{-1}$. McJannet et al. (2014) adjusted the coefficient values based on the finding that 30% of the neutrons counted by the CRNS are actually thermalised neutrons, to 3.007, -48.391, 3.499, and -5.396 (coefficients from left to right in Eq. 2.4). The HMF method was, like the N_0 method, developed with MCNPx simulations, in which a range of observed soil chemistries and vertical pore water distributions were included. Validated with half a year of data from a distributed sensor network at one site and with soil and vegetation calibration data at 35 sites, Franz et al. (2013b) concluded the HMF function predicted more than 79% of neutron count variability at

every site. In their testing of the HMF method, McJannet et al. (2014) concluded that this formula can be especially useful at sites with high biomass, where, they argued, it could pose an advantage over the original N_0 method of Desilets et al. (2010). Baatz et al. (2015) however mentioned that a disadvantage of the HMF method is that the hydrogen molar fraction is bound by a maximum of 0.23 moles moles⁻¹. Baatz et al. (2014) and Franz et al. (2013b) showed the observed hydrogen molar fractions can exceed this value. Moreover, Franz et al. (2013c) showed hydrogen in high above ground biomass (e.g. trees) cannot be conceptualised as a water layer on top of the soil, due to the heterogeneous spatial distribution of hydrogen. Franz et al. (2013c) used the HMF method to estimate biomass at a resolution of $\sim 1\text{ km}^2$, provided soil moisture and other hydrogen pools were known. They expected this technique to be useful in multiple scientific disciplines, including hydrology and forestry, due to its non-destructive nature.

2.4.3 COsmic-ray Soil Moisture Interaction Code (COSMIC)

COSMIC was developed as a data assimilation forward operator³, and is a simpler, computationally less expensive (at least 50 000 times faster) neutron transport model than MCNPX (Shuttleworth et al., 2013; Rosolem et al., 2014). COSMIC considers three processes (Figure 2.6): (1) exponential decay of high-energy neutron intensity with depth, (2) creation of fast neutrons as a consequence of collisions with soil and water particles and (3) exponential decay of fast neutrons while they travel upward from the place where they were created. COSMIC can be written as follows (Eq. 2.5):

$$(2.5) \quad N = N_{COSMIC} \int_0^{\infty} \left[e^{-\left[\frac{m_s(z)}{L_1} + \frac{m_w(t,z)}{L_2} \right]} \cdot [\alpha \rho_s + \theta(t,z) + lw + w_{SOM}] \right. \\ \left. \cdot \frac{2}{\pi} \cdot \int_0^{\frac{\pi}{2}} e^{\left(\frac{-1}{\cos(\beta)} \right) \cdot \left[\frac{m_s(z)}{L_3} + \frac{m_w(t,z)}{L_4} \right]} d\beta \right] dz,$$

where $\beta(-)$ is a dummy variable representing a range of angles and $L_1 = 162.0(\text{gcm}^{-2})$, $L_2 = 129.1(\text{gcm}^{-2})$, and $L_4 = 3.16(\text{gcm}^{-2})$ are universal parameter values, and $L_3(\text{gcm}^{-2})$, $N_{COSMIC}(\text{cph})$, and $\alpha(-)$ are site dependent parameters. Likewise parameter HMF-parameter N_s , parameter N_{COSMIC} is defined as the count rate over water like parameter N_s of the HMF-formula, but is not inhibited by a drawback like the maximum hydrogen molar fraction value of N_s . The parameters m_w and m_s are the integrated mass per unit area (gcm^{-2}) of dry soil and water respectively and ρ_s and ρ_w are the dry soil bulk density and density of water (gcm^{-3}). The original model included soil moisture and lattice water (Shuttleworth et al., 2013), while Baatz et al. (2014) added soil organic matter water equivalent to this. Shuttleworth et al. (2013) found correlations between

³A forward operator is a computational model that has output from another model, for instance a land surface model, and produces output that can be directly compared with observations. Data assimilation is the process of combining model output and observations to obtain an improved estimate of the concerned state variable, in this case soil moisture content.

dry soil bulk density and parameters L_3 and α . The relationship for L_3 was especially strong ($r^2 = 0.98$), but the correlation of the relationship for α was considerably lower ($r^2 = 0.66$).

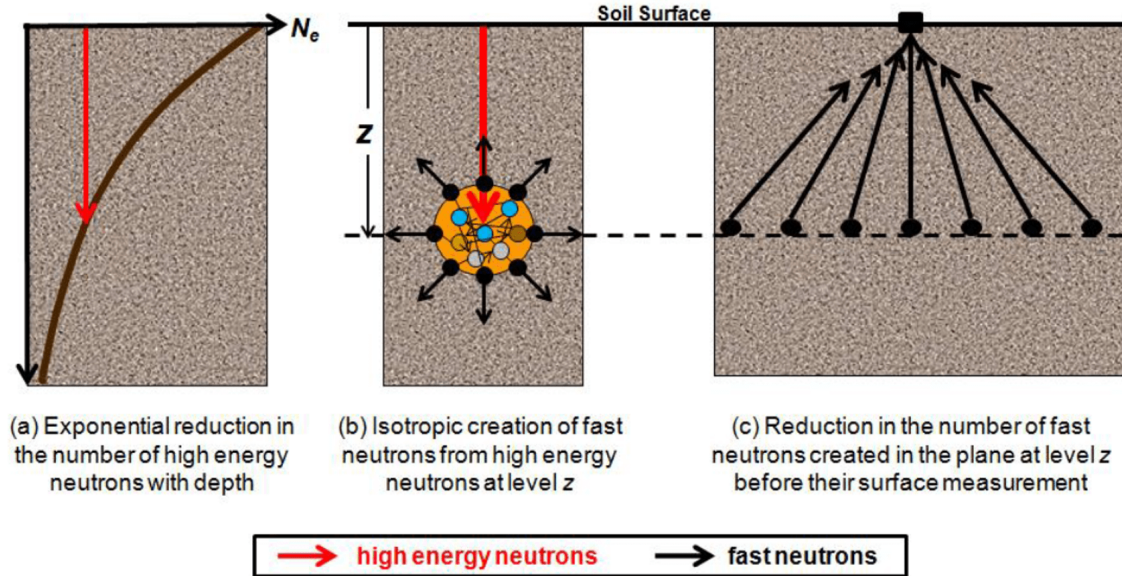


FIGURE 2.6. The three physical processes represented in the COSMIC model that are assumed to control the aboveground fast neutron count rate. Copied with permission from Shuttleworth et al. (2013).

Like the two other neutron – soil moisture models, COSMIC was developed with the help of MCNPx simulations (Shuttleworth et al., 2013). The model was calibrated at 42 sites, using MCNPx as well, in contrast to the other two models, which were site-calibrated with actual soil moisture observations. Baatz et al. (2014) however successfully calibrated COSMIC parameter N_{COSMIC} at ten German sites, while using the before mentioned relationships with dry soil bulk density for parameters L_3 and α .

Shuttleworth et al. (2013) validated COSMIC against neutron and soil moisture observations at a site in Arizona, showing good correspondence between the simulated neutron counts and the observed neutron counts. They tested the use of COSMIC in data assimilation with the Noah land surface model (Ek et al., 2003) at the same site. This resulted in removal of bias between model simulated and observed soil moisture. Rosolem et al. (2014) employed COSMIC to assimilate synthetic soil moisture observations in Noah at sub-kilometre scale and later studies used also real observations. These studies are discussed in Section 2.11.

2.4.4 Comparison of the three methods

In their comparison of the three neutron – soil moisture relationships presented in this chapter (N_0 , HMF, and COSMIC), Baatz et al. (2014) successfully calibrated each method at ten German sites with different soil properties, land use, above ground biomass, and meteorologi-

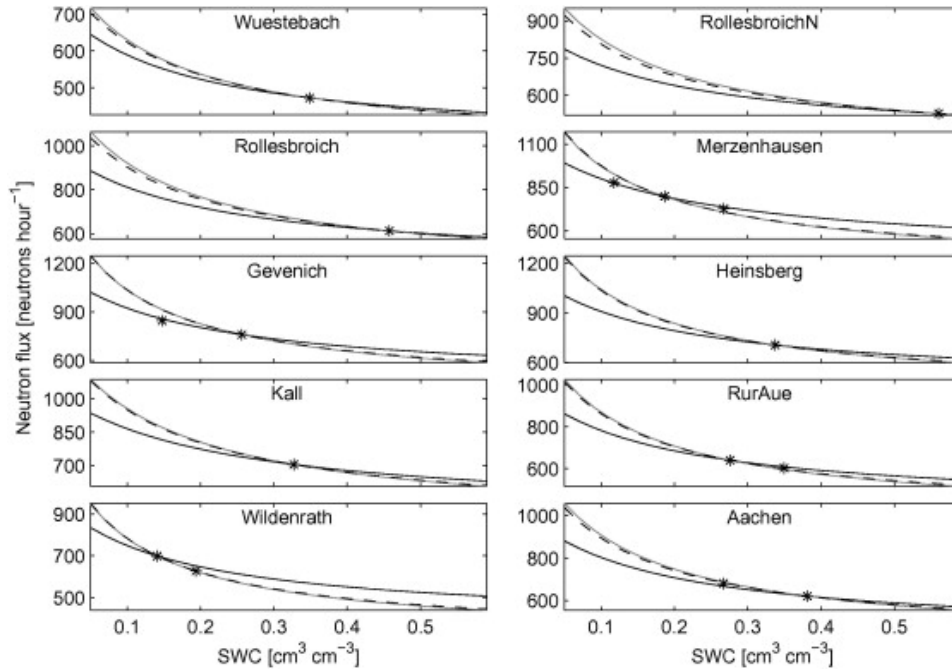


FIGURE 2.7. Calibration curves for ten CRNS sites in Germany. The N_0 method is shown in black, COSMIC is shown as dashed line, and the HMF method is shown as gray line. Copied with permission from Baatz et al. (2014).

cal conditions. The three methods performed similarly well and errors over validation periods ($\leq 0.033 \text{ cm}^3 \text{ cm}^{-3}$) were within the sensor measurement uncertainty. The HMF method and COSMIC yielded especially similar calibration curves (Fig.2.7). The three normalisation parameters (N_0 , N_s , and N_{COSMIC}) showed a strong correlation with above ground biomass in this study. Baatz et al. (2015) also compared the three parameterisations, this time for more CRNS stations in the Rur Catchment. They concluded all three models performed satisfactorily in this area.

In most studies so far the N_0 has been employed, due to its simplicity. The HMF method has not been used often since its development, possibly due to its greater complexity and the limitation of the maximum hydrogen molar fraction value. COSMIC has been used mostly in the context of hydrological modelling and data assimilation, which it was meant to be used for initially. In Chapter 3 of this thesis the COSMIC operator was used, while in Chapter 4 all three soil moisture – neutron parameterisations were evaluated, and in Chapter 5 the N_0 method and the COSMIC operator were used. In Chapter 5 the COSMIC operator was further developed to study the effects of different neutron mitigating factors on neutron count. The result was a model, named COSMIC2, that could be used beyond the context of hydrological modelling; namely to investigate the effects of different neutron mitigating factors on the CRNS measurement, through the means of sensitivity analysis.

2.5 Field calibration of the neutron – soil moisture relationships

As mentioned in Section 2.4.1, Section 2.4.2, and Section 2.4.3, the three neutron – soil moisture parameterisations need to be calibrated for each site separately. This can be done by taking soil samples within the CRNS footprint. The original field sampling strategy for the N_0 method was to take gravimetric soil samples at three to four depths between 5 and 25 cm depth at sixteen to twenty-four spots (Desilets et al., 2010). Franz et al. (2012b) calibrated a CRNS at a site in Arizona by spatially distributing eighteen soil sample points (six layers of 5 cm between 0 and 30 cm at each spot, yielding 108 soil samples per CRNS site) within the sensor footprint in such way that each location weighted the same towards the average. This approach was applied throughout the COSMOS network (Zreda et al., 2012) and has been a standard at other locations since (Bogena et al., 2013; Hawdon et al., 2014; Evans et al., 2016). As explained in further detail in Section 2.7.1, the knowledge of the CRNS footprint has improved and different sampling schemes have been applied.

If feasible, volumetric (i.e. the exact volume is known) samples are taken, or otherwise gravimetric samples are taken, of which the exact volume is not known. A reason to take gravimetric rather than volumetric samples is the presence of many stones, requiring a large Representative Elementary Volume (REV; Moene and Van Dam, 2014). Another reason is that soft or wet soils are possibly compressed inside the soil sampling corer, making it more difficult to obtain volumetric samples (Zreda et al., 2012). Volumetric samples are the preferred option because hydrological models and land surface models express water content in terms of volume. Assigning a field average dry soil bulk density or a dry soil bulk density from literature to compute volumetric water contents from gravimetric water contents can yield substantially different values compared to determining the volumetric water content in each sample directly. The soil samples are weighed first, then dried in a ventilated oven at 105 °C for 24 hours, and then weighed again, yielding the water content value for the sample.

Rivera Villarreyes et al. (2011); Heidbüchel et al. (2016); Lv et al. (2014) calibrated the three coefficients (a_0 , a_1 , and a_2) of the N_0 formula because the fixed shape that the predefined values of these parameters impose, were shown not to correspond with observations. In Chapter 4 of this thesis a similar approach was used. Later Köhli et al. (2015) and Schrön et al. (2017) found the incorrect shape of the N_0 equation to possibly be caused by incorrect spatial averaging of soil moisture samples. Therefore the original fixed parameter values were used in Chapter 5 of this thesis. It was originally assumed that a single calibration day was sufficient for the N_0 method because the shape was assumed to be known and hence only the position of the curve needed to be fixed by calibrating the single parameter N_0 (Desilets et al., 2010; Zreda et al., 2012). However, due to effects of other hydrogen pools on the neutron count rate (Section 2.6), calibrations at different moments could yield different positions of the curve (Fig. 2.8) or could

show the need for a different shape of the curve. Moreover, due to uncertainty in soil samples for all kinds of reasons (e.g. presence of many stones, loss of samples in the process, spatial heterogeneity in soil properties, insufficient number of soil samples) multiple calibration points could provide a better estimation of the curve position than a single calibration. The effect of more than one soil sampling point in time on the quality of the calibration of the three neutron – soil moisture parameterisations was tested in Chapter 4 of this thesis. Later, Heidebüchel et al. (2016) approached, for the N_0 method, the same problem in a different way. They combined different calibration days to obtain an estimate of the N_0 curve that better corresponded with the computed footprint average soil moisture at a sandy, forested site in Germany. Soil moisture contents computed with curves of the different individual calibration days were found to deviate up to $0.1\text{ m}^3\text{ m}^{-3}$. Using two different calibration days, from a dry day and from a wet day to redefine the shape of the curve did however yield satisfactory soil moisture estimates. Franz et al. (2016) recommended, based on results from a mixed agricultural site in North East Austria, three calibration days to calibrate the N_0 parameters. Lv et al. (2014) also recommended multiple calibration days for the N_0 method. Sigouin et al. (2016) did however not find an advantage of multiple calibration days at their Canadian site.

Dutta et al. (2012); Dutta and Terhorst (2013) proposed a different CRNS calibration method. They used a machine learning technique by training non-linear empirical equations to estimate soil moisture from CRNS neutron counts with limited ground truth data. The idea behind this technique is to remove the point-scale sensors at some moment and still be able to use the CRNS to estimate soil moisture.

2.6 Effects of other neutron mitigating factors

As mentioned in Section 2.1, primary cosmic-ray radiation intensity and secondary cosmic-ray high-energy neutron radiation intensity are decreased by multiple factors, varying in space and time (Desilets and Zreda, 2001b). Changes in the cosmic-ray and high-energy neutron intensity affect the epithermal–fast neutron count measured by a Cosmic-Ray Neutron Sensor and hence need to be accounted for to obtain a corrected neutron count time series that reflects the effects of soil moisture (Zreda et al., 2012).

2.6.1 Temporal and spatial variations in cosmic-ray intensity

Interplanetary magnetic fields and the Earth’s magnetic field control how much cosmic-ray radiation reaches our atmosphere (Blasi, 2014). When these magnetic fields are stronger, less cosmic-rays reach the Earth’s atmosphere. Examples are periods of increased solar activity, when less cosmic-rays reach the Earth due to magnetic fields travelling from the Sun (Desilets and Zreda, 2001a). Temporal changes in factors controlling cosmic-ray radiation also vary with our planet’s latitude and are thus also spatially variable (Desilets and Zreda, 2001b). The time scales

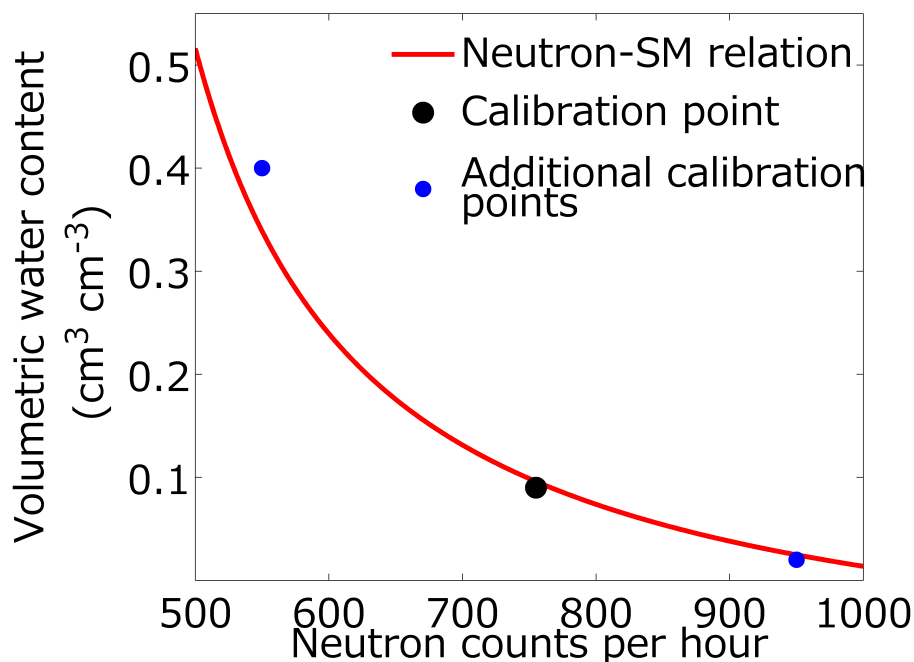


FIGURE 2.8. Schematic of N_0 -calibration curve and calibration points obtained from multiple soil sampling days. Different calibration points do not necessarily line up with a single calibration curve. Arbitrary values.

of the temporal variations vary from minutes to millennia. The temporal changes induced by these factors on the CCRNS counting rate can be corrected for using measurements from a high-energy neutron detector (Simpson, 2000). Such a sensor is for instance located at Jungfraujoch in Switzerland, which is used to correct the neutron counts of the COSMOS network. The measured epithermal-fast neutron count is divided over the intensity correction factor f_i (Eq. 2.6 Zreda et al., 2012):

$$(2.6) \quad N_i = N/f_i = N/(I_m/I_0),$$

where I_m is the high-energy neutron intensity measured at a certain time, I_0 is the intensity measured at a chosen reference date, N (cph) is the raw observed epithermal-fast neutron count, and N_i is the epithermal-fast neutron count corrected for temporal variations in high-energy neutron count (cph).

The shielding strength of the magnetic field of the earth for cosmic-rays varies with latitude and longitude (Desilets and Zreda, 2001a). It is stronger at the equator than at the poles and hence is the high-energy neutron intensity at the equator relatively lower. After primary cosmic-rays have managed to reach the atmosphere and high-energy neutrons are created, the chance of these high-energy neutrons actually reaching the Earth's surface is lowered with thicker or denser atmosphere because they can be stopped by atmospheric nuclei. At some places the

atmosphere is on average thicker or denser than at other places, meaning the long-term average atmospheric air pressure is higher. The global spatial variability in high-energy neutron intensity at a specific sensor site is corrected for effects from spatial variations in the geomagnetic field and the long-term average air pressure with a complicated mathematical procedure (Smart and Shea, 2001). The final local intensity correction factor is however easily computed (Eq. 2.7; Hawdon et al., 2014):

$$(2.7) \quad f_{i,scaled} = (F_i - 1) \times R + 1,$$

where $F_{i,ref}$ is the intensity correction factor (Eq. 2.6 at the reference site, for instance Jungfraujoch), R is a correction factor for latitude and altitude (for instance 0.931 in South England), and $f_{i,scaled}$ is the final local intensity correction factor. This correction factor ($f_{i,scaled}$; Zreda et al., 2012), over which the measured neutron count is divided, is assumed temporally constant over a period of five years (<http://cosmos.hwr.arizona.edu/Util/rigidity.php>) and hence needs to be obtained only once every five years for an individual site.

Within site variation of the local intensity correction factor has been shown to vary significantly; for instance from ~0.95 to 1.15 (Evans et al., 2016) and ~0.86 to 1.22 (Hawdon et al., 2014). Hawdon et al. (2014) tested the effect on the neutron intensity correction factor from using different high-energy neutron detectors. They evaluated the sensor at Jungfraujoch, versus using the high-energy neutron detectors located closest to their Australian sites, and they included their own neutron detector at Kingston in Tasmania. The overall high-energy neutron intensity trends were similar, but the variability (size of peaks) differed between the different detectors. The different neutron intensity correction yielded differences in estimated soil moisture up to $0.015 \text{ cm}^3 \text{ cm}^{-3}$.

2.6.2 Atmospheric pressure

Atmospheric air pressure changes over time and this affects the high-energy neutron intensity. The measured epithermal–fast neutron count at the Earth’s surface decreases exponentially with increasing atmospheric pressure, because more particles were in the neutron’s downward pathway. The measured epithermal–fast neutron count can be corrected for changes in atmospheric pressure by multiplying the measured count with the factor f_p (Eq. 2.8 Zreda et al. (2012) and Bogena et al., 2013):

$$(2.8) \quad N_p = N \times f_p = N \times \exp\left(\frac{P - P_0}{L}\right),$$

where P_0 is a reference atmospheric pressure, for instance the site long term average atmospheric pressure or mean atmospheric pressure at sea level (1013.25 hPa), P is the measured atmospheric pressure (hPa), and L is the mass attenuation length⁴ of high-energy neutrons for dry air in

⁴The attenuation length of a certain type of radiation, for instance neutron radiation (for a certain material with a certain mass density) is a measure of how far a radiation particle can travel before being effectively stopped.

unit gcm^{-2} . Values for L vary between $\sim 128 \text{ gcm}^{-2}$ at high latitudes and 142 gcm^{-2} at low latitudes (Desilets and Zreda, 2001b). N_p is the atmospheric pressure variation corrected neutron count (cph); this would be the neutron count measured had the atmospheric pressure been the same as the reference atmospheric pressure. Differences in altitude between sites can be taken into account in this correction factor by using a single reference pressure value. Due to the exponential relationship, atmospheric pressure changes have a relatively large effect on the measured neutron counts (Zreda et al., 2012; Baatz et al., 2014). Within site variation of the pressure correction factor has been shown to range from for instance ~ 0.80 to 1.20 (Hawdon et al., 2014), and from ~ 0.75 to 1.30 (Evans et al., 2016). Air pressure is therefore always measured at a Cosmic-Ray Neutron Sensor site.

2.6.3 Effects of different hydrogen pools on fast neutron intensity

As described in Section 2.3 hydrogen is the most important element in moderating epithermal-fast neutron radiation intensity. Hydrogen is not only present as soil moisture, but in any other type of water, for instance as surface/ponding water and water in the atmosphere. Hydrogen is also present in other molecules, especially in organic molecules, which constitute an important ($\sim 40\%$) share of both dead and living biomass (Franz et al., 2013a). Besides hydrogen also other atoms like nitrogen, oxygen, and carbon can importantly affect the epithermal-fast neutron radiation (Zreda et al., 2008; Köhli et al., 2015). Carbon, which is abundant near the land surface in the form of biomass, is an important factor. However, carbon is in case of biomass proportionally present with respect to hydrogen (organic molecules contain both), and has therefore not been considered explicitly in most CRNS studies (Franz et al., 2013a; Bogena et al., 2013). For the same reason carbon is not explicitly considered in the methods employed in this thesis. In the following sections the relevance of different hydrogen pools on the CRNS signal is discussed.

2.6.3.1 Atmospheric water vapour

Water is present in the atmosphere in the form of water vapour. Rosolem et al. (2013b) investigated the effects of atmospheric water vapour on the CRNS measured neutron count using both MCNPx simulations and observations at two sites in the US. Fast neutron intensity changed over a range of up to 24% for a water vapour content range of 0 to 23 gm^{-3} based on global observations at the land surface. A change in atmospheric humidity of 23 gm^{-3} was found to change the neutron intensity as much as a change of $0.10 \text{ m}^3 \text{ m}^{-3}$ in soil moisture content would do. Rosolem et al. (2013b) developed a correction factor to correct for temporal changes in atmospheric water vapour content, which needs to be multiplied with the measured neutron count (Eq. 2.9):

$$(2.9) \quad N_h = N \times fh = N \times (1 + 0.0054 \times (\rho_v - \rho_{v,ref})),$$

where ρ_v is the measured absolute humidity (gm^{-3}) and $\rho_{v,ref}$ is a reference absolute humidity, often set to dry air (0 gm^{-3}). N_h is the atmospheric humidity corrected neutron count (cph). To

obtain absolute humidity values for this correction function, relative humidity RM (%) and air temperature T (°C) are measured at Cosmic-Ray Neutron Sensor sites. From these measurements absolute humidity ρ_v can be computed (Eq. 2.10):

$$(2.10) \quad \rho_v = 1000 \times \frac{e_a \times 100}{461.5 \times (T + 273.15)},$$

where e_a is the vapour pressure in hPa:

$$(2.11) \quad e_a = e_s \times \frac{RH}{100},$$

where e_s is the saturation vapour pressure in hPa:

$$(2.12) \quad e_s = 6.112 \times \exp \frac{17.67 \times T}{243.5 + T}.$$

Equation 2.9 can be used when air temperature and relative humidity measurements near the land surface are available, which is the case at CRNS sites. If vertical atmospheric water vapour profile measurements over tens of metres are available, a similar equation from Rosolem et al. (2013b) can be used. This equation, which is not shown here, yields similar correction function values, with a maximum difference of ~ 0.03 compared to Equation 2.9. Rosolem et al. (2013b) found Equation 2.9 to give sufficiently accurate estimates even under temperature inversion conditions in the atmosphere. Baroni and Oswald (2015) however found a significant day-night cycle in neutron counts at a cropped field in Germany. They attributed this, besides to vertical redistribution of water in the soil-biomass system, to redistribution of water in the lower atmosphere. They recommended to further study these patterns and to revisit the assumption by Rosolem et al. (2013b) of a standard atmosphere with neutral stability. Measurement errors in relative humidity and air temperature observed near the land surface could propagate to errors in CRNS soil moisture estimates of up to one order of magnitude less than the effect from atmospheric water vapour on the signal. Value ranges for absolute humidity observed at CRNS sites are $3 - 15 \text{ gm}^{-3}$ (Evans et al., 2016) and $1.8 - 24 \text{ gm}^{-3}$ (Hawdon et al., 2014), corresponding to correction factor values of 0.98 to 1.04, and 1.01 to 1.13, respectively. Within site changes in measured neutron count due to changes in atmospheric water vapour content are hence usually smaller than neutron counts changes due to changes in atmospheric pressure and high-energy neutron intensity.

The presented corrections for sensor counting efficiency, high-energy neutron intensity, atmospheric pressure, and atmospheric water vapour content are usually applied in series, yielding the corrected neutron count N_{epih} (Eq. 2.13):

$$(2.13) \quad N_{epih} = N \times fe \times fp/f_{i,scaled} \times fh,$$

2.6.3.2 Lattice water

Below the land surface not only soil moisture affects the epithermal–fast neutron intensity measured by the above ground Cosmic-Ray Neutron Sensor. A hydrogen pool present in most

soils (Desilets et al., 2010) is so-called interstitial water, also called lattice water. This water is so strongly bound to soil particles that it is actually part of the solid phase and is therefore immobile (it does not move under the force of hydrostatic pressure differences; Hoogsteen et al. (2015); Grim (1953) and Zreda et al., 2012). Such water is especially present in clay soils, where it is found strongly bound in-between clay sheets and as hydroxyl groups that are actually part of clay minerals (Hoogsteen et al., 2015; Grim, 1953). Water can also be present bound to carbonates and hydrated salts, which can be found in chalk soils and sodic soils respectively (Hoogsteen et al., 2015).

The lattice water content can be determined with different laboratory procedures, depending on the soil chemistry. One common approach is to ignite dry soil samples at 1000 °C (Loss on Ignition; LOI) after the soil sample was dried at 105 °C for 24 hours to remove unbound water. Other methods include using an Elemental Analyser (possibly in combination with LOI); a device which measures the abundance of different elements in a (soil) sample, in this case hydrogen (e.g. Bogen et al. (2013) and Franz et al., 2013a). Lattice water content can be expressed in the same unit as soil moisture (gravimetric water content $\text{g water g soil}^{-1}$ or volumetric water content $\text{m}^3 \text{ water m soil}^{-3}$) and can be treated in a similar way in a neutron count – soil moisture relationship as shown for the N_0 method in Section 2.4.1.

Lattice water content has been shown to vary from approximately zero (quartz rich soils) to 0.07 g g^{-1} (e.g. clay rich soils) at most COSMOS sites (Zreda et al., 2012), COSMOS-UK sites (Evans et al., 2016), and Terrestrial ENvironment Observatory sites (TERENO, Baatz et al. (2014), Sec. 2.9). Three COSMOS sites on Hawaii exceeded the value of 0.07 g g^{-1} , with a value of 0.21 g g^{-1} in the soil of site Island Dairy, due to the volcanic ash origin of the soil (Zreda et al., 2012). The quartz rich soil at site Gngangara of the Australian CosmOz network had a lattice water as low as zero and the sodic soil of the Tullochgorum site had a lattice water content as high as 0.27 g g^{-1} (Hawdon et al., 2014). Lattice water is often associated with clay soils, but it can also be a significant hydrogen pool in peat, as reported by Sigouin et al. (2016) for a Canadian site where the peat contained 0.05 g g^{-1} . The effect of the presence of lattice water on the CRNS neutron count signal and the derived soil moisture measured is shown in Fig. 2.5. When more lattice water is present, the neutron count is lower at the same soil moisture content. This shifts the curve to the left (from point A to point B in Fig. 2.5).

2.6.3.3 Soil organic matter

Soil organic matter contains hydrogen within its organic molecules. A way to incorporate the effects of this hydrogen is to compute a water-equivalent from measured Soil Organic Carbon (SOC) or Soil Organic Matter (SOM) values. Water equivalent values are used for the N_0 method and for COSMIC, while in the HMF method hydrogen is represented instead. The organic matter water equivalent is commonly calculated under the assumption that organic matter consists of cellulose (Franz et al., 2013b), with chemical formula $\text{C}_6\text{H}_{10}\text{O}_5$, where C is carbon, H is hydrogen,

and O is oxygen. Based on this assumption soil organic matter has a water equivalent of 56% on mass base.

There are different methods to determine the SOC or SOM content in soil samples. Which method is used depends on the availability of resources and on soil characteristics. Likewise lattice water, an Elemental Analyser can be used to determine total carbon content, from which the organic carbon content can be computed if also the CO₂ content is retrieved with the Elemental Analyser (Franz et al., 2013b). A cheaper and simpler method is, like for lattice water, the Loss On Ignition (LOI) method. In the case of organic matter determination the LOI method involves the burning (ignition) of soil samples at a temperature between ~400 and 800 °C, after evaporation of all water at a temperature of 105 °C. At those high temperatures organic molecules are lost from the sample but other soil particles are assumed to remain. In practice however, a certain amount of lattice water is lost and usually a correction factor is applied based on the soil clay content (Grim, 1953; Howard and Howard, 1990; Hoogsteen et al., 2015). The last step of the LOI laboratory procedure is to determine the weight loss from which the soil organic matter content can be determined. To obtain SOM, SOC, and water equivalent values expressed per unit volume of soil a dry soil bulk density value is needed.

Soil organic matter/carbon water equivalents differ substantially between different soils. At the COSMOS sites originally presented by Zreda et al. (2012) the average SOC was 0.016 gg⁻¹. The lowest recorded SOC value of 0.001 gg⁻¹ was in the sandy soil of site 'OS-beach' and the highest value of 0.061 gg⁻¹ was found in the forest soil of Harvard Forest. Evans et al. (2016) recorded a similarly high value of 0.059 gg⁻¹ in the organically managed grassland soil at the COSMOS-UK Sheepdrove Farm site. The three other original COSMOS-UK sites had SOC values around 0.03 gg⁻¹. Hawdon et al. (2014) reported SOM values for Australian sites, which varied from 0.002 gg⁻¹ to 0.059 gg⁻¹. These values correspond with relatively low SOC values of 0.0009 gg⁻¹ to 0.026 gg⁻¹. Sigouin et al. (2016) found a high average Soil Organic Carbon (SOC) content of 0.12 gg⁻¹ at a Canadian site with a mixed soil that included peat and sand among other materials.

2.6.3.4 Plant roots

The hydrogen contained within dry plant root biomass and liquid water inside plant roots has not been quantified as often as soil organic matter and lattice water. There are two main reasons for this. Firstly plant roots are difficult to sample and the obtained values are relatively inaccurate due to the complex methods and spatial heterogeneity (e.g. Baatz et al., 2014). These methods often involve washing roots from soil samples, resulting in a loss of many small roots. Secondly, it is usually present in substantially smaller amounts than for instance soil organic matter. For instance, Bogena et al. (2013) found plant roots at a German forest site to contain a water equivalent of about 0.015 cm³ cm⁻³. This was small compared to soil organic matter (0.048 cm³ cm⁻³) at the same site, but similar to the lattice water content (0.012 cm³ cm⁻³). The

root biomass water equivalent can be computed under the same assumption used for soil organic matter; that the roots consist of cellulose. In the research presented in Chapter 5 of this thesis root samples were taken and the contribution to the CRNS measured signal was discussed.

2.6.3.5 Organic litter layer

Few studies have investigated the effects of organic litter layer on CRNS measurements. At many sites no significant litter layer is present (e.g. on farmland, in dry ecosystems). In forests however, a substantial litter layer is often present. Bogena et al. (2013) found the litter layer in a German forest to contain a larger share (36 %) of the hydrogen within the CRNS footprint than soil moisture (21 %) for wet soil conditions. This hydrogen was mostly water intercepted by the litter layer and Bogena et al. (2013) was able to improve the soil moisture estimate by modelling water transport within this layer using HYDRUS1D (Šimunek et al., 2008).

2.6.3.6 Ponding water and surface water

Ponding water and surface water have received some attention from CRNS studies. Some studies used a land–water interface to study the CRNS footprint size (Köhli et al., 2015) and other studies reported effects of ponding water, some caused by (flooding) irrigation. At one site in Australia, Montzka et al. (2017) found ponding water to cause discrepancies between CRNS and satellite soil moisture data, indicating the local effects of ponding water on the CRNS signal. Significant effects from ponding water on the CRNS measured signal were reported by Jiao et al. (2014); Zhu et al. (2015) for a dry but flood–irrigated site in the Heihe region of China. Compared with soil moisture estimates from a wireless point-scale sensor network, the Root Mean Squared Deviation⁵ was $0.037\text{cm}^3\text{cm}^{-3}$ during irrigated periods, whereas it was $0.028\text{cm}^3\text{cm}^{-3}$ during non-irrigated periods. This difference was attributed to the flood-irrigation. Zhu et al. (2015) however concluded that despite the effects from additional hydrogen pools like ponding water and vegetation, the CRNS proved to be a robust method for use in irrigated areas.

2.6.3.7 Snow

Desilets et al. (2010) did some pioneering work to investigate the effect of snow cover on the CRNS signal. They found good agreement between CRNS Snow Water Equivalent (SWE⁶) estimates and independent snow measurements. In a wider study on the quality of snow measurements

⁵The Root Mean Squared Deviation (RMSD) and Root Mean Squared Error (RMSE), are both defined as the square root of the mean of the squared differences between two quantities $\sqrt{\text{mean}((A - B)^2)}$. RMSE usually refers to the difference between measurements and simulated values but the term is often used in relation to two different observations. In this case the mathematically identical Root Mean Squared Deviation (RMSD) is often reported. In practice the two terms are used interchangeably.

⁶Snow Water Equivalent (SWE) is the water layer, usually expressed in millimetres, if the snow was melted. It is a quantity that can be measured directly with certain equipment.

Rasmussen et al. (2012) reported good agreement between estimates from the CRNS and independent measurements with a Root Mean Squared Error (RMSE) of 5.1 mm. Sigouin and Si (2016) used a CRNS installed in Canada to establish a relationship between CRNS neutron counts and Snow Water Equivalent (SWE). Soil moisture underneath the snow layer was found to affect the CRNS snow estimates. To correct for this they advised to measure the soil moisture content just before the onset of snow cover, at the beginning of winter. They reported overestimated SWE by the CRNS during substantial snow melt periods. The fit with independent snow measurements had an RMSE of 7.5 to 8.8 mm SWE, similarly to Rasmussen et al. (2012). This compared advantageously with more traditional, large scale SWE estimates which typically have RMSE values between 24 and 77 mm. The knowledge developed could also prove useful to design a snow correction function to estimate soil moisture content.

Tian et al. (2016) used the ratio between thermal and fast neutron counts to estimate SWE. The thermal/fast ratio correlated well with SWE and including a snow correction based on the thermal/fast ratio improved soil moisture estimation compared to TDR sensors from $0.097 \text{ cm}^3 \text{ cm}^{-3}$ to $0.039 \text{ cm}^3 \text{ cm}^{-3}$.

Currently periods with snow cover are removed from time series when soil moisture content is studied. Improved knowledge could possibly facilitate these periods to be kept by applying a snow correction function.

2.6.3.8 Above ground biomass

Above ground vegetation has received significant attention in CRNS studies (e.g. Rivera Villarreyes et al. (2011); Franz et al. (2013b,c); Bogena et al. (2013); Baatz et al. (2014, 2015); Coopersmith et al. (2014); Baroni and Oswald (2015) and Heidbüchel et al., 2016). Vegetation contains hydrogen within its dry biomass as well as water inside. Changes in these hydrogen pools vary differently over time. Biomass can be relatively constant in time, for instance in established forests, or it can vary more quickly, for instance on agricultural lands. Rivera Villarreyes et al. (2011) and Hornbuckle et al. (2012) were some of the first to look at the effects of above ground biomass on the CRNS signal. They however drew different conclusions for cropped fields. Rivera Villarreyes et al. (2011) concluded that crop biomass did not substantially affect the CRNS signal but hypothesised this could be different in, for instance, forests. Hornbuckle et al. (2012) on the other hand, found fresh above ground biomass changes in the order of 1 kg m^{-2} in a maize field to significantly affect the neutron count. Bogena et al. (2013) found dry above ground biomass to contain 39–48 % of hydrogen within the CRNS footprint in a German coniferous forest. These values corresponded with a wet above ground biomass value of 68 kg m^{-2} (Baatz et al., 2014). Heidbüchel et al. (2016) found similar values for the contribution to total hydrogen for dry above ground biomass (50–65 %) at a deciduous forest with ~35 % coniferous trees and grass. They could not find effects of seasonally varying hydrogen in above ground vegetation on neutron counts and CRNS calibration results. At a heterogeneous cropped field, Coopersmith et al.

(2014) were able to decrease the RMSD between CRNS soil moisture estimates and those from a distributed sensor network from about $0.04 \text{ cm}^3 \text{ cm}^{-3}$ to $0.03 \text{ cm}^3 \text{ cm}^{-3}$ by using Leaf Area Index (LAI) estimates to correct neutron counts with an empirical linear function. Baroni and Oswald (2015) concluded that at a sunflower, maize, and winter rye cropped German site with a relatively dry soil ($0.05 - 0.20 \text{ cm}^3 \text{ cm}^{-3}$), fast biomass growth strongly affected the CRNS measured signal. In addition to these effects they observed effects on measured neutron counts with a higher temporal resolution from crop water stress.

Tian et al. (2016) used the ratio between thermal and fast neutron counts to estimate above ground Biomass Water Equivalent (BWE). Their results showed above ground biomass to affect the thermal/fast neutron count ratio substantially more than soil moisture did. They therefore argued the thermal/fast neutron count correction method could improve CRNS soil moisture estimates significantly. Avery et al. (2016) mentioned that fast-growing crops, grassland, and forest mainly affect the CRNS neutron counts with the water contained in them, more than with the hydrogen in the dry biomass. They also concluded that effects on the CRNS measured signal from relatively small changes in above ground biomass ($\sim 1 \text{ kg m}^{-2}$) are nearly indistinguishable from noise. Correspondingly, Franz et al. (2016) found relatively small changes ($\sim 1.8\%$) in parameter N_0 between sites with different land uses and vegetation conditions consistent with biomass changes of less than 2 kg m^{-2} . Results from Sigouin et al. (2016) seemed to correspond with this. Despite obvious vegetation growth between their calibration of the N_0 -formula in one summer and validations a year later, no obvious biomass effect was noticed. This was possibly caused by the drier soil conditions or by the still relatively small biomass.

Hawdon et al. (2014) evaluated the effects of biomass at their Australian sites and established a non-linear relationship between parameter N_0 and biomass. Their relationship showed a strong change in N_0 for a change in biomass from 0 to 8 kg m^{-2} . This finding contrasted with results from Baatz et al. (2015); Avery et al. (2016); Franz et al. (2016); Sigouin et al. (2016) that showed limited effects from small biomass changes. Baatz et al. (2015) found a linear relationship between parameter N_0 and above ground biomass. They found a reduction in neutron counts of $0.9\% \text{ kg}^{-1}$ of dry biomass increase and $0.5\% \text{ kg}^{-1}$ Biomass Water Equivalent (BWE) increase. The uncertainty at small biomass amounts ($< 5 \text{ kg m}^{-2}$) was however large.

2.6.3.9 Water intercepted by above ground vegetation

Heidbüchel et al. (2016) found vegetation intercepted water to contribute significantly to the total hydrogen and together with water intercepted in the soil litter layer, this contribution was up to 5%. Baroni and Oswald (2015) investigated the effects of intercepted water in a sunflower / winter rye field. Intercepted water affected the neutron count during rain events, with maximum intercepted water contents of 6 mm (or kg m^{-2}) in sunflower and 4 mm in winter rye. They observed daily fluctuations of up to 1.5 mm in CRNS SM estimates, partly attributed to rainfall interception.

2.6.3.10 Animals

No scientific papers on the effects of animals on the CRNS signal have been published. The only instance of research on this topic was when researchers installed a CRNS at the venue of the ‘Fall Meeting’ of the American Geophysical Union in San Francisco, December 2006 (Desilets et al., 2007). The sensor was used to count the number of people at the venue over time. Animals contain hydrogen, for instance in the form of body water. It is difficult to measure the effect of animals, for instance sheep or cattle, on the neutron radiation in a field because they move. Tracking the animals is probably not feasible in many cases.

2.6.4 The relative contributions from different hydrogen pools at different sites

The CRNS was developed at sites with favourable conditions, with limited additional hydrogen pools besides soil moisture. To see if the method was also suitable under rather unfavourable conditions like a forest in a humid climate, Bogen et al. (2013) tested the uncertainty of the sensor in their ‘worst case scenario’ study. They analysed the contributions from different hydrogen pools on the CRNS measured neutron count in a forest in Germany. Depending on soil wetness conditions, different hydrogen pools contributed differently to the total hydrogen amount within the CRNS footprint (Fig. 2.9). Under wet conditions the litter layer contained most hydrogen (36%) and under dry conditions soil moisture (31%) contributed most towards the total hydrogen, although followed closely by water intercepted in the canopy (27%). Quantifying the relative contributions towards the total hydrogen pool is just an indicator of the relative effects on the neutron counts. A more accurate approach could take into account the spatial distributions of different hydrogen pools (i.e. an organic litter layer has a different distribution and effect than trees biomass). Therefore, in Chapter 5, COSMIC2 was used to study the relative effects of different hydrogen pools on CRNS neutron counts and the accuracy and precision of the CRNS neutron count and soil moisture estimates (see Section 2.8 about accuracy and precision). Baroni and Oswald (2015) concluded, based on their study on biomass changes and rainfall interception in a cropped field, that all hydrological processes in the soil-vegetation-atmosphere continuum need to be considered to properly evaluate the CRNS signal. They used the N_0 method and represented all additional hydrogen pools as an additional water layer in the soil. They employed a so-called scaling approach to do this, in which CRNS footprint average soil moisture was estimated from soil moisture measured with one point-scale profile. They used knowledge of the hydrogen pools on specific days to establish a linear relationship between the two.

Below the ground, either lattice water or soil organic matter is usually the largest hydrogen pool after soil moisture (Zreda et al., 2012; Franz et al., 2013b; Hawdon et al., 2014; Evans et al., 2016). Which of these two is more important differs between sites, with soil organic matter often high in forest soils and lattice water highest in clay soils and especially in volcanic and sodic soils. The lattice water range reported (zero – $0.27 \text{ cm}^3 \text{ cm}^{-3}$) was larger than the water equivalent

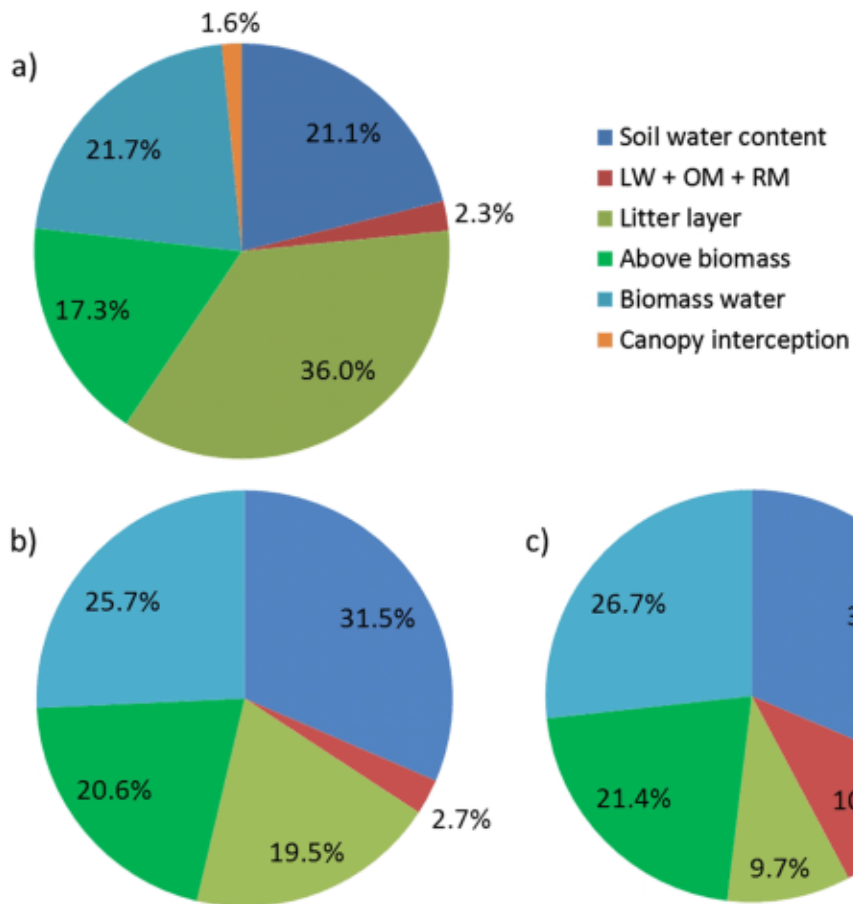


FIGURE 2.9. This figure from Bogaena et al. (2013) shows the relative contributions to the total hydrogen at three wetness levels in the German Wüstebach forest. *a* maximal wetness, *b* average wetness, *c* driest conditions. OM is organic matter, LW is lattice water and RM is root biomass. Copied with permission.

of the soil organic matter range ($0.001 - 0.077 \text{ cm}^3 \text{ cm}^{-3}$ water equivalent) reported. Lattice water and soil organic matter content affect the neutron counts in a similar way because they are distributed similarly within the CRNS support volume. Differences in vertical distribution exist, with soil organic matter content in many soils being higher near the surface than in the subsoil. Another below ground hydrogen pool discussed is plant roots. This hydrogen pool has been investigated less due to the difficult sampling process Baatz et al. (2015). In cases where it has been investigated it was found to be of less importance than lattice water and soil organic matter (e.g. Bogaena et al., 2013).

2.7 Cosmic-Ray Neutron Sensor footprint and measurement depth

The soil volume measured by a CRNS placed within a few metres above the ground is characterised by its horizontal areal dimension and by its vertical depth dimension. The horizontal dimension is often referred to as the *footprint*. The vertical dimension is usually conceptualised with the term *measurement depth*. Both dimensions have been an important topic of debate in the CRNS community (Desilets and Zreda, 2013; Franz et al., 2013a; Köhli et al., 2015). Due to these developments the support volume size is now known to be smaller than originally thought Köhli et al. (2015). The exact support volume size is especially important when, among others, soil, land cover, topography conditions are strongly spatially heterogeneous (Franz et al., 2013a). In this section the footprint is discussed first and then the knowledge of the measurement depth is presented.

2.7.1 Footprint

Zreda et al. (2008) derived a first estimate of the footprint size using MNCPx. The footprint size is defined as the area from which 86 % of neutrons originates. They found the footprint size not to depend on soil moisture content, but it was found to be inversely proportional to atmospheric pressure. Between sea level and an altitude of ~3000 m the footprint size was found to increase with about 25 %. The diameter of the circular footprint at sea level was found to be ~670 m at sea level (Zreda et al., 2008). The relative contribution of neutrons that reach the CRNS decreases non-linearly with distance from the sensor and can best be described mathematically with an exponential function. This property of the CRNS measured signal is depicted in the top panel of Figure 2.10. The (mathematically approximate) exponential decrease in relative influence with distance is the basis for the standard CRNS calibration soil sampling scheme of the COSMOS network (Zreda et al., 2012). In this scheme soil samples are taken at such spatial interval that each point has the same weight towards the CRNS measured signal (Fig. 2.11). The circular area around the sensor is divided by six radii (every 60 degrees) and circles at 25, 75, and 200 m from the CRNS. At each radius – circle intersection one of the eighteen sampling points is located.

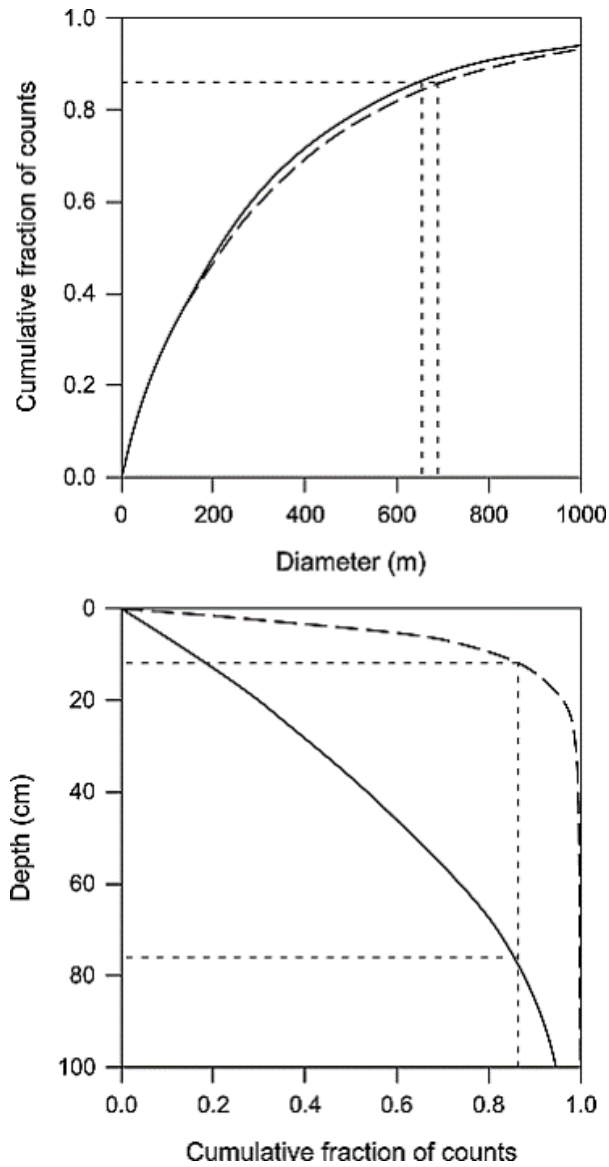


FIGURE 2.10. This figure from Zreda et al. (2008) shows the relative contributions of neutrons originating from different distances (top panel) and different depths (bottom panel). Copied with permission.

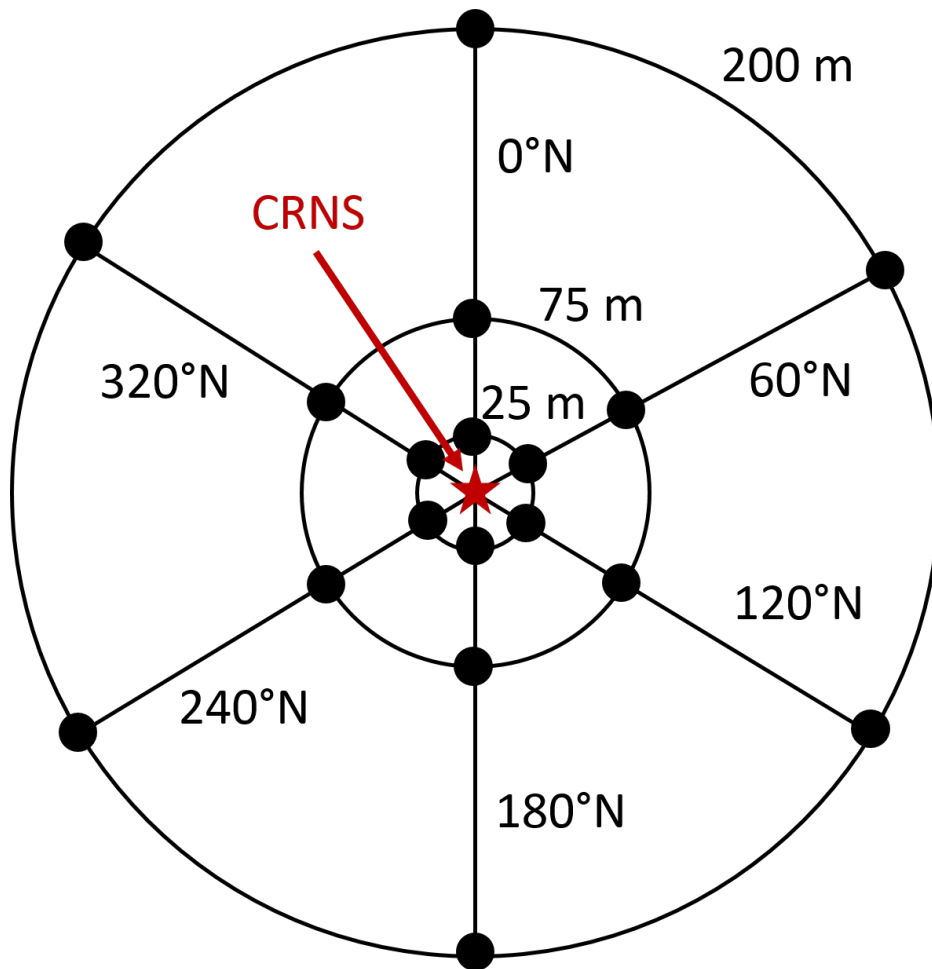


FIGURE 2.11. COsmic-ray Soil Moisture Observation System (COSMOS) standard soil sampling scheme (Franz et al., 2012b; Zreda et al., 2012). The sampling points are distributed such that, according to the knowledge at the time, each point has the same weight towards the CRNS measured signal (Franz et al., 2012b).

Desilets and Zreda (2013) investigated the footprint size in more detail and updated the estimated diameter slightly smaller at 600 m. They based their investigation on the assumption that free neutrons in the air can be modelled similar to a gas, as a diffusion process. The neutron intensity ϕ around a point source (from where fast-epithermal neutrons originate), at distance r from that point source is (Eq. 2.14; Desilets and Zreda, 2013):

$$(2.14) \quad \phi(r) = \frac{S_{pt}}{4\pi D} \times \frac{e^{-\frac{r}{L}}}{r},$$

where S_{pt} is the intensity at the source ($r = 0$), D is the diffusion constant, and L is the e-folding length that describes the fast-epithermal neutron mitigation due to de-acceleration and absorption. Two times L is equal to the radius of the area from which 86 % of neutrons reaching the CRNS originates. The implication of this theory is that neutrons travel randomly through the air and therefore the length a neutron travels after leaving the soil is on average 150 m in dry air at sea level. The effect of atmospheric pressure on L was quantified based on the assumptions, which implied the footprint size was mainly determined by the properties of air (Eq. 2.15):

$$(2.15) \quad L = L_0 \frac{P_0}{P},$$

where L_0 is the moderation length at reference pressure level P_0 (e.g. mean pressure at sea level), and P is the pressure. They confirmed the finding by Zreda et al. (2008) that the dependence of the footprint size on soil moisture content is small (5 % decrease in L). The effect of atmospheric humidity on the footprint was quantified at a decrease of 40 m diameter for every 0.01 kg kg^{-1} . Finally, Desilets and Zreda (2013) discussed the effect of the installation height of the CRNS on the footprint size. They concluded height differences of a few metres should not affect the footprint size substantially.

More recently Köhli et al. (2015) however found the horizontal footprint radius, based on modelling and observations, to be considerably smaller (86 % of neutrons originate 130 to 240 m from the CRNS). They found the footprint radius to be substantially affected by soil moisture content under humid climates when soil moisture is between 0.10 and $0.40 \text{ cm}^3 \text{ cm}^{-3}$ and when soil moisture content is below $0.03 \text{ cm}^3 \text{ cm}^{-3}$). Similarly, the radius decreased 10 m for each additional $4 - 6 \text{ gm}^{-3}$ atmospheric water vapour. The horizontal weighting of Köhli et al. (2015) is a function of mean soil moisture, mean soil organic matter, mean lattice water, mean plant root biomass etc., and relative humidity (Eq. 2.16):

$$(2.16) \quad W_r \approx \begin{cases} F_1 e^{-F_2 r} + F_3 e^{-F_4 r}, & r \leq 0.5 \text{ m} \\ F_5 e^{-F_6 r} + F_7 e^{-F_8 r}, & 0.5 \text{ m} < r \leq 50 \text{ m} \end{cases},$$

where the parameter functions F_i are dependent on atmospheric humidity and soil moisture and r is the radial distance from the CRNS (Köhli et al., 2015). The effects of atmospheric pressure, atmospheric water vapour, and vegetation on the footprint size were quantified. The conceptualisation of the effect of atmospheric pressure was practically the same as Equation 2.15.

The decrease of the footprint size with increasing atmospheric water vapour content as modelled by Köhli et al. (2015) did not differ substantially from earlier outcomes (Zreda et al., 2012; Desilets and Zreda, 2013; Rosolem et al., 2013b). The dependency of the footprint size on vegetation was captured with multiplication factor f_{veg} (Eq. 2.17):

$$(2.17) \quad f_{veg}(\theta) = 1 - 0.17(1 - e^{-0.41H_{veg}}) \times (1 + e^{-7\theta}),$$

where θ is the volumetric soil moisture content ($\text{cm}^3\text{cm}^{-3}$) and H_{veg} (m) is the vegetation height. This was however a first approximation based on modelling results and Köhli et al. (2015) therefore recommended to investigate the vegetation effect with observation based studies at sites with different vegetation conditions.

These new insights by Köhli et al. (2015) on the CRNS footprint size are based on different assumptions on how neutrons travel air and soil. They showed that the diffusion theory assumption by Desilets and Zreda (2013) was not valid for neutrons travelling through air. Moreover, assuming diffusive behaviour of neutrons in a single layer of air above the soil neglected the influence of soil on the neutrons, yielding too few soil – neutron collisions. According to Köhli et al. (2015), neutrons interact with the soil more often than hypothesised by Desilets and Zreda (2013). Köhli et al. (2015) also showed that defining the sensor footprint based on exponential decay Desilets and Zreda (2013) was not a valid assumption because the decay of influence with distance cannot be described by a simple exponential function. However, using any other value than 86 % would also be an arbitrary choice, so they kept this percentage as the footprint definition. Based on their results, Köhli et al. (2015) recommended to take more samples close (within 10 m) to the CRNS.

Multiple studies have addressed the footprint – spatial heterogeneity question from a more applied point of view, to accommodate for site specific conditions. Coopersmith et al. (2014) used so-called Voronoi diagrams to spatially interpolate point-scale network soil moisture to the CRNS footprint. The Voronoi method assigns weights to different locations according to how much of a total area (in this case the CRNS footprint) they represent. They used this method to circumvent disadvantages from other interpolation methods that suffer from the effects of sensor malfunctioning and from the too high weights attributed to sensors located close to each other. Baroni and Oswald (2015) used a linear relationship between a single point-scale soil moisture sensor profile and CRNS estimated soil moisture to have an independent soil moisture estimate without the need for an entire point-scale sensor network. Almeida et al. (2014) used a machine learning technique to determine CRNS within footprint spatial variability. Using the machine learning technique in combination with a network of point-scale soil moisture sensors allowed to remove the point-scale sensors at some moment but still be able to estimate within footprint spatial variability afterwards.

2.7.2 Measurement depth

Zreda et al. (2008) modelled the CRNS measurement depth, yielding a strong dependency on soil moisture content but no dependency on atmospheric pressure. The measurement depth was conceptualised similar to the horizontal footprint size; with an exponential decrease of the relative contribution to the above ground neutron count. The modelled measurement depth varied between 12 cm for wet soil and 76 cm for dry soil Franz et al. (2012a) studied the measurement depth in more detail. First of all their simulations showed that if a pure water layer of 5.8 cm covers the soil surface, 86 % of CRNS measured neutrons originates from this layer, so that the measurement depth does not reach the soil. They reported measurement depth z^* values similar to Zreda et al. (2008) with the formula they derived for uniform soil bulk density and soil hydrogen pools (Eq. 2.18):

$$(2.18) \quad z^* = \frac{5.8}{\theta_{tot} + 0.0829},$$

where θ_{tot} is the total water equivalent in the soil ($\text{cm}^3 \text{cm}^{-3}$). Based on HYDRUS1D modelling a non-uniform depth-weighting function was developed (Eq. 2.19):

$$(2.19) \quad wt(z) = a \times \left(1 - \frac{z}{z^*}\right), 0 \leq wt \leq z^*,$$

where a is a constant (Eq. 2.20):

$$(2.20) \quad a = \frac{1}{z^* - \frac{(z^*r)}{2z^*}},$$

where z^* is the measurement depth. This formula can be used to compute a depth-weighted average from independent soil moisture measurements at different depths (e.g. soil samples to calibrate a CRNS).

Bogena et al. (2013) developed a similar formula to compute profile average soil moisture contents with exponentially decreasing weights (w_s) with depth (Eq. 2.21):

$$(2.21) \quad w_s = 1 - e^{-\frac{z}{y}}$$

and

$$(2.22) \quad y = \frac{-5.8}{\ln(0.14) \cdot (H_p + 0.0829)},$$

where z represents the measurement depth (cm) and H_p represents the total below ground hydrogen pool in the respective soil layer in $\text{g H}_2\text{O cm}^{-3}$.

Köhli et al. (2015) also investigated the measurement depth of the Cosmic-Ray Neutron Sensor, and found measurement depths (15 – 83 cm) to be similar to those from Zreda et al. (2008) (12 – 76 cm). They took horizontal distance from the Cosmic-Ray Neutron Sensor into consideration and found the maximum measurement depth at 300 m from the sensor to be no

more than 46 cm instead of 83 cm just below the sensor. The measurement depth can be calculated as ((Köhli et al., 2015), Eq. 2.23):

$$(2.23) \quad D_{86}(r, \theta) = \rho_{bd}^{-1} (p_0 + p_1 \cdot (p_2 + e^{-r/100}) \frac{p_3 + \theta}{p_4 + \theta}),$$

where D_{86} is the maximum depth 86% of the detected neutrons reached. r is the radial distance from the CRNS, θ is the total volumetric soil water equivalent (including for instance soil organic matter), and ρ_{bd} is the dry soil bulk density. Parameters p_{0-4} are numerical parameters (Köhli et al., 2015). The vertical weight (W_d) for each point as distance r from the CRNS can be calculated as: (Eq. 2.24):

$$(2.24) \quad W_d(r, \theta) = e^{-2d/D_{86}(r, \theta)},$$

where d is the depth in *cm*.

Multiple studies on the effects of using different depth-weighting schemes and of different hydrogen pools on the measurement depth have been done. Franz et al. (2012a) reported a strong effect of shallow wetting fronts in sandy soils on the measurement depth based on simulations with non-uniform soil moisture profiles. Baroni and Oswald (2015) tested three different depth-weighting techniques (vertically varying weights, uniform weights, and taking the effect of above ground biomass into account), which yielded different measurement depths varying from 23 to 28 cm. Using vertically varying weights and taking into the account other hydrogen pools gave the best measurement depth estimates. The argued that a lower measurement depth percentage value (e.g. 63% instead of 86%) could avoid the need to elaborate the CRNS signal with vertical weights and make comparison with independent soil moisture measurements easier.

Measurement depth reported across the world vary with soil type and land cover type. Bogena et al. (2013) reported soil organic matter to importantly affect the measurement depth in a forest soil during high soil moisture content. Across their Australian sites, Hawdon et al. (2014) the measurement depth varied in both cases from 14 to 46 cm. Han et al. (2014) reported measurement depths of 10 to 20 cm for a cropped site in China. Sigouin et al. (2016) reported average measurement depth of 13 cm at a Canadian oil sand reclamation site with a soil that contained peat. Zhu et al. (2016) reported a rather deep measurement depth of about 31 cm on average at a dry high-altitude site in China.

2.8 Measurement quality and prediction error

The first research with the sensor was done at a relatively dry site with little vegetation in the San Pedro River Valley in Arizona, US (Zreda et al., 2008). Zreda et al. (2008) found a clear correlation with independent soil moisture measurements and with precipitation events. Since this first study the CRNS has been tested at many different sites and clear correlations with independent soil moisture measurements and precipitation have been found at locations across

different climates, land cover types, and soil types (e.g. Baatz et al. (2014)). Good agreement with independent co-located soil moisture measurements, from for instance distributed point-scale networks, can indicate good agreement with the actual areal average soil moisture content. It is then assumed that the distributed sensor network soil moisture estimate is sufficiently close to the *true* soil moisture content. When, under this assumption, a CRNS soil moisture time series is compared with a distributed sensor network average soil moisture time series, the measurement quality is mainly assessed on its accuracy. Accuracy indicates a systematic bias from the truth (or *target*; Fig. 2.12). High accuracy means the average of the estimates is close to the true value. Another indication of the measurement quality of a sensor is *precision*. Precision shows how spread out different estimates of the true value are. A high precision means the variation in estimates is small. The precision value can be used to determine how many digits of the (soil moisture) value should be displayed, because digits below the precision have no actual meaning. A measurement can have a high accuracy (so mean is close to the truth), but a low precision (large spread of the estimates) or vice versa.

As mentioned above, the performance of CRNS data can be assessed using other, co-located, soil moisture data. The RMSD is than often used to measure the performance. Whereas it is usually assumed the accuracy is thereby assessed, also precision contributes to the RMSD. The RMSD is computed over all timesteps of a timeseries. Splitting the RMSD (or MSD; see Section 3.2.2) of a timeseries between accuracy and precision is not straightforward. The main reason is that the bias component (which could be an indicator of accuracy) is computed as the difference between the mean values of the two timeseries. The difference between these two mean values would be equivalent to the accuracy only if the length of the timeseries would be one.

In Section 2.8.1 the accuracy of the CRNS will be addressed followed by a discussion on the precision in Section 2.8.2. In Chapter 5 the difference between the accuracy and precision of the CRNS are addressed. The effects of different neutron mitigating factors on both metrics are investigated for three humid sites with distinct soil and land-cover types, in England.

2.8.1 Accuracy

As mentioned, the accuracy of the CRNS has often been addressed by comparing its soil moisture estimates with the mean of co-located distributed sensor networks. Under favourable conditions high accuracies have been found. Franz et al. (2012b) for instance found an RMSD value of $0.011\text{ cm}^3\text{ cm}^{-3}$ at a dry, sparsely vegetated site in Arizona. Using a 12-hour moving average, Schreiner-Mcgraw et al. (2016) found, at two other semiarid sites in Arizona, RMSD values of $0.009 - -0.013\text{ cm}^3\text{ cm}^{-3}$. Under favourable conditions (i.e. relatively dry sites) for the CRNS technique at a Desert Steppe site in China, Pang et al. (2016) found high similarity between CRNS and colocated FDR network soil moisture (RMSD of $0.016\text{ cm}^3\text{ cm}^{-3}$). Zhu et al. (2016) investigated the accuracy of the CRNS under favourable conditions (4600 metre above sea level, relatively dry) at a Chinese alpine meadow on the northern Tibetan Plateau. The RMSD with soil

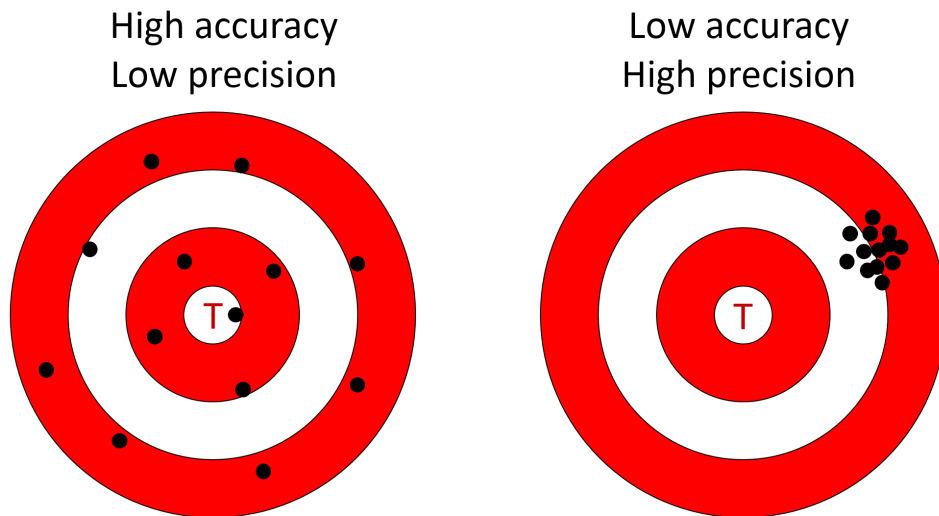


FIGURE 2.12. The difference between accuracy and precision explained with an ‘archery’ target. The target is indicated with the red T. The estimates (or ‘arrow shots’) are indicated with the black dots.

samples was low with $0.011\text{cm}^3\text{cm}^{-3}$. The accuracy of the CRNS however depends on how well secondary hydrogen pools are accounted for. If for instance the effect of biomass is corrected for sufficiently, the accuracy is improved. For this reason lower RMSD values with distributed point scale networks have been reported at sites with less favourable conditions (e.g. dense vegetation). At many sites across the world, RMSD values are around $0.03\text{cm}^3\text{cm}^{-3}$ (Bogena et al., 2013; Coopersmith et al., 2014; Zhu et al., 2015; Franz et al., 2016; Sigouin et al., 2016).

An issue that affects the accuracy of the CRNS is the neutron count integration time (Zreda et al., 2008, 2012). A too long neutron count integration time can be insufficient to, for instance, study the effects of irrigation scheduling. Hydrological processes with short response time, like rapid surface runoff at arid sites (minutes to hours) are smoothed out when a longer integration time is used, causing information content loss. Therefore, the neutron count integration time should be as short as possible, depending on the purpose of the data (e.g. runoff modelling, irrigation scheduling, studying land surface energy fluxes). However, sufficient precision requires minimum temporal supports that can be higher than desired (see next section for explanation). Typical integration times used currently vary from less than 1 hour at sites with high neutron count rates (Zreda et al., 2008; Han et al., 2014) to a day at sites with low neutron count rates (e.g. Bogena et al., 2013). Schreiner-Mcgraw et al. (2016) reported higher predicted runoff based on CRNS soil moisture estimates than for the distributed sensor network. The reason was probably the daily temporal support of the CRNS values, whereas runoff at these sites is quick, in minutes to hours. Compared to a point-scale sensor network, CRNS soil moisture dried out slower, possibly due to the presence of other sorts of water that affected the CRNS neutron counts. Baroni and Oswald (2015) quantified the effects of temporal variation of different hydrogen pools

on CRNS accuracy with the differences in N_0 values from four different calibration days. These differences were up to 100 cph, which yielded differences in estimated soil moisture of up to $0.05 \text{ cm}^3 \text{ cm}^{-3}$. Using a calibration result from one day to estimate soil moisture on the three other days yielded RMSE values (between soil moisture measured and estimated on three days) between $0.011 \text{ cm}^3 \text{ cm}^{-3}$ and $0.019 \text{ cm}^3 \text{ cm}^{-3}$. Tian et al. (2016) reported substantial improvement in comparison with independent TDR soil moisture measurements after correcting neutron counts for Biomass Water Equivalent. RMSE values decreased from $0.039 - 0.051 \text{ cm}^3 \text{ cm}^{-3}$ to $0.028 - 0.030 \text{ cm}^3 \text{ cm}^{-3}$ and the coefficient of determination increased from 0.68-0.73 to 0.77-0.79. Han et al. (2014) evaluated the performance of the CRNS at a heterogeneously covered farmland in China. They concluded the CRNS provided good soil moisture estimates with an RMSD of $0.04 \text{ cm}^3 \text{ cm}^{-3}$ and a value of 0.72 for the coefficient of determination, while using a neutron count integration time of one hour only. Lv et al. (2014) evaluated the CRNS against a TDT network in a forest in Utah. They found a bias (with differences after heavy rain up to $0.08 \text{ cm}^3 \text{ cm}^{-3}$) between CRNS and TDT network average soil moisture and reported an RMSE of $0.023 \text{ cm}^3 \text{ cm}^{-3}$. The differences were attributed to the lack of shallow ($< 10 \text{ cm}$) TDT sensors. The TDT sensors did not respond as strongly to rain events as the CRNS measurements. To improve the fit between CRNS and TDT, HDRUS1D was used to model the soil moisture at shallower depth with TDT soil moisture measured at greater depths as input. This reduced biases after heavy rain to $0.02 \text{ cm}^3 \text{ cm}^{-3}$. This last example shows an important scale advantage of the CRNS.

2.8.2 Precision

First of all the precision of the measured neutron count itself is of importance. The neutron count precision (E_N) is usually defined with the standard deviation. The standard deviation is, based on Poissonian statistics, equal to the square root of the neutron count N (Knoll (2000); Zreda et al. (2008), second panel of Figure 2.13; Eq. 2.25):

$$(2.25) \quad E_N = \sqrt{N},$$

A Poissonian distribution applies to a non-continuous quantity like neutron count, and becomes a Gaussian (i.e. normal) distribution for neutron counts above 30 cph. The neutron count signal therefore has a normal distribution with the domain between the mean minus one standard deviation and the mean plus one standard deviation containing about 64 % of the spread. The standard deviation is usually divided over the neutron count to obtain the coefficient of variation (Eq. 2.26):

$$(2.26) \quad CV = E_N^{-1/2},$$

The CV increases with decreasing neutron count (third panel of Fig. 2.13), indicating the higher uncertainty at a lower neutron count. The CV is calculated over the actually measured neutron count. However, this neutron count is usually corrected for different factors (e.g. high-energy

neutron intensity, atmospheric pressure, atmospheric water vapour, biomass), yielding a different neutron count value from which the soil moisture estimate is derived. To obtain the neutron count precision (or error) for this corrected neutron count, the CV is multiplied with the corrected neutron count N_{corr} (Eq. 2.27):

$$(2.27) \quad E_{N,sm} = CV \times N_{corr},$$

To increase the neutron count precision the neutron count should be increased (Fig. 2.14). This can be done by either using a longer integration time or by using larger or more efficient CRNS tubes (Sec. 2.3.3), or by adding more tubes at the same location. The effect of increasing the neutron count on E_N , CV, or $E_{N,sm}$ can be computed with (Eq. 2.28):

$$(2.28) \quad Y_n = \frac{Y}{\sqrt{n}},$$

where Y is the original neutron count and n is the multiplication factor, representing the relative increase in integration time (Eq. 2.29):

$$(2.29) \quad n = \frac{T_Y n}{T_Y},$$

where T_Y is the original integration time and T_{Yn} is the new integration time. Alternatively, it represents the relative increase in neutron count rate within the certain integration time (Eq. 2.30):

$$(2.30) \quad n = \frac{X_n}{X},$$

where X is the original neutron count rate and X_n is the new neutron count rate due to increased count rate. In contrast with the accuracy, the precision of the neutron sensor cannot be improved by accounting for different neutron mitigating factors. The CRNS precision is a property of the natural neutron intensity at a certain location, of the CRNS itself (size, type), and of the neutron count integration time. The precision can therefore be improved to a desired level by increasing the neutron count with the efforts mentioned.

At the end the quantity of interest is the precision of the soil moisture estimate (E_{sm}). The soil moisture error is related non-linearly to the neutron count error, due to the non-linear relationship between neutron count and soil moisture content (Fig. 2.15). The error at a high soil moisture content can therefore be a magnitude higher at saturation than at dry soil conditions (lowest panel of Fig. 2.13). Bogena et al. (2013) produced a Monte Carlo sample of neutron counts with a normal distribution and the mean at the observed neutron count. They then computed the soil moisture values for all N_0 runs and derived the standard deviation of the soil moisture error. In Chapter 5 of this thesis a different method was used, to estimate neutron count errors computed with the newly developed model COSMIC2. While the neutron count has a normally distributed precision, the soil moisture estimate does theoretically not, due to the non-linear

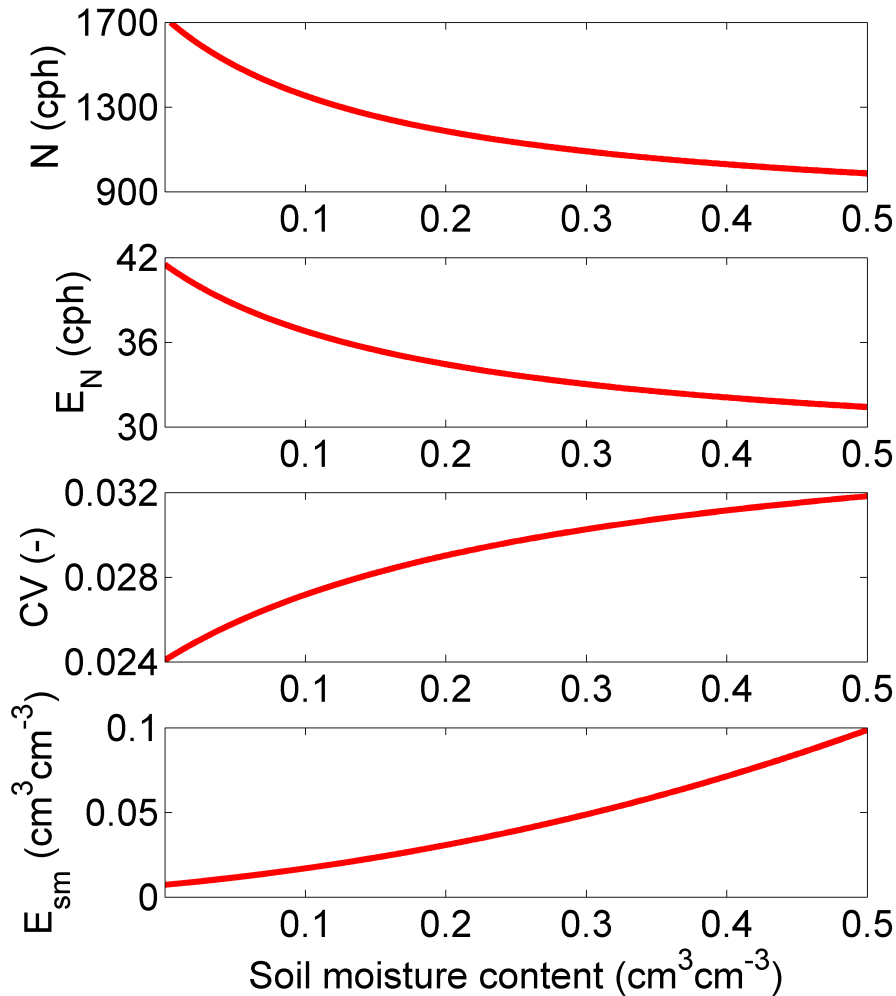


FIGURE 2.13. Neutron count (N), Coefficient of Variation (CV), neutron count error on the soil moisture – neutron curve ($E_{N,sm}$), and soil moisture error (E_{sm}) as a function of soil moisture content.

error propagation. At a low soil moisture content, where the slope of the soil moisture versus neutron count curve is flatter than -1 , the error is larger on the left side of the mean than on the right side of the mean. At wet soil conditions this is the other way around. The difference between the soil moisture errors on both sides of the neutron count mean is largest where the steepness of the curve changes quickest.

The precision of the CRNS has received somewhat less attention than the accuracy. Zreda et al. (2008) described the theory behind the CRNS precision when they introduced the CRNS. Bogena et al. (2013) paid attention to the precision of the CRNS in their ‘worst case scenario’ study. They estimated the soil moisture precision, reporting a value of $0.013 \text{cm}^3 \text{cm}^{-3}$ at a soil

moisture content of $0.1 \text{ cm}^3 \text{ cm}^{-3}$ and $0.183 \text{ cm}^3 \text{ cm}^{-3}$ at a soil moisture content of $0.7 \text{ cm}^3 \text{ cm}^{-3}$, for a neutron count integration time of 1 hour. To obtain an error below $0.04 \text{ cm}^3 \text{ cm}^{-3}$ an integration time of 12 hours was needed and to obtain an error below $0.03 \text{ cm}^3 \text{ cm}^{-3}$ an integration time of 24 hours was needed, at a soil moisture content of $0.7 \text{ cm}^3 \text{ cm}^{-3}$. Baroni and Oswald (2015) found substantially increased neutron count randomness at a soil moisture content of $0.20 \text{ cm}^3 \text{ cm}^{-3}$ compared to at a soil moisture content of $0.05 \text{ cm}^3 \text{ cm}^{-3}$. In multiple studies (e.g. Baatz et al. (2014) and Baatz et al., 2015), error bars were shown around neutron count and soil moisture time series to indicate the CRNS' performance.

In many studies accuracy and precision are not clearly distinguished and used interchangeably. Therefore both accuracy and precision of the CRNS are often compared with precision values for satellite remote sensing soil moisture products and with precision values of point-scale soil moisture sensors. The target precision value of the SMOS satellite soil moisture product is $0.04 \text{ cm}^3 \text{ cm}^{-3}$ (Kerr et al., 2001) and the estimated precision value of TDT sensors is $0.04 \text{ cm}^3 \text{ cm}^{-3}$ (Topp et al., 2001). The common RMSD value between CRNS and distributed sensor network soil moisture ($0.03 \text{ cm}^3 \text{ cm}^{-3}$) is of comparable magnitude. The same holds for the 12 hour and 24 hour

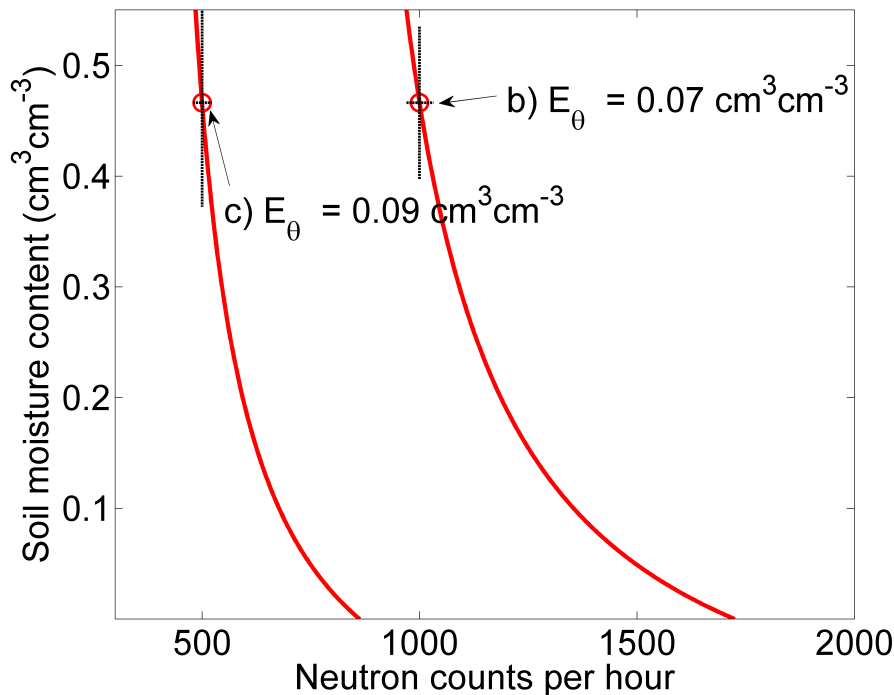


FIGURE 2.14. Soil moisture plotted against neutron count, with arbitrary values. This figure shows how the precision of the soil moisture estimate can be increased by increasing the neutron count by for instance increasing the integration time. In this specific synthetic case the count rate is doubled, improved soil moisture precision by $0.02 \text{ cm}^3 \text{ cm}^{-3}$.

integration time precision values of Bogen et al. (2013). As mentioned before, the advantage of the CRNS is that the neutron count can be increased, however at a financial cost (more sensor tubes or more efficient counters) or at the price of reduced temporal resolution. Because the precision of the CRNS has received relatively less attention than other issues, the effects of different neutron mitigating factors on these two separate quantities are addressed in Chapter 5 of this thesis.

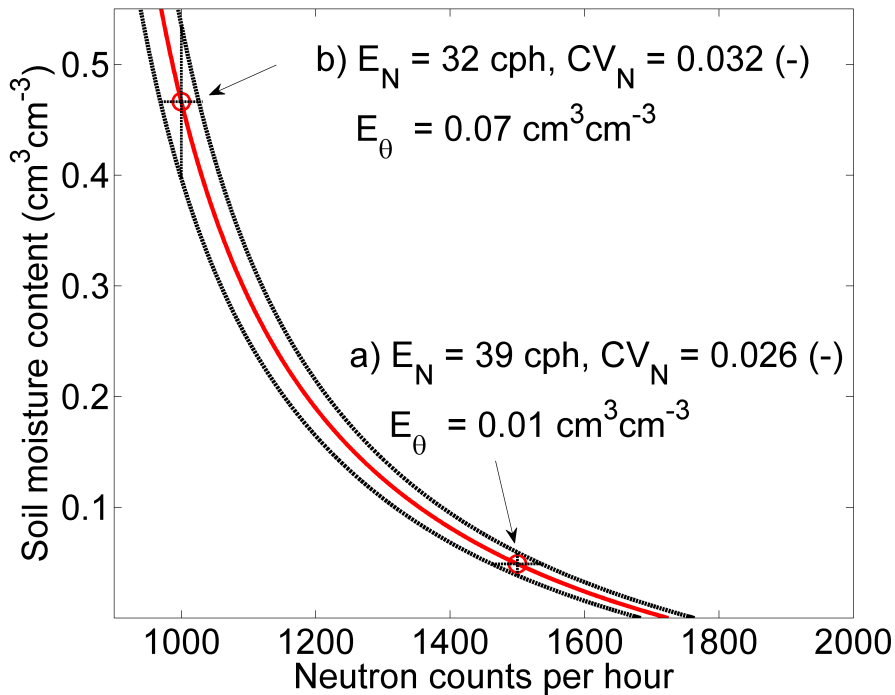


FIGURE 2.15. Soil moisture plotted against neutron count, with arbitrary values. This figure shows that due to the non-linear shape of the neutron count – soil moisture relationship, the soil moisture precision is considerably higher at dry soil conditions than at wet soil conditions. Arbitrary values.

2.9 CRNS networks around the world

Large scale networks, with CRNSs spread over countries or even continents, have been established in different parts of the world over the past seven years. The first network, the Cosmic-ray Soil Moisture Observation System (COSMOS; Zreda et al., 2012) was established in the United States and has been expanded to other regions of the world since. The purpose of the COSMOS network was initially to create a publicly available CRNS soil moisture dataset for the US, to help fill the scale mismatch between point scale measurements and satellite remote sensing soil moisture measurements. Outside the US, CRNSs have been installed in Africa, Europe, and

South-America. Over a hundred CRNS have been installed as part of the COSMOS network. The sites of the Australian CosmOz CRNS network, i.e. the Australian National Cosmic Ray Soil Moisture Monitoring Facility (Hawdon et al., 2014), are also included in the COSMOS database. The Australian CosmOz network also has a data website of its own (<http://cosmoz.csiro.au/>) showing the same data. This network currently includes seventeen CRNS stations across the islands of Australia and Tasmania.

In Germany CRNSs have been installed within the Terrestrial Environment Observatory (TERENO; Baatz et al., 2015). This Earth observation network covers multiple areas across Germany. The purpose of this network is to enable the study of longterm impacts of global change on ecology, society, and economy at a regional level. Besides CRNSs a wide range of other measurement instruments have been installed, like point scale sensor networks and eddy-covariance towers.

A relatively new network is COSMOS-UK, the equivalent of COSMOS in the United Kingdom (Evans et al., 2016). Within the United Kingdom 41 CRNSs have been installed at sites with different climatic conditions, land cover types, and soil types. The CRNS at these sites is accompanied by, among other instruments, a phenological camera, point-scale soil moisture sensors, and an automatic weather station.

2.10 Cosmic-ray Rover

Chrisman and Zreda (2013) introduced a mobile CRNS, the Cosmic-ray Rover or CRNS Rover. The Cosmic-ray Rover is a vehicle on which a CRNS is installed, so that soil moisture maps can be established at horizontal scales of hectares to tens of square kilometres. This is especially useful for calibration and validation of satellite soil moisture products and for studying spatial patterns in soil moisture. Other useful applications are precision agriculture and irrigation scheduling. The width (perpendicular to the driving direction) of the footprint of the CRNS Rover is equal to that of a fixed CRNS. The length of the footprint is however the distance travelled during the neutron count integration time. The size of the footprint therefore depends on the driving speed and the neutron count integration time. This integration time needs to be as short as possible to obtain a fine resolution, but it needs to be long enough to ensure sufficient precision of the soil moisture estimate. Chrisman and Zreda (2013) found for their study in the Tucson Basin, Arizona, US, that in that region applying a seven-minute averaging window over one minute count integration times yielded optimal results. They used an average driving speed of 55 km h^{-1} , but the speed varied from standing still to 100 km h^{-1} . With the driving speed the footprint size changed from 6.4 km at 55 km h^{-1} to 12 km at 100 km h^{-1} . At slower driving speed the precision was higher (especially when stationary) but represented a smaller footprint.

Franz et al. (2015) used a CRNS Rover in combination with three fixed CRNSs in a 12 by 12 km agricultural area in Nebraska, US. They found linear relationships between the fixed

CRNSs and the Rover estimates for grid cells of with sizes of 1, 3, and 12 km. They could provide a temporal resolution of 8 hours for the 12 by 12 km area. To validate the linear relationships between the fixed and mobile CRNSs they recommended to repeat their experiment with study periods significantly longer than their five months.

Dong et al. (2014) evaluated the precision of the CRNS Rover's soil moisture estimates in Oklahoma and they showed the Rover's calibration and validation process. The CRNS soil moisture estimates corresponded well with spatially distributed point-scale soil moisture measurements with RMSD (i.e. RMSE) values of $0.03 \text{ cm}^3 \text{ cm}^{-3}$. This accuracy could be improved on by using a slower driving speed or by increasing the size of the CRNS tubes. They did not explicitly consider hydrogen pools other than soil moisture and atmospheric water vapour content. They did however estimate the effects from lattice water to be approximately $0.034 \text{ cm}^3 \text{ cm}^{-3}$, from soil organic matter approximately $0.018 \text{ cm}^3 \text{ cm}^{-3}$, and vegetation approximately $0.0066 \text{ cm}^3 \text{ cm}^{-3}$. Avery et al. (2016) later investigated whether these effects could be quantified from globally available maps rather than local measurements, because that would enhance the effectiveness of the Rover technique substantially (see Sec. 2.11 for details). They concluded certain variables, especially soil bulk density should be measured locally for sufficient accuracy. In Section C.3 of Appendix C, a study in which CRNS Rover data was used, is presented.

2.11 Cosmic-Ray Neutron Sensor in hydrological studies

So far most studies on the application of CRNS data in hydrological studies have focussed on data assimilation, soil hydraulic parameter calibration, and the calibration and validation of satellite remote sensing products. In this section the studies published so far on these issues are discussed.

Rivera Villarreyes et al. (2014) were the first to investigate the potential of CRNS data to estimate soil hydraulic parameters. They did this for soil hydrological model HYDRUS1D. Traditionally, soil hydraulic parameters are estimated from local soil characteristics with pedotransfer functions (i.e. formulas that relate soil textural properties to soil hydraulic parameter values). Another method used often is to estimate these parameters using point-scale soil moisture data. The alleged advantage of the CRNS is here again the larger support volume. Compared to results from pedotransfer functions and parameter estimation with point-scale sensor data, parameter estimation with CRNS data derived water storage, yielded improved water storage but not necessarily more accurate soil moisture content and hydraulic pressure profiles. Using the CRNS data also resulted in better hourly variation in soil moisture profiles than when using point-scale data. They found some different parameter values with the CRNS technique than with the point-scale data, for instance higher permeability, which could be explained from the larger soil volume, which includes relatively more macro-pores. Finally, they recommended to include other field scale hydrological data, like eddy-covariance evapotranspiration data, to further investigate the

potential of CRNS data for hydraulic parameter estimation.

Sigouin et al. (2016) tested the CRNS for the specific purpose of reclaiming oil sand mining locations. Oil companies must re-establish soil and vegetation after oil mining is finished at these sites. That is done by rebuilding the soil and vegetation regrowth. An appropriate soil moisture content is needed to properly establish new vegetation because a short period of drought can mean seedlings will not mature. Soil moisture therefore needs to be measured at such locations. They installed a CRNS at an oil sand reclamation site in Canada. Sigouin et al. (2016) concluded the CRNS is a suitable means to measure soil moisture at such a site despite soil and vegetation heterogeneity. The advantage of the CRNS technique is that the sensor can be installed at remote locations and then needs little maintenance and disturbance of the soil. Limitations mentioned were the relatively shallow (< 15 cm) measurement depth and possible significant biomass increase over time.

Schreiner-Mcgraw et al. (2016) compared CRNS measured soil moisture with change in soil moisture computed with a water balance equation. This yielded good agreement with RMSE values of $0.001\text{ cm}^3\text{ cm}^{-3}$ and $0.082\text{ cm}^3\text{ cm}^{-3}$ at two distinct US sites. Large infiltration events at a site with a more rocky soil were not well captured by the CRNS, yielding underestimated soil moisture compared to the water balance method. They quantified the link between soil moisture and evapotranspiration at both sites and found predictive relationships for both sites, which could be applicable to semiarid ecosystems in the southwestern US. At one of the sites CRNS soil moisture showed a stronger link with evapotranspiration than the distributed sensor network soil moisture did. They attributed this to the CRNS' ability to detect drier soil conditions than the sensor network and to the decreased spatial scale mismatch with evapotranspiration data measured with eddy-covariance. They also concluded that the CRNS can discriminate between dry soil conditions better and so predict bare soil evaporation more accurately.

Avery et al. (2016) tested if lattice water, soil bulk density, soil organic carbon, and vegetation estimates from globally available datasets could be used instead of local samples. Such less labour intensive data acquisition could be especially advantageous to CRNS Rover studies and (distributed) modelling. They used the Global Soil Dataset, a soil taxonomic classes map, and correlation between soil clay percentages and lattice water content to establish a lattice water map. They found positive relationships between local sample data and their lattice water soil bulk density, soil organic carbon, and vegetation estimates with low correlations (coefficient of determination of 0.18 for soil organic carbon and 0.68 for clay percentage). They found the relationship between clay percentage and lattice water to be strong for one soil group (Mollisols) only. This soil group is however important for worldwide agricultural production. They recommended to take local soil bulk density samples at all sites and to take local soil organic carbon samples in case of strong soil organic carbon vertical gradients. Finally, they recommended to, especially for Rover applications, to establish maps that discriminate between rainfed cropland and irrigated cropland, and to include features such as roads and natural areas explicitly.

Chapter 3 of this thesis addresses the topic of the potential of CRNS data to calibrate soil hydraulic and evapotranspiration parameters. One difference with the studies discussed here before is that the performance of a land surface model after calibration with CRNS data is compared with the performance of the model after calibration with point scale soil moisture data. This comparison provided some insight in the significance of the spatial scale mismatch to improve hydrological modelling.

One application of CRNS soil moisture estimates is by assimilating these data into hydrological models to improve estimates of soil moisture, hydrological and surface energy fluxes, and to obtain effective parameter values. Soil moisture data assimilation is the technique of adjusting the soil moisture model state to a value between the original model state and an observed value. As mentioned in Section 2.4.3, Shuttleworth et al. (2013) and Rosolem et al. (2014) were the first to assimilate CRNS data in a land surface model; Noah. Rosolem et al. (2014) assimilated synthetic CRNS data for three sites with distinct climatic and land-cover conditions; a semi-arid shrubland, a rainfed agricultural field, and a mixed forest. At the semi-arid site both bi-daily and hourly assimilation of CRNS data with a measurement depth of 12–20 cm improved soil moisture profiles up to 100 cm remarkably well. At the other two sites however, hourly data assimilation led to considerably better soil moisture profile estimates than bi-daily data assimilation. These outcomes show potential for hydrometeorological modelling when high-frequency CRNS data is available. Han et al. (2015) investigated whether bias in simulated soil moisture contents could be removed by assimilating real neutron count data into the Community Land Model (CLM). In their case there was no irrigation input available for their model in an area in Area in the irrigated Heihe catchment in China. Assimilating neutron counts into CLM did yield improved soil moisture profile estimation and was able to remove the bias. Compared to independent point-scale soil moisture measurements the RMSE improved from $0.20\text{cm}^3\text{cm}^{-3}$ to $0.09\text{cm}^3\text{cm}^{-3}$. Evapotranspiration / latent heat flux and sensible heat flux also improved by over 50%. Most improvement was obtained if not only CRNS data was used to update soil moisture, but when more accurate LAI values were used and if land surface temperature was updated simultaneously using MODIS satellite data. Han et al. (2016) used synthetic CRNS data to remove soil moisture bias and to estimate soil hydraulic properties. Their goal was to improve irrigation scheduling. Estimation of required irrigation amount improved with 86% while evapotranspiration estimation did not improve, due to excessive irrigation, which resulted in sustained potential evapotranspiration. They concluded improvements are needed to make CRNS data assimilation a practical tool for irrigation scheduling. Recommended improvements included modelling of neutrons under high vegetation coverage, precise weather forecasts, and especially cooperation of farmers.

Baatz et al. (2017) also assimilated CRNS data into CLM. They updated both soil moisture state and soil hydraulic parameters over time with data from CRNS stations in the Rur area in Germany. Compared to simulations with soil parameter values based on an erroneous, biased

soil map, soil moisture state update improved soil moisture estimation, but also updating the parameters yielded a more substantial improvement. On average RMSE values improved from $0.12\text{ cm}^3\text{ cm}^{-3}$ for simulations without any data assimilation to $0.05\text{ cm}^3\text{ cm}^{-3}$ for simulations with updates soil moisture and parameters. Improvement was seen compared to the erroneous soil map, but not compared to a more detailed, local soil map. They therefore concluded that assimilation of CRNS data could be useful to regions with little soil information.

Another use of CRNS data is to calibrate and validate satellite remote sensing data to improve the use of such soil moisture sensor data in hydrological investigations. A potential advantage of CRNS data compared to point-scale data is the larger footprint. Multiple studies have been done to identify the potential of CRNS data in this context. Hornbuckle et al. (2012) were the first to look at this issue, by analysing the effects of vegetation on the CRNS signal. They concluded CRNS sensor data must be corrected for the effects of growing vegetation to be used to validate soil moisture and vegetation satellite remote sensing products. Renzullo et al. (2014) combined investigating the potential of the CRNS in the context of satellite remote sensing with studying the potential of CRNS data for both hydrological modelling and calibration / validation of remotely sensed soil moisture data. Using a range of Australian sites, they found it a disadvantage that most CRNS in Australia were located in places with higher error in satellite remote sensing data due to dense vegetation cover and close proximity to the sea. They recommended further work on assimilating CRNS data into hydrological models. Pang et al. (2016) also concluded, for a Desert Steppe site in China, that based on high similarity (a zero RMSE and an R^2 of 0.97) between CRNS soil moisture and remotely sensed soil moisture, CRNS is a viable means to validate remotely sensed soil moisture.

Kędzior and Zawadzki (2016) compared CRNS soil moisture data from a site in Poland with Soil Moisture and Ocean Salinity (SMOS) satellite remote sensing soil moisture data and soil moisture data from the Global Land Data Assimilation System (GLDAS)⁷. Correspondence between CRNS and SMOS data was better than with GLDAS data. CRNS and SMOS data showed similar dynamics. CRNS soil moisture data described soil moisture in deeper soil layers better than the SMOS data, possibly due to the deeper measurement depth (maximum 24 cm for CRNS versus maximum 5 cm for SMOS). Montzka et al. (2017) did a more elaborate comparison of CRNS data with satellite remote sensing data (and GLDAS data); they included different regions of the world (Germany, Arizona, California, Australia, Kenya, and India). They evaluated four different satellite remote sensing soil moisture products in their comparison: SMOS, Soil Moisture Active Passive (SMAP), Advanced Microwave Scanning Radiometer-2 (AMSR-2), and METOP-A/B Advanced Scatterometer (ASCAT). Overall, SMAP showed a relatively low bias, similar dynamics, and highest-signal-to-noise ratio compared to CRNS data. They argued that to better use CRNS data to calibrate or validate satellite remote sensing data, an operational biomass neutron count correction model is needed.

⁷GLDAS data is generated by running distributed land surface models to obtain a spatially and temporally continuous soil moisture product for use in hydrological models.

2.12 Outlook

Based on this chapter it should be clear that there have been developments on multiple fronts of the CRNS topic. The knowledge of the sensor footprint size and measurement depth has been improved especially (Köhli et al., 2015; Schrön et al., 2017). The effects of different hydrogen pools on CRNS soil moisture estimates have been the subject of a relatively large number of CRNS studies. As mentioned in Section 2.6.4, it differs between sites which hydrogen pools are most important to the correct interpretation of the CRNS neutron counts. The magnitude of the effects of above ground vegetation on the CRNS signal is not a finished topic either. For these reasons it is not completely clear yet which should hydrogen pools should be quantified at which types (i.e. land cover, soil type, climate, altitude) of sites.

Two other topics on which more improved knowledge can be expected are the value of CRNS data for hydrological studies and calibration and validation of satellite remote sensing soil moisture products (Sec. 2.11). These topics were the most important intended applications of the CRNS. With regard to calibration and validation of satellite remote sensing soil moisture products, vegetation correction methods can be investigated. Satellite remote sensing – CRNS Studies can be expanded to new regions where CRNS have been installed. CRNS data can be used in the context of different hydrological models, given studies have so far focussed on the Community Land Model, Noah, and Hydrus1D. Studies with catchment hydrological models can be expected in the future (personal communication with M. Schrön). Another opportunity for research is the simultaneous use of CRNS soil moisture data and Eddy-Covariance heat flux data. So far, hydrological modelling studies and land surface modelling studies have used CRNS data alone for calibration and data assimilation. However, to better understand the potential scale advantage of the CRNS, the effect of improved model soil moisture due to using CRNS data on simulated evapotranspiration should be evaluated. This topic is addressed in Chapter 3.

Another issue that has received attention is the question how many calibration days are need at different sites, especially at humid sites. This question is addressed in Chapter 4. A final open question that has not been addressed by the CRNS community yet, is the separation of the CRNS accuracy and precision and the question how much different neutron mitigating factors influence these two separate metrics. Therefore, in Chapter 5 the effects of different relevant neutron mitigating factors on the CRNS accuracy and precision at three humid sites with different soil types and land cover types in South-England are investigated.

BIBLIOGRAPHY

- Albertson, J. D. and Montaldo, N.: Temporal dynamics of soil moisture variability: 1. Theoretical basis, *Water Resour. Res.*, 39, doi: 10.1029/2002WR001616, 2003.
- Almeida, A., Dutta, R., Franz, T., Terhorst, A., Smethurst, P., Baillie, C., and Worledge, D.: Combining Cosmic-Ray Neutron and Capacitance Sensors and Fuzzy Inference to Spatially Quantify Soil Moisture Distribution, *IEEE Sensors J.*, 14, 3465–3472, doi: 10.1109/JSEN.2014.2345376, 2014.
- Anderson, R. G. and Goulden, M. L.: Relationship between climate, vegetation, and energy exchange across a montane gradient, *J. Geophys. Res.*, 116, doi: 10.1029/2010JG001476, 2011.
- Andreasen, M., Jensen, K. H., Zreda, M., Desilets, D., Bogaen, H., and Looms, M. C.: Modeling cosmic ray neutron field measurements, *Water Resources Research*, 52, 6451–6471, doi: 10.1002/2015WR018236, 2016.
- Aubinet, M., Feigenwinter, C., Heinesch, B., Bernhofer, C., Canepa, E., Lindroth, A., Montagnani, L., Rebmann, C., Sedlak, P., and Van Gorsel, E.: Direct advection measurements do not help to solve the night-time CO₂ closure problem: Evidence from three different forests, *Agr. Forest Meteorol.*, 150, 655–664, doi: 10.1016/j.agrformet.2010.01.016, 2010.
- Avery, W. A., Finkenbiner, C., Franz, T. E., Wang, T., Nguy-Robertson, A. L., Suyker, A., Arkebauer, T., and Muñoz Arriola, F.: Incorporation of globally available datasets into the roving cosmic-ray neutron probe method for estimating field-scale soil water content, *Hydrology and Earth System Sciences*, 20, 3859–3872, doi: 10.5194/hess-20-3859-2016, 2016.
- Baatz, R., Bogaen, H. R., Hendricks Franssen, H.-J., Huisman, J. A., Qu, W., Montzka, C., and Vereecken, H.: Calibration of a catchment scale cosmic-ray probe network: A comparison of three parameterization methods., *J. Hydrol.*, 516, 231–244, doi: 10.1016/j.jhydrol.2014.02.026, 2014.
- Baatz, R., Bogaen, H. R., Hendricks Franssen, H.-J., Huisman, J., Montzka, C., and Vereecken, H.: An empirical vegetation correction for soil water content quantification using cosmic ray probes., *Water Resour. Res.*, 51, 2030–2046, doi: 10.1002/2014WR016443, 2015.

BIBLIOGRAPHY

- Baatz, R., Hendricks Franssen, H.-J., Han, X., Hoar, T., Bogena, H. R., and Vereecken, H.: Evaluation of a cosmic-ray neutron sensor network for improved land surface model prediction, *Hydrology and Earth System Sciences Discussions*, 21, 2509–2530, doi: 10.5194/hess-21-2509-2017, 2017.
- Baldocchi, D., Falge, E., Gu, L., Olson, R., Hollinger, D., Running, S., Anthoni, P., Bernhofer, C., Davis, K., Evans, R., Fuentes, J., Goldstein, A., Katul, G., Law, B., Lee, X., Malhi, Y., Meyers, T., Munger, W., Oechel, W., Paw, K. T., Pilegaard, K., Schmid, H. P., Valentini, R., Verma, S., Vesala, T., Wilson, K., and Wofsy, S.: FLUXNET: A New Tool to Study the Temporal and Spatial Variability of Ecosystem–Scale Carbon Dioxide, Water Vapor, and Energy Flux Densities, *B. Am. Meteorol. Soc.*, 82, 2415–2434, doi: 10.1175/1520-0477(2001)082<2415:FANTTS>2.3.CO;2, 2001.
- Baroni, G. and Oswald, S.: A scaling approach for the assessment of biomass changes and rainfall interception using cosmic-ray neutron sensing, *Journal of Hydrology*, 525, 264 – 276, doi: 10.1016/j.jhydrol.2015.03.053, 2015.
- Bartelink, H.: Allometric relationships for biomass and leaf area of beech (*Fagus sylvatica* L), in: *Annales des sciences forestières*, vol. 54, pp. 39–50, EDP Sciences, 1997.
- Best, M. J., Pryor, M., Clark, D. B., Rooney, G. G., Essery, R. L. H., Menard, C. B., Edwards, J. M., Hendry, M. A., Porson, A., Gedney, N., Mercado, L. M., Sitch, S., Blyth, E., Boucher, O., Cox, P. M., Grimmond, C. S. B., and Harding, R. J.: The Joint UK Land Environment Simulator (JULES), model description - Part 1: Energy and water fluxes, *Geosci. Model. Dev.*, 4, 677–699, doi: 10.5194/gmd-4-677-2011, 2011.
- Bethe, H. A., Korff, S. A., and Placzek, G.: On the Interpretation of Neutron Measurements in Cosmic Radiation, *Phys. Rev.*, 57, 573–587, doi: 10.1103/PhysRev.57.573, 1940.
- Beven, K.: Linking parameters across scales: Subgrid parameterizations and scale dependent hydrological models, *Hydrological Processes*, 9, 507–525, doi: 10.1002/hyp.3360090504, 1995.
- Beven, K. and Germann, P.: Macropores and water flow in soils revisited, *Water Resour. Res.*, 49, 3071–3092, doi: 10.1002/wrcr.20156, 2013.
- Beven, K. J.: *Rainfall-runoff modelling: The primer*, John Wiley and Sons, Chichester, UK, 2001.
- Beven, K. J. and Cloke, H. L.: Comment on 'Hyperresolution global land surface modeling: Meeting a grand challenge for monitoring Earth's terrestrial water' by Eric F. Wood et al., *Water Resour. Res.*, 48, doi: 10.1029/2011WR10982, 2012.
- Blasi, P.: Recent results in cosmic ray physics and their interpretation., *Braz. J. Phys.*, 44(5), 426–440, doi: 10.1007/s13538-014-0223-9, 2014.

- Blonquist, J. M., Jones, S. B., and Robinson, D. A.: Standardizing characterization of electromagnetic water content sensors: Part 2. Evaluation of seven sensing systems., *Vadose Zone J.*, 4, 1059–1069, doi: 10.1007/s13538-014-0223-9, 2015.
- Blöschl, G.: Scaling in hydrology, *Hydrological Processes*, 15, 709–711, doi: 10.1002/hyp.432, 2001.
- Blöschl, G. and Sivapalan, M.: Scale issues in hydrological modelling: A review, *Hydrol. Process.*, 9, 251–290, doi: 10.1002/hyp.3360090305, 1995.
- Blyth, E. Clark, D., Ellis, R., Huntingford, C., Los, S., Pryor, M. Best, M., and Sitch, S.: A comprehensive set of benchmark tests for a land surface model of simultaneous fluxes of water and carbon at both the global and seasonal scale, *Geosci. Model Dev.*, 4, 255–269, doi: 10.5194/gmd-4-255-2011, 2011.
- Blyth, E., Gash, J., Lloyd, A., Pryor, M., Weedon, G. P., and Shuttleworth, J.: Evaluating JULES Land Surface Model Energy Fluxes Using FLUXNET Data, *J. Hydrometeor.*, 11, 509–519, doi: 10.1175/2009JHM1183.1, 2010.
- Blyth, E. M., Dolman, A. J., and Wood, N.: Effective resistance to sensible-and latent-heat flux in heterogeneous terrain, *Q. J. Roy. Meteorol. Soc.*, 119, 423–442, doi: 10.1002/qj.49711951104, 1993.
- Bogena, H. R., Huisman, J. A., Meier, H., Rosenbaum, U., and Weuthen, A.: Hybrid wireless underground sensor networks: Quantification of signal attenuation in soil, *Vadose Zone J.*, 8, 755–761, doi: 10.2136/vzj2008.0138, 2009.
- Bogena, H. R., Herbst, M., Huisman, J. A., Rosenbaum, U., Weuthen, A., and Vereecken, H.: Potential of Wireless Sensor Networks for Measuring Soil Water Content Variability, *Vadose Zone J.*, 9, 1002–1013, doi: 10.2136/vzj2009.0173, 2010.
- Bogena, H. R., Huisman, J. A., Baatz, R., Hendricks Franssen, H. J., and Vereecken, H.: Accuracy of the cosmic-ray soil water content probe in humid forest ecosystems: The worst case scenario., *Water Resour. Res.*, 49, 5778–5791, doi: 10.1002/wrcr.20463, 2013.
- Bogena, H. R., Bol, R., Borchard, N., Brüggemann, N., Diekkrüger, B., Drüe, C., Groh, J., Gottselig, N., Huisman, J., Lücke, A., Missong, A., Neuwirth, B., Pütz, T., Schmidt, M., Stockinger, M., Tappe, W., Weihermüller, L., Wiekenkamp, I., and Vereecken, H.: A terrestrial observatory approach to the integrated investigation of the effects of deforestation on water, energy and matter fluxes., *Sci. China Earth. Sci.*, 58, 61–75, doi: 10.1007/s11430-014-4911-7, 2014.
- Braden, H.: Ein energiehaushalts- und verdunstungsmodell für wasser und stoffhaushaltsuntersuchungen landwirtschaftlich genutzter einzugsgebiete., *Mitt. Deut. Bodenk. Ges.*, 42, 294–299, 1985.

BIBLIOGRAPHY

- Brady, N. C. and Weil, R. R.: The nature and properties of soils, Prentice Hall, New York, 11th edn. edn., 1956.
- Breuer, L., Eckhardt, K., and Frede, H.-G.: Plant parameter values for models in temperate climates, *Ecological Modelling*, 169, 237 – 293, doi: 10.1016/S0304-3800(03)00274-6, 2003.
- Brocca, L., Morbidelli, R., Melone, F., and Moramarco, T.: Soil moisture spatial variability in experimental areas of central Italy, *Journal of Hydrology*, 333, 356 – 373, doi: 10.1016/j.jhydrol.2006.09.004, 2007.
- Budyko, M.: Heat Balance of the Earth's Surface, Department of Commerce, Weather Bureau, 1956.
- Budyko, M.: Climate and Life, International geophysics series, Academic Press, 1974.
- Campbell Scientific Inc.: CS650 and CS655 Water Content Reflectometers Instruction Manual, Campbell Scientific Inc., Logan, USA, revision: 2/14 edn., 2014.
- Campbell Scientific Inc.: CS616 and CS625 Water Content Reflectometers Instruction Manual, Campbell Scientific Inc., Logan, USA, revision: 2/16 edn., 2016.
- Cardell-Oliver, R., Kranz, M., Smettem, K., and Mayer, K.: A Reactive Soil Moisture Sensor Network: Design and Field Evaluation, *International Journal of Distributed Sensor Networks*, 1, 149–162, doi: 10.1080/15501320590966422, 2005.
- Cavanaugh, M. L., Kurc, S. A., and Scott, R. L.: Evapotranspiration partitioning in semiarid shrubland ecosystems: A two-site evaluation of soil moisture control on transpiration., *Ecohydrology*, 4, 671–681, doi: 10.1002/eco.157, 2011.
- Chen, X., Rubin, Y., Ma, S., , and Baldocchi, D.: Observations and stochastic modelling of soil moisture control on evapotranspiration in a Californian oak savanna., *Water Resour. Res.*, 44, doi: 10.1029/2007WR006646, 2008.
- Chrisman, B. and Zreda, M.: Quantifying mesoscale soil moisture with the cosmic-ray rover., *Hydrol. Earth Syst. Sci.*, 17, 5097–5108, doi: 10.5194/hess-17-5097-2013, 2013.
- Clark, D. B., Mercado, L. M., Sitch, S., Jones, C. D., Gedney, N., Best, M. J., Pryor, M., Rooney, G. G., Essery, R. L. H., Blyth, E., Boucher, O., Harding, R. J., Huntingford, C., and Cox, P. M.: The Joint UK Land Environment Simulator (JULES), model description – Part 2: Carbon fluxes and vegetation dynamics., *Geosci. Model Dev.*, 4, 701– 722, doi: 10.5194/gmd-4-701-2011, 2011.
- Coopersmith, E. J., Cosh, M. H., and Daughtry, C. S.: Field-scale moisture estimates using {COS-MOS} sensors: A validation study with temporary networks and Leaf-Area-Indices, *Journal of Hydrology*, 519, Part A, 637 – 643, doi: 10.1016/j.jhydrol.2014.07.060, 2014.

- Crow, W. T., Berg, A. A., Cosh, M. H., Loew, A., Mohanty, B. P., Panciera, R., Rosnay, P., Ryu, D., and Walker, J. P.: Upscaling sparse ground-based soil moisture observations for the validation of coarse-resolution satellite soil moisture products, *Rev. Geophys.*, 50, 1–20, doi: 10.1029/2011RG000372, 2012.
- Cullen, M. J. P.: The unified forecast/climate model, *Meteorol. Mag.*, 122, 81–94, 1993.
- De Lannoy, G. J. M., Koster, R. D., Reichle, R. H., Mahanama, S. P. P., and Liu, Q.: An updated treatment of soil texture and associated hydraulic properties in a global land modeling system, *J. Adv. Model. Earth Syst.*, 6, 957–979, doi: 10.1002/2014MS000330, 2014.
- De Vries, D. A.: Thermal properties of soils, in: *Physics of plant environment*, edited by van Wijk, W. R., pp. 210–235, North Holland Publishing Co., Amsterdam, Netherlands, 1963.
- Dee, D. P.: Bias and data assimilation., *Q.J.R. Meteorol. Soc.*, 131, 3323–3343, doi: 10.1256/qj.05.137, 2005.
- Delta-T Devices: ML3 ThetaProbe User Manual, Delta-T Devices Ltd, Cambridge, UK, version ml3-um-1.0 edn., 2013.
- Demaria, E. M., Nijssen, B., and Wagener, T.: Monte Carlo sensitivity analysis of land surface parameters using the Variable Infiltration Capacity model., *J. Geophys. Res.*, 112, D11113, doi: 10.1029/2006JD007534, 2007.
- Desilets, D. and Zreda, M.: On scaling cosmogenic nuclide production rates for altitude and latitude using cosmic-ray measurements., *Earth Planet. Sci. Lett.*, 193, 213–225, doi: 10.1016/S0012-821X(01)00477-0, 2001a.
- Desilets, D. and Zreda, M.: Spatial and temporal distribution of secondary cosmic-ray neutron intensities and applications to in-situ cosmogenic dating., *Earth Planet. Sci. Lett.*, 206, 41–42, doi: 10.1016/S0012-821X(02)01088-9, 2001b.
- Desilets, D. and Zreda, M.: Footprint diameter for a cosmic-ray soil moisture probe: Theory and Monte Carlo simulations., *Water Resour. Res.*, 49, 3566–3575, doi: 10.1002/wrcr.20187, 2013.
- Desilets, D., Zreda, M., and Ferré, T.: Scientist water equivalent measured with cosmic rays at 2006 AGU Fall Meeting, *Eos, Transactions American Geophysical Union*, 88, 521–522, doi: 10.1029/2007EO480001, 2007.
- Desilets, D., Zreda, M., and Ferré, T. P. A.: Nature’s neutron probe: Land surface hydrology at an elusive scale with cosmic rays., *Water Resour. Res.*, 46, W11505, doi: 10.1029/2009WR008726, 2010.
- Dingman, S.: *Physical hydrology*, Prentice Hal, Upper Saddle River, NJ, USA, 2nd edn., 2002.

BIBLIOGRAPHY

- Dirmeyer, P.: The terrestrial segment of soil moisture-climate coupling, *Geophys. Res. Lett.*, 38, doi: 10.1029/2011GL048268, 2011.
- Dirmeyer, P., Dolman, A. J., and Sato, N.: The Pilot Phase of the Global Soil Wetness Project, *Bulletin of the American Meteorological Society*, 80, 851–878, doi: 10.1175/1520-0477(1999)080<0851:TPPOTG>2.0.CO;2, 1999.
- Dirmeyer, P. A., Zeng, F. J., Ducharne, A., Morrill, J. C., and Koster, R.: The Sensitivity of Surface Fluxes to Soil Water Content in Three Land Surface Schemes, *J. Hydrometeorol.*, 1, 121–134, doi: 10.1175/1520-0477(1999)080<0851:TPPOTG>2.0.CO;2, 2000.
- Dirmeyer, P. A., Jin, Y., Singh, B., and Yan, X.: Trends in Land-Atmosphere Interactions from CMIP5 Simulations, *J. Hydrometeorol.*, 14, 829–849, doi: 10.1175/JHM-D-12-0107.1, 2013.
- Dong, J., Ochsner, T. E., Zreda, M., Cosh, M. H., and Zou, C. B.: Calibration and Validation of the COSMOS Rover for Surface Soil Moisture Measurement., *Vadose Zone J.*, 13, doi: 10.2136/vzj2013.08.0148, 2014.
- Downer, C. W. and Ogden, F. L.: Appropriate vertical discretization of Richards's equation for two-dimensional watershed-scale modelling., *Hydrol. Process.*, 18, 1–22, doi: 10.1002/hyp.1306, 2004.
- Dunne, T., Moore, T., and Taylor, C.: Recognition and prediction of runoff-producing zones in humid regions., *Hydrol. Sci. Bull.*, 20, 305–327, 1975.
- Durre, I., Wallace, J. M., and Lettenmaier, D. P.: Dependence of extreme daily maximum temperatures on antecedent soil moisture in the contiguous United States during summer, *J. Climate*, 13, 2641–2651, doi: 10.1175/1520-0442(2000)013<2641:DOEDMT>2.0.CO;2, 2000.
- Dutta, R. and Terhorst, A.: Adaptive Neuro-Fuzzy Inference System-Based Remote Bulk Soil Moisture Estimation: Using CosmOz Cosmic Ray Sensor., *IEEE Sensors J.*, 13, doi: 10.1109/JSEN.2013.2254710, 2013.
- Dutta, R., Terhorst, A., Hawdon, A., and Cotching, B.: Bulk soil moisture estimation using CosmOz cosmic ray sensor and ANFIS, in: 2012 IEEE Sensors, pp. 1–4, doi: 10.1109/ICSENS.2012.6411570, 2012.
- DWD: WebWerdis: Web-based Weather Request and Distribution System (WebWerdis) of the German Weather Service (DWD)., URL <http://www.dwd.de/webwerdis>, last accessed:15 December 2014, 2014.
- Ek, M., Mitchell, K., Lin, Y., Rogers, E., Grummann, P., Koren, V., Gayno, G., and Tarpley, J.: Implementation of Noah land surface model advances in the National Centers for Environmental Prediction operational Mesoscale Eta Model., *J. Geophys. Res.*, 108(8851), doi: 10.1029/2002JD003296, 2003.

- Entekhabi, D.: Recent advances in land-atmosphere interaction research, *Reviews of Geophysics*, 33, 995–1003, doi: 10.1029/95RG01163, 1995.
- Entin, J. K., Robock, A., Vinnikov, K. Y., Hollinger, S. E., Liu, S., and Namkhai, A.: Temporal and spatial scales of observed soil moisture variations in the extratropics, *Journal of Geophysical Research: Atmospheres*, 105, 11 865–11 877, doi: 10.1029/2000JD900051, 2000.
- Etmann, M.: Dendrologische Aufnahmen im Wassereinzugsgebiet Oberer Wüstebach anhand verschiedener Mess- und Schätzverfahren., Ph.D. thesis, Westfälische Wilhelms-Universität Münster, Münster, 2009.
- Evans, J. G., Ward, H. C., Blake, J. R., Hewitt, E. J., Morrison, R., Fry, M., Ball, L. A., Doughty, L. C., Libre, J. W., Hitt, O. E., Rylett, D., Ellis, R. J., Warwick, A. C., Brooks, M., Parkes, M. A., Wright, G. M. H., Singer, A. C., Boorman, D. B., and Jenkins, A.: Soil water content in southern England derived from a cosmic-ray soil moisture observing system – COSMOS-UK, *Hydrological Processes*, 30, 4987–4999, doi: 10.1002/hyp.10929, 2016.
- FAO/IIASA/ISRIC/ISS-CAS/JRC: Harmonized World Soil Database (version 1.1.), 2009.
- Ferré, P. A., Knight, J. H., Rudolph, D. L., and Kachanoski, R. G.: The sample areas of conventional and alternative time domain reflectometry probes, *Water Resources Research*, 34, 2971–2979, doi: 10.1029/98WR02093, 1998.
- Finch, J. W. and Haria, A.: The representation of chalk soils in the JULES/MOSES soil hydrology model, Rept., 2014.
- Finkelstein, P. L. and Sims, P. F.: Sampling error in eddy correlation flux measurements., *J. Geophys. Res.*, 106, 3503–3509, doi: 10.1029/2000JD900731, 2001.
- Fischer, E. M., Seneviratne, S. I., Luthi, D., and Schar, C.: The contribution of land-atmosphere coupling to recent European summer heatwaves, *Geophys. Res. Lett.*, 34, 1–6, doi: 10.1029/2006GL029068, 2007a.
- Fischer, E. M., Seneviratne, S. I., Vidale, P. L., Luthi, D., and Schar, C.: Soil moisture-atmosphere interactions during the 2003 European summer heatwave, *J. Climate*, 20, 5081–5099, doi: 10.1175/JCLI4288.1, 2007b.
- Forstreuter, M.: Ergebnisbericht: Ökologie der Gehölze i. Report SS99, Institut für Ökologie und Biologie, Technische Universität Berlin, Königin-Luise-Str. 22, Berlin 14195, 1999.
- Franz, T. E., Zreda, M., Rosolem, R., and Ferré, T. P. A.: Measurement depth of the cosmic ray soil moisture probe affected by hydrogen from various sources., *Water Resour. Res.*, 48, doi: 10.1029/2012WR011871, 2012a.

BIBLIOGRAPHY

- Franz, T. E., Zreda, M., Rosolem, R., and Ferré, T. P. A.: Field Validation of a Cosmic-Ray Neutron Sensor Using a Distributed Sensor Network., *Vadose Zone J.*, 11, doi: 10.2136/vzj2012.0046, 2012b.
- Franz, T. E., Zreda, M., Ferré, T. P. A., and Rosolem, R.: An assessment of the effect of horizontal soil moisture heterogeneity on the area-average measurement of cosmic-ray neutrons., *Water Resour. Res.*, 49, 6450–6458, doi: 10.1002/wrcr.20530, 2013a.
- Franz, T. E., Zreda, M., Rosolem, R., and Ferré, T. P. A.: A universal calibration function for determination of soil moisture with cosmic-ray neutrons., *Hydrol. Earth Syst. Sci.*, 17, 453–460, doi: 10.5194/hess-17-453-2013, 2013b.
- Franz, T. E., Zreda, M., Rosolem, R., Hornbuckle, B. K., Irvin, S. L., Adams, H., Kolb, T. E., Zweck, C., and Shuttleworth, W. J.: Ecosystem-scale measurements of biomass water using cosmic ray neutrons., *Geophys. Res. Lett.*, 40, 3929–3933, doi: 10.1002/grl.50791, 2013c.
- Franz, T. E., Wang, T., Avery, W., Finkenbiner, C., and Brocca, L.: Combined analysis of soil moisture measurements from roving and fixed cosmic ray neutron probes for multiscale real-time monitoring, *Geophysical Research Letters*, 42, 3389–3396, doi: 10.1002/2015GL063963, 2015GL063963, 2015.
- Franz, T. E., Wahbi, A., Vreugdenhil, M. and Weltin, G., Heng, L., Oismueller, M., Strauss, P., Dercon, G., and Desilets, D.: Using Cosmic-Ray Neutron Probes to Monitor Landscape Scale Soil Water Content in Mixed Land Use Agricultural Systems., *Applied and Environmental Soil Science*, 2016, 4323742, doi: 10.1155/2016/4323742, 2016.
- Galagedara, L. W., Redman, J. D., Parkin, G. W., Annan, A. P., and Endres, A. L.: Numerical Modeling of GPR to Determine the Direct Ground Wave Sampling Depth, *Vadose Zone J.*, 4, 1096–1106, doi: 10.2136/vzj2004.0143, 2005.
- Gardner, W. and Kirkham, D.: Determination of soil moisture by neutron scattering., *Soil Sci.*, 5, 391–402, 1952.
- Gaskin, G. and Miller, J.: Measurement of Soil Water Content Using a Simplified Impedance Measuring Technique, *Journal of Agricultural Engineering Research*, 63, 153 – 159, doi: <http://dx.doi.org/10.1006/jaer.1996.0017>, 1996.
- Goldhagen, P., Reginatto, M., Kniss, T., Wilson, J., Singleterry, R., Jones, I., and Steveninck, W. V.: Measurement of the energy spectrum of cosmic-ray induced neutrons aboard an ER-2 high-altitude airplane., *Nucl. Instrum. Methods Phys. Res., Sect. A*, 476(12), 42–51, doi: 10.1016/S0168-9002(01)01386-9, 2002.
- Goulden, M. L.: Measurement of Energy, Carbon and Water Exchange Along California Climate Gradients., URL <http://www.ess.uci.edu/~california/>, last accessed: July 2016, 2015.

- Goulden, M. L., Munger, J. W., Fan, S. M., Daube, B. C., and Wofsy, S. C.: Measurements of carbon sequestration by long-term eddy covariance: Methods and a critical evaluation of accuracy, *Glob. Change Biol.*, 2, 169–182, doi: 10.1111/j.1365-2486.1996.tb00070.x, 1996.
- Goulden, M. L., Winston, G. C., McMillan, A. M. S., Litvak, M. E., Read, E. L., Rocha, A. V., and Elliot, J. R.: An eddy covariance mesonet to measure the effect of forest age on land-atmosphere exchange., *Glob. Change Biol.*, 12, 2146–2162, doi: 10.1111/j.1365-2486.2006.01251.x, 2006.
- Goulden, M. L., Anderson, R. G., Bales, R. C., Kelly, A. E., Meadows, M., and Winston, G. C.: Evapotranspiration along an elevation gradient in California’s Sierra Nevada., *J. Geophys. Res.*, 117, doi: 10.1029/2012JG002027, 2012.
- Grim, R.: *Clay Mineralogy*, McGraw–Hill Book Company Inc., New York, 1953.
- Gudima, K., Mashnik, S., and Toneev, V.: Cascade-exciton model of nuclear reactions, *Nuclear Physics A*, 401, 329 – 361, doi: 10.1016/0375-9474(83)90532-8, 1983.
- Guericke, M.: Growth dynamics of mixed stands of beech and European larch. Technical report., Fakultät für Forstwissenschaften und Waldökologie, Georg-August-Universität, Göttingen, Germany, 2001.
- Gupta, H. V. and Sorooshian, S.: Toward improved calibration of hydrologic models: Multiple and noncommensurable measures of information, *Water Resour. Res.*, 34, 751–763, doi: 10.1029/97WR03495, 1998.
- Gupta, H. V., Bastidas, L. A., Sorooshian, S., Shuttleworth, W. J., and Yang, Z. L.: Parameter estimation of a land surface scheme using multicriteria methods, *J. Geophys. Res.*, 104, 19 491–19 503, doi: 10.1029/1999JD900154, 1999.
- Gupta, H. V., King, H., Yilmaz, K. K., and Martinez, G. F.: Decomposition of the mean squared error and NSE performance criteria: Implications for improving hydrological modelling, *J. Hydrol.*, 377, 80–91, doi: 10.1016/j.jhydrol.2009.08.003, 2009.
- Hadka, D. and Reed, P.: Borg: an auto-adaptive many-objective evolutionary computing framework, *Evolut. Compt.*, 21, 231–259, doi: 10.1162/EVCO_a_00075, 2013.
- Han, X., Jin, R., Li, X., and Wang, S.: Soil Moisture Estimation Using Cosmic-Ray Soil Moisture Sensing at Heterogeneous Farmland, *IEEE Geosci. Rem. Sens. Lett.*, 11, 1659–1663, doi: 10.1109/LGRS.2014.2314535, 2014.
- Han, X., Hendricks Franssen, H.-J., Rosolem, R., Jin, R., Li, X., and Vereecken, H.: Correction of systematic model forcing bias of CLM using assimilation of cosmic-ray Neutrons and land surface temperature: a study in the Heihe Catchment, China, *Hydrology and Earth System Sciences*, 19, 615–629, doi: 10.5194/hess-19-615-2015, 2015.

BIBLIOGRAPHY

- Han, X., Hendricks Franssen, H.-J., Jiménez Bello, M., Rosolem, R., Bogaen, H., Martínez Alzamora, F., Chanzy, A., and Vereecken, H.: Simultaneous soil moisture and properties estimation for a drip irrigated field by assimilating cosmic-ray neutron intensity, *Journal of Hydrology*, 539, 611 – 624, doi: 10.1016/j.jhydrol.2016.05.050, 2016.
- Hawdon, A., McJannet, D., and Wallace, J.: Calibration and correction procedures for cosmic-ray neutron soil moisture probes located across Australia, *Water Resources Research*, 50, 5029–5043, doi: 10.1002/2013WR015138, 2014.
- Heidbüchel, I., Günter, A., and Blume, T.: Use of cosmic-ray neutron sensors for soil moisture monitoring in forests, *Hydrol. Earth Syst. Sci.*, 20, 1269–1288, doi: 10.5194/hess-20-1269-2016, 2016.
- Henderson-Sellers, A., McGuffie, K., and Pitman, A. J.: The Project for Intercomparison of Land-Surface Parameterization Schemes (PILPS): 1992 to 1995, *Clim. Dynam.*, 12, 849–859, doi: 10.1175/1520-0477(1993)074<1335:TPFIOL>2.0.CO;2, 1996.
- Hendrick, L. D. and Edge, R. D.: Cosmic-Ray Neutrons near the Earth, *Phys. Rev.*, 145, 1023–1025, doi: 10.1103/PhysRev.145.1023, 1966.
- Hess, W., Canfield, E. H., and Lingenfelter, R. E.: Cosmic-ray neutron demography., *J. Geophys. Res.*, 66, 665–677, doi: 10.1029/JZ066i003p00665, 1961.
- Hess, W. N., Patterson, H. W., and Wallace, R.: Cosmic-ray neutron energy spectrum, *Physical Rev. Lett.*, 116, 445–457, doi: 10.1103/PhysRev.116.445, 1959.
- Hoogsteen, M. J. J., Lantinga, E. A., Bakker, E. J., Groot, J. C. J., and Tittonell, P. A.: Estimating soil organic carbon through loss on ignition: effects of ignition conditions and structural water loss, *European Journal of Soil Science*, 66, 320–328, doi: 10.1111/ejss.12224, 2015.
- Hornbuckle, B., Irvin, S., Franz, T., Rosolem, R., and Zweck, C.: The potential of the COSMOS network to be a source of new soil moisture information for SMOS and SMAP, in: 2012 IEEE International Geoscience and Remote Sensing Symposium, pp. 1243–1246, doi: 10.1109/IGARSS.2012.6351317, 2012.
- Howard, P. J. A. and Howard, D. M.: Use of organic carbon and loss-on-ignition to estimate soil organic matter in different soil types and horizons, *Biology and Fertility of Soils*, 9, 306–310, doi: 10.1007/BF00634106, 1990.
- Hu, W., Shao, M., Han, F., and Reichardt, K.: Spatio-temporal variability behavior of land surface soil water content in shrub- and grass-land, *Geoderma*, 162, 260 – 272, doi: 10.1016/j.geoderma.2011.02.008, 2011.

- Hübner, C., Cardell-Oliver, R., Becker, R., Spohrer, K., Jotter, K., and Wagenknecht, T.: Wireless soil moisture sensor networks for environmental monitoring and vineyard irrigation., Helsinki University of Technology, 1, 408–415, 2009.
- Huisman, J., Sperl, C., Bouten, W., and Verstraten, J.: Soil water content measurements at different scales: accuracy of time domain reflectometry and ground-penetrating radar, *Journal of Hydrology*, 245, 48 – 58, doi: 10.1016/S0022-1694(01)00336-5, 2001.
- Ishida, T., Makino, T., and Wang, C. J.: Dielectric-relaxation spectroscopy of kaolinite, montmorillonite, allophane, and imogolite under moist conditions, *Clays Clay. Miner.*, 48, 75–84, 2000.
- Iwema, J., Rosolem, R., Baatz, R., Wagener, T., and Bogen, H. R.: Investigating temporal field sampling strategies for site-specific calibration of three soil moisture – neutron intensity parameterisation methods, *Hydrol. Earth Syst. Sci.*, 19, 3203–3216, doi: 10.5194/hess-19-3203-2015, 2015.
- Iwema, J., Rosolem, R., Rahman, M., Blyth, E., and Wagener, T.: Land surface model performance using cosmic-ray and point-scale soil moisture measurements for calibration, *Hydrol. Earth Syst. Sci.*, 21, 2843–2861, doi: 10.5194/hess-21-2843-2017, 2017.
- Jana, R. B.: Scaling characteristics of soil hydraulic parameters at varying spatial resolutions, Ph.D. thesis, Department of Biological and Agricultural Engineering, Texas AM University, 2010.
- Jarraud, M.: Guide to meteorological instruments and methods of observation (WMO-No. 8), World Meteorological Organisation: Geneva, Switzerland, 2008.
- Jenkins, C., Chojnacky, D., Heath, L. S., and Birdsey, R.: National-Scale Biomass Estimators for United States Tree Species, *Forest Science*, 49, 12–35, doi: 10.5194/hess-19-3203-2015, 2003.
- Jiao, Q., Zhu, Z., and Du, F.: Theory and application of measuring mesoscale soil moisture by cosmic-ray fast neutron probe, in: 35th International Symposium on Remote Sensing of Environment (ISRSE35), IOP Conf. Series: Earth and Environmental Science, vol. 17, doi: 10.1088/1755-1315/17/1/012147, 2014.
- Journel, A. G. and J., H. C.: *Mining Geostatistics*, Academic, London, UK, 1st edn., 1978.
- Katul, G. G., Oren, R., Manzoni, S., Higgins, C., and Parlange, M. B.: Evapotranspiration: A process driving mass transport and energy exchange in the soil-plant-atmosphere-climate system, *Reviews of Geophysics*, 50, doi: 10.1029/2011RG000366, rG3002, 2012.
- Kędzior, M. and Zawadzki, J.: Comparative study of soil moisture estimations from {SMOS} satellite mission, {GLDAS} database, and cosmic-ray neutrons measurements at {COSMOS} station in Eastern Poland, *Geoderma*, 283, 21 – 31, doi: 10.1016/j.geoderma.2016.07.023, 2016.

BIBLIOGRAPHY

- Kerr, Y. H., Waldteufel, P., Wigneron, J.-P., Martinuzzi, J.-M., Font, J., and Berger, M.: Soil Moisture Retrieval from Space: The Soil Moisture and Ocean Salinity (SMOS) Mission., *IEEE T. Geosci. Remote*, 39, 1729–1735, doi: 10.1109/36.942551, 2001.
- Kerr, Y. H., Waldteufel, P., Wigneron, J.-P., Delwart, S., Cabot, F., Boutin, J., Escorihuela, M.-J., Font, J., Reul, N., Gruhier, C., Enache Juglea, S., Drinkwater, M. R., Hahne, A., Martin-Neira, M., and Mecklenburg, S.: The SMOS Mission: New Tool for Monitoring Key Elements of the Global Water Cycle, *IEEE T. Geosci. Remote*, 98, 1729–1735, doi: 10.1109/JPROC.2010.2043032, 2010.
- Knight, R.: Ground Penetrating Radar for Environmental Applications, *Annual Review of Earth and Planetary Sciences*, 29, 229–255, doi: 10.1146/annurev.earth.29.1.229, 2001.
- Knoll, G. F.: *Radiation detection and measurement.*, Wiley, New York, 1st edn., 2000.
- Knoll, G. F.: *Radiation detection and measurement.*, Wiley, New York, 3rd edn., 2010.
- Kodama, M.: Continuous monitoring of snow water equivalent using cosmic-ray neutrons., *Cold Region Sci. Technol.*, 3, 295–303, doi: 10.1016/0165-232X(80)90036-1, 1980.
- Kodama, M., Kudo, S., and Kosuge, T.: Application of atmospheric neutrons to soil moisture measurement., *Soil Sci.*, 140, 237–242, doi: 10.1091/00010694-198510000-00001, 1985.
- Köhli, M., Schrön, M., Zreda, M., Schmidt, U., Dietrich, P., and Zacharias, S.: Footprint characteristics revised for field-scale soil moisture monitoring with cosmic-ray neutrons, *Water Resour. Res.*, 51, doi: 10.1002/2015WR017169, 2015.
- Kollat, J. B., Reed, P. M., and Wagener, T.: When are multiobjective calibration trade-offs in hydrological models meaningful?, *Water Resour. Res.*, 48, doi: 10.1029/2011WR011534, 2012.
- Koster, R. D., Dirmeyer, P. A., Guo, Z., Bonan, G., Chan, E., Cox, P., Gordon, C. T., Kanae, S., Kowalczyk, E., Lawrence, D. and Liu, P., Lu, G.-H., Malyshev, S., McAvaney, B., Mitchell, K., Mocko, D., Oki, T., Oleson, K., Pitman, A., Sud, Y. C., Taylor, C. M., Versegny, D., Vasic, R., Xue, Y., and Yamada, T.: Regions of Strong Coupling Between Soil Moisture Precipitation, *Science*, 305, 1138–1140, doi: 10.1126/science.1100217, 2004.
- Koster, R. D., Guo, Z., Yang, R., Dirmeyer, P. A., Mitchell, K., and Puma, M. J.: On the nature of soil moisture in land surface models, *J. Climate*, 22, 4322–4335, doi: 10.1175/2009JCLI2832.1, 2009.
- Kroes, J., Van Dam, J., Groenendijk, P., Hendriks, R., and Jacobs, C.: *SWAP version 3.2. Theory description and user manual.*, Alterra, Research Institute, Wageningen, The Netherlands, alterra-report 1649, 262 pp, 2008.

- Kurc, S. A. and Small, E. E.: Soil moisture variations and ecosystem-scale fluxes of water and carbon in semiarid grassland and shrubland, *Water Resour. Res.*, 43, 4322–4335, doi: 10.1029/2006WR005011, 2007.
- Larson, K. M., Small, E. E., Gutmann, E. D., Bilich, A. L., Braun, J. J., and Zavorotny, V. U.: Use of GPS receivers as a soil moisture network for water cycle studies, *Geophysical Research Letters*, 35, doi: 10.1029/2008GL036013, l24405, 2008.
- Larson, K. M., Braun, J. J., Small, E. E., Zavorotny, V. U., Gutmann, E. D., and Bilich, A. L.: GPS Multipath and Its Relation to Near-Surface Soil Moisture Content, *IEEE Journal of Selected Topics in Applied Earth Observations and Remote Sensing*, 3, 91–99, doi: 10.1109/JSTARS.2009.2033612, 2010.
- Lee, D. H. and Abriola, L. M.: Use of Richards equation in land surface parameterizations, *J. Geophys. Res.*, 104, 27 519–27 526, doi: 10.1029/1999JD900951, 1999.
- Letaw, J. R. and Normand, E.: Guidelines for predicting single-event upsets in neutron environments [RAM devices], *IEEE Transactions on Nuclear Science*, 38, 1500–1506, doi: 10.1109/23.124138, 1991.
- Lingenfelter, R. E., Canfield, E. H., and Hess, W. N.: The lunar neutron flux, *Journal of Geophysical Research*, 66, 2665–2671, doi: 10.1029/JZ066i009p02665, 1961.
- Lv, L., Franz, T. E., Robinson, D. A., and Jones, S. B.: Measured and Modeled Soil Moisture Compared with Cosmic-Ray Neutron Probe Estimates in a Mixed Forest., *Vadose Zone J.*, 13, doi: 10.2136/vzj2014.06.0077, 2014.
- Manabe, S.: Climate and ocean circulation, Part I: the atmospheric circulation and the hydrology of the earth's surface, *Mon. Weather Rev.*, 97, 739–774, 1969.
- McJannet, D., Franz, T., Hawdon, A., Boadle, D., Baker, B., Almeida, A., Silberstein, R., Lambert, T., and Desilets, D.: Field testing of the universal calibration function for determination of soil moisture with cosmic-ray neutrons, *Water Resour. Res.*, 50, 5235–5248, doi: 10.1002/2014WR015513, 2014.
- MetOffice: Marlborough Climate., URL <http://www.metoffice.gov.uk/public/weather/climate/gcnu88xky>, last accessed:15 December 2016, 2016.
- Mittelbach, H. and Seneviratne, S. I.: A new perspective on the spatio-temporal variability of soil moisture: temporal dynamics versus time-invariant contributions, *Hydrology and Earth System Sciences*, 16, 2169–2179, doi: 10.5194/hess-16-2169-2012, 2012.
- Mittelbach, H., Lehner, I., and Seneviratne, S. I.: Comparison of four soil moisture sensor types under field conditions in Switzerland, *Journal of Hydrology*, 430-431, 39 – 49, doi: 10.1016/j.jhydrol.2012.01.041, 2012.

BIBLIOGRAPHY

- Moene, A. F. and Van Dam, J.: *Transport in the Atmosphere-Vegetation-Soil continuum.*, Cambridge University Press, New York, 1st edn., 2014.
- Montzka, C., Bogen, H. R., Zreda, M., Monerris, A., Morrison, R., Muddu, S., and Vereecken, H.: Validation of Spaceborne and Modelled Surface Soil Moisture Products with Cosmic-Ray Neutron Probes, *Remote Sensing*, 9, doi: 10.3390/rs9020103, 2017.
- Morris, M.: Factorial Sampling Plans for Preliminary Computational Experiments, *Technometrics*, 33, 161–174, doi: 10.1080/00401706.1991.10484804, 1991.
- Mualem, Y.: A new model for predicting the hydraulic conductivity of unsaturated porous media, *Water Resour. Res.*, 12, 513–522, doi: 10.1029/WR012i003p00513, 1976.
- Oki, T. and Kanae, S.: Global Hydrological Cycles and World Water Resources, *Science*, 313, 1068–1072, doi: 10.1126/science.1128845, 2006.
- ORNL-DAAC: AmeriFlux Web Page, URL <http://ameriflux.ornl.gov>, last accessed: 26 October 2015, 2015.
- Osbornová, J., Kovářová, M., Lepš, J., and Prach, K.: *Succession in Abandoned Fields. Studies in Central Bohemia, Czechoslovakia.*, Kluwer, Dordrecht, Netherlands, 1st edn., 1990.
- Pang, Z., Cai, J., Song, W., and Lu, Y.: Measuring and verifying of soil moisture in desert steppe from different spatial scaling, in: 2016 IEEE International Geoscience and Remote Sensing Symposium (IGARSS), pp. 2985–2988, doi: 10.1109/IGARSS.2016.7729771, 2016.
- Pelowitz, D. B.: *MCNPX User's Manual*, Los Alamos National Laboratory, Los Alamos, New Mexico, version 2.5.0 edn., LA-CP-05-0369, 2005.
- Pianosi, F. and Wagener, T.: A simple and efficient methods for global sensitivity analysis based on cumulative distribution functions., *Environ. Model. Software*, 67, doi: 10.1016/j.envsoft.2015.01.004, 2015.
- Pianosi, F., Sarrazin, F., and Wagener, T.: A Matlab toolbox for Global Sensitivity Analysis, *Environmental Modelling and Software*, 70, 80 – 85, doi: 10.1016/j.envsoft.2015.04.009, 2015.
- Pianosi, F., Iwema, J., Rosolem, R., and Wagener, T.: A multimethod global sensitivity analysis approach to support the evaluation of land surface models, in: *Sensitivity Analysis in Earth Observation Modelling*, edited by Petropoulos, G. and Srivastava, P., chap. 7, pp. 125–142, Elsevier Inc., Amsterdam, Netherlands, 2017.
- Pitman, A. J.: The evolution of, and revolution in, land surface schemes designed for climate models., *Int. J. Climatol.*, 23, 479–510, doi: 10.1002/joc.893, 2003.

- Prihodko, L., Denning, A. S., Hanan, N. P., Baker, I., and Davis, K.: Sensitivity, uncertainty and time dependence of parameters in a complex land surface model., *Agr. Forest Meteorol.*, 148, 268–287, doi: 10.1016/j.agrformet.2007.08.006, 2008.
- Qu, W., Bogaen, H. R., Huisman, J. A., Martinez, G., Pachepsky, Y. A., and Vereecken, H.: Calibration of a Novel Low-Cost Soil Water Content Sensor Based on a Ring Oscillator., *Vadose Zone J.*, 12, doi: 10.2136/vzj2012.0139, 2013.
- Qu, W., Bogaen, H. R., Huisman, J. A., Martinez, G., Pachepsky, Y. A., and Vereecken, H.: Effects of Soil Hydraulic Properties on the Spatial Variability of Soil Water Content: Evidence from Sensor Network Data and Inverse Modeling., *Vadose Zone J.*, 13, doi: 10.2136/vzj2014.07.0099, 2014.
- Rahman, M. and Rosolem, R.: Towards a simple representation of chalk hydrology in land surface modelling, *Hydrol. Earth Syst. Sci.*, 21, 459–471, doi: 10.5194/hess-21-459-2017, 2017.
- Rasmussen, R., Baker, B., Kochendorfer, J., Meyers, T., Landolt, S., Fischer, A. P., Black, J., Thériault, J. M., Kucera, P., Gochis, D., Smith, C., Nitu, R., Hall, M., Ikeda, K., and Gutmann, E.: How Well Are We Measuring Snow: The NOAA/FAA/NCAR Winter Precipitation Test Bed, *Bulletin of the American Meteorological Society*, 93, 811–829, doi: 10.1175/BAMS-D-11-00052.1, 2012.
- Rebmann, C., Göckede, M., Foken, T., Aubinet, M., Aurela, M., Berbigier, P., Bernhofer, C., Buchmann, N., Carrara, A., Cescatti, A., et al.: Quality analysis applied on eddy covariance measurements at complex forest sites using footprint modelling, *Theoretical and Applied Climatology*, 80, 121–141, doi: 10.1007/s00704-004-0095-y, 2005.
- Reichle, R. H. and Koster, R. D.: Bias reduction in short records of satellite soil moisture., *Geophys. Res. Lett.*, 31, L19501, doi: 10.1029/2004GL020938, 2004.
- Renzullo, L., van Dijk, A., Perraud, J.-M., Collins, D., Henderson, B., Jin, H., Smith, A., and McJannet, D.: Continental satellite soil moisture data assimilation improves root-zone moisture analysis for water resources assessment, *Journal of Hydrology*, 519, Part D, 2747 – 2762, doi: 10.1016/j.jhydrol.2014.08.008, 2014.
- Richter, H., Western, A. W., and Chiew, F. H. S.: The Effect of Soil and Vegetation Parameters in the ECMWF Land Surface Scheme, *J. Hydrometeor.*, 5, 1131–1146, doi: 10.1175/JHM-362.1, 2004.
- Ritsema, C. J., Kuipers, H., Kleiboer, L., van den Elsen, E., Oostindie, K., Wesseling, J. G., Wolthuis, J.-W., and Havinga, P.: A new wireless underground network system for continuous monitoring of soil water contents, *Water Resources Research*, 45, doi: 10.1029/2008WR007071, 2009.

BIBLIOGRAPHY

- Rivera Villarreyes, C. A., Baroni, G., and Oswald, S. E.: Integral quantification of seasonal soil moisture changes in farmland by cosmic-ray neutrons., *Hydrol. Earth Syst. Sci.*, 15, 3843–3859, doi: 10.5194/hess-15-3843-2011, 2011.
- Rivera Villarreyes, C. A., Baroni, G., and Oswald, S. E.: Inverse modelling of cosmic-ray soil moisture for field-scale soil hydraulic parameters, *European Journal of Soil Science*, 65, 876–886, doi: 10.1111/ejss.12162, 2014.
- Robinson, D. A., Campbell, C. S., Hopmans, J. W., Hornbuckle, B. K., Jones, S. B., Knight, R., Ogden, F., Selker, J., and Wendroth, O.: Soil Moisture Measurement for Ecological and Hydrological Watershed-Scale Observatories: A Review., *Vadose Zone J.*, 7, 358–389, doi: 10.2136/vzj2007.0143, 2008.
- Rodriguez-Iturbe, I. and Porporato, A.: *Ecohydrology of water-controlled ecosystems: Soil moisture and plant dynamics.*, Cambridge University Press, Cambridge, United Kingdom, 1st edn., 2004.
- Romano, N.: Soil moisture at local scale: Measurements and simulations, *Journal of Hydrology*, 516, 6 – 20, doi: <https://doi.org/10.1016/j.jhydrol.2014.01.026>, 2014.
- Rosenbaum, U., Bogaen, H. R., Herbst, M., Huisman, J. A., Peterson, T. J., Weuthen, A., Western, A. W., and Vereecken, H.: Seasonal and event dynamics of spatial soil moisture patterns at the small catchment scale., *Water Resour. Res.*, 48, W10544, doi: 10.1029/2011WR011518, 2012.
- Rosolem, R., Shuttleworth, W. J., Zeng, X., Saleska, S. R., and Huxman, T. E.: Land surface modeling inside the Biosphere 2 tropical rain forest biome, *J. Geophys. Res.*, 115, doi: 10.1029/2010JG001443, 2010.
- Rosolem, R., Gupta, H. V., Shuttleworth, W. J., and Gonalves de Gonalves, L. G.: Towards a comprehensive approach to parameter estimation in land surface parameterization schemes., *Hydrol. Process.*, 27, 2075–2097, doi: 10.1002/hyp.9362, 2013a.
- Rosolem, R., Shuttleworth, W. J., Zreda, M., Franz, T. E., Zeng, X., and Kurc, S. A.: The Effect of Atmospheric Water Vapor on Neutron Count in the Cosmic-Ray Soil Moisture Observing System., *J. Hydrometeorol.*, 14, 1659–1671, doi: 10.1175/JHM-D-12-0120.1, 2013b.
- Rosolem, R., Hoar, T., Arellano, A., Anderson, J. L., Shuttleworth, W. J., Zeng, X., and Franz, T. E.: Translating aboveground cosmic-ray neutron intensity to high-frequency soil moisture profiles at sub-kilometer scale., *Hydrol. Earth Syst. Sci.*, 18, 4363–4379, doi: 10.5194/hess-18-4363-2014, 2014.
- Running, S. W., Baldocchi, D. D., and Turner, D.: A global terrestrial monitoring network, scaling tower fluxes with ecosystem modelling and EOS satellite data, *Remote Sensing*, 70, 108–127, doi: 10.1016/S0034-4257(99)00061-9, 1999.

- Saltelli, A., Ratto, M., Andres, T., Campolongo, F., Cariboni, J., Gatelli, D., Saisana, M., and Tarantola, S.: *Global sensitivity analysis: the primer*, John Wiley & Sons, 2008.
- Sato, T. and Niita, K.: Analytical functions to predict cosmic-ray neutron spectra in the atmosphere., *Radiat. Res.*, 166(3), 544–555, doi: 10.1667/RR0610.1, 2006.
- Schreiner-Mcgraw, A., Vivoni, E., Mascaro, G., and Franz, T.: Closing the water balance with cosmic-ray soil moisture measurements and assessing their relation to evapotranspiration in two semiarid watersheds, *Hydrol. Earth Syst. Sci.*, 20, 329–345, doi: 10.5194/hess-20-329-2016, 2016.
- Schrön, M., Köhli, M., Rosolem, R., Piussi, L., Kasner, M., Kögler, S., Iwema, J., Schröter, I., Mollenhauer, H., Bumberger, J., Wollschläger, U., and Zacharias, S.: Soil moisture estimation across scales with mobile sensors for cosmic-ray neutrons – The influence of roads, in: *EGU General Assembly 2017*, Vienna, Austria, 2017.
- Schrön, M., Köhli, M., Scheiffle, L., Iwema, J., Bogena, H. R., Lv, L., Martini, E., Baroni, G., Rosolem, R., Weimar, J., Mai, J., Cuntz, M., Rebmann, C., Oswald, S. E., Dietrich, P., Schmidt, U., and Zacharias, S.: Improving Calibration and Validation of Cosmic-Ray Neutron Sensors in the Light of Spatial Sensitivity – Theory and Evidence, *Hydrology and Earth System Sciences Discussions*, 2017, 1–30, doi: 10.5194/hess-2017-148, 2017.
- Scott, R. L., Cable, W. L., and Hultine, K. R.: The ecohydrologic significance of hydraulic redistribution in a semiarid savanna, *Water Resour. Res.*, 44, doi: 10.1029/2007wr006149, 2008.
- Sellers, P. J. and Hall, F. G.: FIFE in 1992: Results, scientific gains, and future research directions, *J. Geophys. Res.*, 97, 19 091–19 109, doi: 10.1029/92JD02173, 1992.
- Sellers, P. J., Dickinson, R. E., Randall, D. A., Betts, A. K., Hall, F., Berry, J., Collatz, G., Denning, A., Mooney, H., Nobre, C., Sato, N., Field, C., and Henderson-Sellers, A.: Modeling the exchanges of energy, water, and carbon between continents and the atmosphere, *Science*, 275, 502–509, doi: 10.1126/science.275.5299.502, 1997.
- Seneviratne, S. I., Luthi, D., Litschi, M., and Schar, C.: Land-atmosphere coupling and climate change in Europe, *Nature*, 443, 205–209, doi: 10.1038/nature05095, 2006.
- Seneviratne, S. I., Corti, T., Davin, E. L., Hirschi, M., Jaeger, E. B., Lehner, I., Orlowsky, B., and Teuling, A. J.: Investigating soil moisture-climate interactions in a changing climate: A review., *Earth-Sci. Rev.*, 99, 125–161, doi: 10.1016/j.earscirev.2010.02.004, 2010.
- Shiklomanov, I.: World fresh water resources, in: *Water in Crisis: A Guide to the World's Fresh Water Resources*, edited by Gleick, P., Oxford University Press, New York, 1993.

BIBLIOGRAPHY

- Shuttleworth, W. J., Rosolem, R., Zreda, M., and Franz, T.: The COsmic-ray Soil Moisture Interaction Code (COSMIC) for use in data assimilation., *Hydrol. Earth Syst. Sci.*, 17, 3205–3217, doi: 10.5194/hess-17-3205-2013, 2013.
- Siebert, S., Doll, P., Hoogeveen, J., Faures, J.-M., Frenken, K., and Feick, S.: Development and validation of the global map of irrigation areas., *Hydrol. Earth Syst. Sci.*, 9, 535–547, doi: 10.5194/hess-9-535-2005, 2005.
- Sigouin, M. J. P. and Si, B. C.: Calibration of a non-invasive cosmic-ray probe for wide area snow water equivalent measurement, *The Cryosphere*, 10, 1181–1190, doi: 10.5194/tc-10-1181-2016, 2016.
- Sigouin, M. J. P., Dyck, M., Si, B. C., and Hu, W.: Monitoring soil water content at a heterogeneous oil sand reclamation site using a cosmic-ray soil moisture probe, *Journal of Hydrology*, 543, 510–522, doi: 10.1016/j.jhydrol.2016.10.026, 2016.
- Simpson, J.: The cosmic-ray nucleonic component: The invention and scientific uses of the neutron monitor - (Keynote Lecture)., *Space Sci. Rev.*, 93, 11–32, 2000.
- Simpson, J. A.: Neutrons Produced in the Atmosphere by the Cosmic Radiations, *Phys. Rev.*, 83, 1175–1188, doi: 10.1103/PhysRev.83.1175, 1951.
- Smart, D. and Shea, M.: Geomagnetic cutoff rigidity computer program: Theory, software description and example., The University of Alabama, Huntsville, Alabama, USA, URL <http://ccmc.gsfc.nasa.gov/modelweb/sun/cutoff.html>, nAG5-8009, 2001.
- Smirnova, T. G., Brown, J. M., and Benjamin, S. G.: Performance of temperature and surface fluxes., *Mon. Weather Rev.*, 125, 1871–1884, doi: 10.1175/1520-0493(1997)125<1870:PODSMC>2.0.CO;2, 1997.
- Smith, A. B., Walker, J. P., Western, A. W., Young, R. I., Ellett, K. M., Pipunic, R. C., Grayson, R. B., Siriwardena, L., Chiew, F. H. S., and Richter, H.: The Murrumbidgee soil moisture monitoring network data set, *Water Resour. Res.*, 48, doi: 10.1029/2012WR011976, 2012.
- Smits, K. M., Sakaki, T., Limsuwat, A., and Illangasekare, T. H.: Thermal conductivity of sands under varying moisture and porosity in drainage-wetting cycles, *Vadose Zone. J.*, 9, 172–180, doi: 10.2136/vzj2009.0095, 2010.
- Sobol, I.: Sensitivity analysis for non-linear mathematical models, *Mathematical Modelling and Computational Experiment*, 1, 407–414, translated from Russian: I.M. Sobol', Sensitivity estimates for nonlinear mathematical models, *Matematicheskoe Modelirovanie* 2 (1990) 112–118, 1993.

- Spear, R. and Hornberger, G.: Eutrophication in peel inlet. II. Identification of critical uncertainties via generalized sensitivity analysis, *Water Research*, 14, 43 – 49, doi: 10.1016/0043-1354(80)90040-8, 1980.
- Stöckli, R., Lawrence, D. M., Niu, G. Y., Oleson, K. W., Thornton, P. E., Yang, Z. L., Bonan, G. B., Denning, A. S., and Running, S. W.: Use of FLUXNET in the community land model development, *J. Geophys. Res.*, 113, doi: 10.1029/2007JG000563, 2008.
- Teuling, A. J.: Soil moisture dynamics and land surface-atmosphere-interaction., Ph.D. thesis, Wageningen Universiteit, 2007.
- Teuling, A. J. and Troch, P. A.: Improved understanding of soil moisture variability dynamics, *Geophysical Research Letters*, 32, doi: 10.1029/2004GL021935, 2005.
- Teuling, A. J., Uijlenhoet, R., Hupet, F., van Loon, E. E., and Troch, P. A.: Estimating spatial mean root-zone soil moisture from point-scale observations, *Hydrol. Earth Syst. Sci.*, 10, 755–767, doi: 10.5194/hess-10-755-2006, 2006.
- Teuling, A. J., Hirschi, M., Ohmura, A., Wild, M., Reichstein, M., Ciais, P., Buchmann, N., Ammann, C., Montagnani, L., Richardson, A. D., Wohlfahrt, G., and Seneviratne, S. I.: A regional perspective on trends in continental evaporation, *Geophysical Research Letters*, 36, doi: 10.1029/2008GL036584, 2009a.
- Teuling, A. J., Uijlenhoet, R., Van den Hurk, B., and Seneviratne, S. I.: An Analysis Using Stochastic Soil Moisture Models and ELDAS Soil Parameters, *J. Hydrometeorol.*, 10, 751–765, doi: 10.1175/2008JHM1033.1, 2009b.
- Tian, Z., Li, Z., Liu, G., Li, B., and Ren, T.: Soil water content determination with cosmic-ray neutron sensor: Correcting aboveground hydrogen effects with thermal/fast neutron ratio, *Journal of Hydrology*, 540, 923–933, doi: 10.1016/j.jhydrol.2016.07.004, 2016.
- Topp, G. C. and Ferré, P. A.: Thermogravimetric method using convective oven-drying., in: *Methods of Soil Analysis*, edited by Dane, J. H. and Topp, G. C., vol. Part 4: Physical methods of *Soil Science Society of America Book Series*, pp. 422–424, Soil Science Society of America, Madison, Wisconsin, 2002.
- Topp, G. C., Davis, J. L., and Annan, A. P.: Electromagnetic determination of soil water content: Measurements in coaxial transmission lines, *Water Resources Research*, 16, 574–582, doi: 10.1029/WR016i003p00574, 1980.
- Topp, G. C., Lapen, D., Young, G., and Edwards, M.: Evaluation of the shaft-mounted TDT readings in disturbed and undisturbed media., in: *Second International Symposium and Workshop on Time Domain Reflectometry for Innovative Geotechnical Applications.*, URL <http://www.iti.northwestern.edu/tdr/tdr2001/proceedings>, 2001.

BIBLIOGRAPHY

- Trenberth, K. E., Fasullo, J. T., and Kiehl, J.: Earth's Global Energy Budget, *B. Am. Meteorol. Soc.*, 90, 311–323, doi: 10.1175/2008BAMS2634.1, 2009.
- Trubilowicz, J., Cai, K., and Weiler, M.: Viability of motes for hydrological measurement, *Water Resources Research*, 45, doi: 10.1029/2008WR007046, 2009.
- Vachaud, G., Passerat De Silans, A., Balabanis, P., and Vauclin, M.: Temporal Stability of Spatially Measured Soil Water Probability Density Function, *Soil Sci. Soc. Am. J.*, 49, 822–828, doi: 10.2136/sssaj1985.03615995004900040006x, 2008.
- Van Dam, J. and Feddes, R. A.: Numerical simulation of infiltration, evaporation, and shallow groundwater levels with the Richards equation., *J. Hydrol.*, 233, 72–85, doi: 10.1016/S0022-1694(00)00227-4, 2000.
- Van Dam, J., Groenendijk, P., R.F.A., H., and Kroes, J.: Advances of modeling water flow in variably saturated soils with SWAP., *Vadose Zone J.*, 7, doi: doi:10.2136/vzj2007.0060, 2008.
- Van Genuchten, M. T.: A closed-form equation for predicting the hydraulic conductivity of unsaturated soils, *Soil Sci. Soc. Am. J.*, 44, 892–898, 1980.
- Vanderlinden, K., Vereecken, H., Hardelauf, H., Herbst, M., Martinez, G., Cosh, M. H., and Pachepsky, Y. A.: Temporal Stability of Soil Water Contents: A Review of Data and Analyses, *Vadose Zone J.*, 11, doi: 10.2136/vzj2011.0178, 2012.
- Vaz, C. M., Jones, S., Meding, M., and Tuller, M.: Evaluation of Standard Calibration Functions for Eight Electromagnetic Soil Moisture Sensors, *Vadose Zone J.*, 12, doi: 10.2136/vzj2012.0160, 2013.
- Vereecken, H., Huisman, J. A., Bogaen, H., Vanderborght, J., Vrugt, J. A., and Hopmans, J. W.: On the value of soil moisture measurements in vadose zone hydrology: A review., *Water Resour. Res.*, 44, W00D06, doi: 10.1029/2008WR006829, 2008.
- Vereecken, H., Huisman, J. A., Hendricks Franssen, H.-J., Brüggemann, N., Bogaen, H. R., Kollet, S., Javaux, M., van der Kruk, J., and Vanderborght, J.: Soil hydrology: Recent methodological advances, challenges, and perspectives, *Water Resources Research*, 51, 2616–2633, doi: 10.1002/2014WR016852, 2015.
- Vinnikov, K. Y., Robock, A., Shuang, W., and Schlosser, A.: Scales of temporal and spatial variability of midlatitude soil moisture, *J. Geophys. Res.*, 101, 7163–7174, doi: 10.1029/95JD02753, 1996.
- Vivoni, E. R., Moreno, H. A., Mascaro, G., Rodriguez, J. C., Watts, C. J., Garatuza-Payan, J., and Scott, R. L.: Observed relation between evapotranspiration and soil moisture in the North American monsoon region, *Geophys. Res. Lett.*, 35, doi: 10.1029/2008GL036001, 2008.

- Von Hoyningen-Huene, J.: Die Interzeption Des Niederschlags in landwirtschaftlichen Pflanzenbeständen. Arbeitsbericht Deutscher Verband für Wasserwirtschaft und Kulturbau, DVWK, Braunschwig, Germany, 1981.
- Šimuněk, J., van Genuchten, M. T., and Šejna, M.: Development and Applications of the HYDRUS and STANMOD Software Packages and Related Codes., *Vadose Zone J.*, 7, 587–600, doi: 10.2136/vzj2007.0077, 2008.
- Wang, C., Zuo, Q., and Zhang, R.: Estimating the necessary sampling size of surface soil moisture at different scales using a random combination method, *Journal of Hydrology*, 352, 309 – 321, doi: <https://doi.org/10.1016/j.jhydrol.2008.01.011>, 2008.
- Weihermüller, L.: Mapping the spatial variation of soil water content at the field scale with different ground penetrating radar techniques, *Journal of Hydrology*, 340, 205 – 216, doi: 10.1016/j.jhydrol.2007.04.013, 2007.
- Western, A. W. and Blöschl, G.: On the spatial scaling of soil moisture, *Journal of Hydrology*, 217, 203 – 224, doi: 10.1016/S0022-1694(98)00232-7, 1999.
- Western, A. W., Blöschl, G., and Grayson, R. B.: Geostatistical characterisation of soil moisture patterns in the Tarrawarra catchment, *Journal of Hydrology*, 205, 20 – 37, doi: 10.1016/S0022-1694(97)00142-X, 1998.
- Western, A. W., Grayson, R. B., and Blöschl, G.: Scaling of Soil Moisture: A Hydrologic Perspective, *Annual Review of Earth and Planetary Sciences*, 30, 149–180, doi: 10.1146/annurev.earth.30.091201.140434, 2002.
- Western, A. W., Zhou, S.-L., Grayson, R. B., McMahon, T. A., Blöschl, G., and Wilson, D. J.: Spatial correlation of soil moisture in small catchments and its relationship to dominant spatial hydrological processes, *Journal of Hydrology*, 286, 113 – 134, doi: 10.1016/j.jhydrol.2003.09.014, 2004.
- Widłowski, J., for Environment, I., and Sustainability: Allometric Relationships of Selected European Tree Species: Parametrizations of Tree Architecture for the Purpose of 3-D Canopy Reflectance Models Used in the Interpretation of Remote Sensing Data : *Betula Pubescens*, *Fagus Sylvatica*, *Larix Decidua*, *Picea Abies*, *Pinus Sylvestris*, Office for Official Publications of the European Communities, URL <https://books.google.co.uk/books?id=D7paewAACAAJ>, 2003.
- Wood, E. F., Roundy, J. K., Troy, T. J., Van Beek, L. P. H., Bierkens, M. F. P., Blyth, E., De Roo, A., Döll, P., Ek, M., Famiglietti, J., Gochis, D., Van de Giesen, N., Houser, P., Jaffé, P. R., Kollet, S., Lehner, B., Lettenmaier, D. P., Peters-Lidard, C., Sivapalan, M., Sheffield, J., Wade, A., and Whitehead, P.: Hyperresolution global land surface modeling: Meeting a grand

BIBLIOGRAPHY

- challenge for monitoring Earth's terrestrial water, *Water Resour. Res.*, 47, W05301, doi: 10.1029/2010WR010090, 2011.
- Wösten, J.: Pedotransfer functions to evaluate soil quality, in: *Soil Quality for Crop Production and Ecosystem Health*, pp. 221–246, Elsevier, Amsterdam, Netherlands, 1997.
- Wösten, J., Pachepsky, Y. A., and Rawls, W.: Pedotransfer functions: Bridging the gap between available basic soil data and missing soil hydraulic characteristics, *J. Hydrol.*, 251, 123–150, doi: 10.1016/S0022-1694(01)00464-4, 2001.
- Wraith, J. M., Robinson, D. A., Jones, S. B., and Long, D. S.: Spatially characterizing apparent electrical conductivity and water content of surface soils with time domain reflectometry, *Computers and Electronics in Agriculture*, 46, 239 – 261, doi: 10.1016/j.compag.2004.11.009, 2005.
- WRCC: Santa Rita Exp Range, Arizona (027593): Period of Record Monthly Climate Summary - Temperature., URL <http://www.wrcc.dri.edu/cgi-bin/cliMAIN.pl?azsant>, last accessed: 16 January 2015, 2006.
- Young, P. C., Spear, R. C., and Hornberger, G. M.: Modeling badly defined systems: Some further thoughts, in: *Proceedings SIMSIG Conference*, Canberra, pp. 24–32, 1978.
- Zadeh, F. K., Nossent, J., Sarrazin, F., Pianosi, F., van Griensven, A., Wagener, T., and Bauwens, W.: Comparison of variance-based and moment-independent global sensitivity analysis approaches by application to the {SWAT} model, *Environmental Modelling and Software*, 91, 210 – 222, doi: 10.1016/j.envsoft.2017.02.001, 2017.
- Zhu, X., Shao, M., Zeng, C., Jia, X., Huang, L., Zhang, Y., and Zhu, J.: Application of cosmic-ray neutron sensing to monitor soil water content in an alpine meadow ecosystem on the northern Tibetan Plateau, *Journal of Hydrology*, 536, 247–254, doi: 10.1016/j.jhydrol.2016.02.038, 2016.
- Zhu, Z., Tan, L., Gao, S., and Jiao, Q.: Observation on Soil Moisture of Irrigation Cropland by Cosmic-Ray Probe, *IEEE Geoscience and Remote Sensing Letters*, 12, 472–476, doi: 10.1109/LGRS.2014.2346784, 2015.
- Zianis, D., Muukkonen, P., Makipaa, R., and Mencuccini, M.: Biomass and stem volume equations for tree species in Europe., *Silva fennica monographs*, pp. 1–2,5–63, 2005.
- Zreda, M., Desilets, D., Ferré, T. P. A., and Scott, R. L.: Measuring soil moisture content non-invasively at intermediate spatial scale using cosmic-ray neutrons., *Geophys. Res. Lett.*, 35, L21402, doi: 10.1029/2008GL035655, 2008.
- Zreda, M., Shuttleworth, W. J., Zeng, X., Zweck, C., Desilets, D., Franz, T., and Rosolem, R.: COSMOS: the COsmic-ray Soil Moisture Observing System., *Hydrol. Earth Syst. Sci.*, 16, 4079–4099, doi: 10.5194/hess-16-4079-2012, 2012.